

**41st German Conference on
Liquid Crystals
Magdeburg
March 25–27, 2014**



Table of Contents

Foreword	7
Timetable	9
Oral Presentations	13
I1 H. Takezoe, et al.: “Azo–dendrimer for Manipulating Molecular Orientations in Microparticle Systems”	15
O1 A. Bogner, et al.: “Compensation of smectic layer contraction in carbosilane ‘de Vries’–type liquid crystals”	19
O2 P. V. Dolganov, et al.: “Behaviour of complex polar structures in external field”	21
O3 R.K. Shukla, et al.: “Ferroelectric liquid crystalline nanocolloids: Effect of harvested nanoparticles on electro–optic and material parameters of FLC”	23
O4 V.S.R. Jampani, et al.: “Microfluidic droplet production in a nematic matrix under AC electric fields”	27
O5 N. Chattham, et al.: “Observation of Polarization in the Leaning Plane of a Bent–Core Molecular Compound”	29
E1 P. Pieranski: “Yes, but what is the question?”	31
O6 A. Lorentz, et al.: “Polymer stabilized short pitch chiral nematic liquid crystals: Electro–optics with interdigitated electrodes”	33
O7 R. Rix, et al.: “Thermotropic Liquid Crystal Elastomer Micro Actuators with Integrated Heating”	37
O8 S. Bedjaoui, et al.: “Liquid Crystalline polymers networks as molecular imprinting materials” CANCELLED.....	41
O9 Y. Derouiche, et al.: “Preferential solubility effects of a commercial nematic LC blend towards Poly(methylphenylsiloxane)”	43

O10	J. Bruckner, et al.: “Solvent induced twist grain boundary phase in a lyotropic liquid crystal”	45
O11	M.M. Neidhardt, et al.: “Novel ionic liquid crystals designed from amino acids”	47
O12	K. Harth, et al.: “Coalescence of Islands in Smectic Membranes”	49
I2	J.P.F. Lagerwall: “With an open attitude new doors open: Reflections on interdisciplinarity, knowledge sharing and the future of liquid crystal research and applications in Europe and in South Korea”	53
O13	M. Wahle, et al.: “Group velocity dispersion in liquid crystal filled photonic crystal fibers”	55
O14	G.H. Mehl, et al.: “Design and investigation of liquid crystal superlattice forming gold nanoparticles – a route to plasmonic metamaterials”	61
I3	A.R. Bausch: “Cytoskeletal pattern formation: Self organization of topology”	63
O15	F. Jenz, et al.: “Two dimensional X-ray diffraction patterns of liquid crystalline Gay–Berne phases: reliability of orientational order parameters”	65
O16	A.M. Menzel, et al.: “Unidirectional laning and migrating cluster crystals in confined active systems”	67
O17	M. Alaasar, et al.: “Synthesis and liquid crystalline properties of new azobenzene based bent–core liquid crystals”	73
O18	M. Lehmann, et al.: “Shape–Persistent, Star–Shaped Host–Guest Supermesogens”	75
O19	M.–G. Tamba, et al.: “Investigation of dimeric systems with a nematic – nematic phase transition”	77
	Poster Presentations	83
P1	B. Atorf, et al.: “Switching between the resonance modes of split ring resonators”	85

P2	S. Bedjaoui, et al.: “Phase separation effect on polymer/liquid crystal systems including nano-sized diamond particles”	89
P3	S. Bedjaoui, et al.: “Optical transmission relaxation processes of polymer/liquid crystal blends“	91
P4	Y. Derouiche, et al.: “Polymer/Liquid Crystal networks : Correlation between morphologies and electrical, optical and electro-optical properties“	93
P5	Y. Derouiche, et al.: “Polymer Dispersed Liquid Crystal Systems: Electron Beam and UV-light induced polymerization/crosslinking Processes“	95
P6	F. Knecht, et al.: “Structure and order parameters of an antiferroelectric liquid crystal with exceptionally high director tilt angle”	97
P7	J. Schmidtke, et al.: “Emissive cholesteric films: Dye depletion, dye diffusion and helix distortion”	99
P8	R.K. Shukla, et al.: “Investigations on structural and dielectric dynamics of non-aqueous lyotropic mesophases”	101
P9	M. Urbanski, et al.: “Dispersions of functionalized gold nanoparticles in nematic liquid crystals”	105
P10	N. Zimmermann, et al.: “Dispersion of micro- and nanoparticles in a chromonic liquid crystal”	111
P11	K. Bahndorf, et al.: “Recent advances in the synthesis of amino acid based arms and their conversion to C ₃ -symmetric star mesogens“	113
P12	J.C. Hänle, et al.: “Liquid crystalline guanidinium Phenylalkoxybenzoates”	115
P13	M. Harjung, et al.: “Photoresponsive ionic liquid crystals”	117
P14	M. Hügel, et al.: “Star-shaped oligo-p-phenylenevinylene mesogens with fullerene guests”	119
P15	D. Janietz, et al.: “Polyphilic Hydrogen-Bonded Complexes Bearing Oligoethyleneglycol and Semiperfluorinated Molecular Segments”	121

P16	M. Kohout, et al.: “Bent-shaped liquid crystals – Quantum chemical calculations or de novo synthesis?”	125
P17	P. Maier, et al.: “Star-shaped mesogens with a hexasubstituted C ₃ -symmetric benzene centre”	127
P18	S. Maisch, et al.: “Shape-persistent V-shaped nematogens with cyclohexane units”	129
P19	R. Pashmeah, et al.: “Synthesis of Novel Liquid Crystal Materials for Ferroelectric Display“	131
P20	M. Poppe, et al.: “4-Cyanoresorcinol derived bent-core mesogens with different wing groups”	133
P21	S. Poppe, et al.: “Bolapolyphiphiles with liquid crystalline and membrane modifying properties”	135
P22	A. Poryvai, et al.: “Design and synthesis of chiral liquid crystals with „de Vries-like“ mesomorphic behaviour“	137
P23	T. Rieth, et al.: “Luminescent Discotic Liquid Crystals based on a Nitrogen-rich Core”	139
P24	S. Roth, et al.: ”Synthesis and Properties of Differently Equipped Four-Armed Star-Shaped Mesogens”	141
P25	M.-G. Tamba, et al.: “Oligomeric materials composed of bent-core and calamitic mesogenic units – mesomorphic and electro-optical properties”	143
P26	T. Vojtylová, et al.: “Chiral HPLC for a study of the optical purity of liquid-crystalline materials derived from lactic acid”	149
P27	J. Vollbrecht, et al.: “Optical and electronic properties of unilaterally and bilaterally extended perylene cores”	153
P28	T. Wöhrle, et al.: “Novel liquid crystals containing a boroxine central unit”	157
P29	S. Dölle, et al.: “Coalescence of Lentil-Like Droplets on Freely Suspended Smectic Films”	158
P30	K. May, et al.: “Dynamics of Free-Floating Smectic Bubbles”	160

P31	K. Harth, et al.: “Dynamics of Point Defects in Free-Standing SmC Films”	162
P32	K. Harth, et al.: “Interface Tension of Smectic Membranes in Water”	166
	List of Presenting Authors	171

Dear Participant,

We would like to welcome you to the 41st German Conference on Liquid Crystals. This conference continues the tradition of bringing together researchers from various fields of science active in the field of liquid crystals. The first meeting started in Freiburg in the early seventies. The annual German meeting on Liquid Crystals has long become an international-scale workshop, promoting exchange of views among scientists working with soft matter and, in particular, liquid crystals.

The activities at the meeting will consist of a few invited lectures from internationally distinguished researchers, and oral presentation and posters mainly by young researchers. Diverse topics cover a wide range of chemistry, physics, and application technologies of thermotropic and lyotropic liquid crystals, including relevant areas such as materials science, optics, colloid chemistry and physics, nanoscience, and biophysics.

We would like to thank all the participants for coming, and we acknowledge generous support by our sponsors and the Otto von Guericke Society.

Enjoy your stay in Magdeburg, and do not hesitate to address the organisers with requests or suggestions!

With kind regards,

The Organising Committee

Prof. Dr. Ralf Stannarius
PD Dr. Alexey Eremin

Tuesday March 25, 2014

Time	Number	Name	Title of Talk
14:00 - 14:15	Introduction		
14:15 - 15:00	I1	Takezoe	Azo-dendrimer for Manipulating Molecular Orientations in Microparticle Systems
15:00 - 15:25	O1	Bogner	Compensation of smectic layer contraction in carbosilane 'de Vries'-type liquid crystals
15:25 - 15:50	O2	Dolganov	Behaviour of complex polar structures in external field
15:50 - 16:20	Pause		
16:20 - 16:45	O3	Shukla	Ferroelectric liquid crystalline nanocolloids: Effect of harvested nanoparticles on electro-optic and material parameters of FLC
16:45 - 17:10	O4	Jampani	Droplet production in nematic liquid crystals under AC electric fields
17:10 - 17:35	O5	Chattham	Observation of polarization in the leaning plane of a bent-core molecular compound
17:35 - 19:00	Poster Session		
19:00 - 19:45	E1	Pieranski	Evening Talk: "Yes, but what is the question?"
>19:45	Reception		

Wednesday March 26, 2014

Time	Number	Name	Title of Talk
8:30 - 8:55	O6	Lorentz	Polymer stabilized short pitch chiral nematic liquid crystals: Electro-optics with interdigitated electrodes.
8:55 - 9:20	O7	Rix	Thermotropic Liquid Crystal Elastomer Micro-Actuators with Integrated Heating
9:20 - 9:45			
9:45 - 10:10	O9	Derouiche	Preferential solubility effects of a commercial nematic LC blend towards Poly(methylphenylsiloxane)
10:10 - 10:40	Pause		
10:40 - 11:05	O10	Bruckner	Solvent induced twist grain boundary phase in a lyotropic liquid crystal
11:05 - 11:30	O11	Neidhardt	Novel ionic liquid crystals designed from amino acids
11:30 - 11:55	O12	Harth	Coalescence of Islands in Smectic Membranes
11:55 - 14:00	Lunch		
14:00 - 14:15	Laudatio		
14:15 - 15:00	I2 (Vorländervorlesung)	Lagerwall	With an open attitude new doors open Reflections on interdisciplinarity, knowledge sharing and the future of liquid crystal research and applications in Europe and in South Korea
15:00 - 15:25	O13	Wahle	Group velocity dispersion in liquid crystal-filled photonic crystal fibers
15:25 - 15:50	O14	Mehl	Design and investigation of liquid crystal superlattice forming gold nanoparticles - a route to plasmonic metamaterials
15:50 - 18:00	Poster Session		
18:00 - 19:00	GLCS Meeting		
20:00 -	Dinner		

Thursday March 27, 2014

Time	Number	Name	Title of Talk
8:30 - 9:15	I3	Bausch	Cytoskeletal pattern formation: Self organization of topology
9:15-9:40	O15	Jenz	Two dimensional X-ray diffraction patterns of liquid crystalline Gay-Berne phases: reliability of orientational order parameters
9:40 - 10:05	O16	Menzel	Unidirectional laning and migrating cluster crystals in confined active systems
10:05 - 10:35	Pause		
10:35 - 11:00	O17	Alaasar	Synthesis and liquid crystalline properties of new azobenzene based bent-core liquid crystals
11:00 - 11:25	O18	Lehmann	Shape-Persistent, Star-Shaped Host-Guest Supermesogens
11:25 - 11:50	O19	Tamba	Investigation of dimeric systems with a nematic – nematic phase transition
11:50-12:20			Award Ceremonies and Closing

Oral Presentations

Azo-dendrimer for Manipulating Molecular Orientations in Microparticle Systems

P. Hirankittiwong,^{a,b} N. Chattham,^{a,b} O. Haba,^c K. Yonetake,^c M.-G. Tamba,^a
A. Eremin,^a R. Stannarius,^a and H. Takezoe^{a,d,*}

^aDepartment of Nonlinear Phenomena, Institute for Experimental Physics, Otto-von-Guericke-Universität Magdeburg, Magdeburg, Germany

^bDepartment of Physics, Faculty of Science, Kasetsart University, Bangkok, Thailand

^cOrganic Device Engineering, Yamagata University, Yonezawa, Japan

^dDepartment of Organic and Polymeric Materials, Tokyo Institute of Technology, Tokyo, Japan

e-mail: takezoe.h.aa@m.titech.ac.jp

Liquid crystal (LC) orientation is specified by interfaces giving an anchoring condition, and is varied by external stimuli such as electric, magnetic, and optical fields. Here, we introduce azo-dendrimer molecules, which spontaneously attach to the interfaces and act as a command surface.^[1] Momoi et al.^[2] showed that the polyimide-free vertical alignment (VA) for display application can be achieved just by dissolving poly(propyleneimine)-based LC dendrimers^[3] in a nematic LC (NLC) mixture. Dendritic azobenzene derivatives (Fig. 1, azo-dendrimer)^[4] are more interesting, since optical surface manipulation (command surface) is possible through photo-induced trans-to-cis isomerization (Fig. 2). Actually, some of the present authors have already reported the usefulness of the azo-dendrimer for optical devices.^[5,6] In the last decades much attention has been devoted to the study of micro-/nano-sized particles, particularly for optically controlling or manipulating the structures for new applications. Here, we study two new systems for azo-dendrimer application; (1) microdroplets of banana nematic in glycerol matrix and (2) microspheres (Slica particle of 3.78 μm in diameter) in nematic (5CB) matrix.

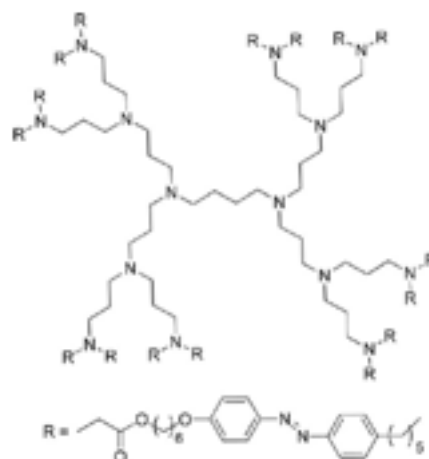


Fig. 1: chemical structure of dendrimer used.

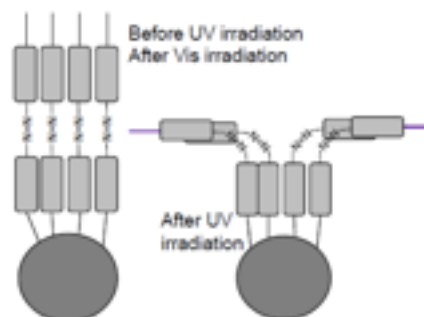


Fig. 2: Schematic molecular shapes before and after UV irradiation and after Vis irradiation.

In both systems, the azo-dendrimers are spontaneously adsorbed at the interfaces between the particles and the matrix just by dissolving a small amount of dendrimer (0.1–0.3 wt%) into NLC materials.

Lee et al.^[6] have already reported photo-induced ordering transition in microdroplets of N, Ch, and SmA LCs. For instance, a reversible structure change between radial and bipolar was induced by UV and Vis light irradiation.^[6] The situation is slightly different in banana NLC (system (1)). In contrast to a sharp extinction cross in 5CB droplet (Fig. 3a), we often observed a curved extinction cross in the radial orientation before light irradiation (Fig. 3b). However, after turning off the UV irradiation, a blurred non-curved extinction cross emerged (Fig. 3c).

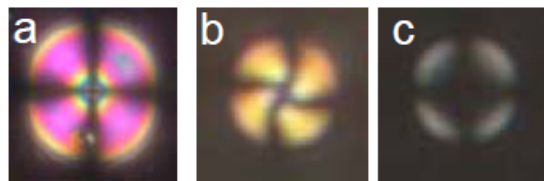


Fig. 3: Nematic droplets in glycerol, (a) 5CB, before irradiation, (b) banana nematic, before irradiation, (c) banana nematic, after UV irradiation.

It is well known that many kinds of topological defects, such as hyperbolic hedgehog defects, Saturn rings, and boojums, emerge around a microparticle situated in an oriented NLC field (Fig. 4).⁷ In our system (2), we originally observed a hedgehog defect (Fig. 4(d)). Upon UV irradiation, the defect structure changes to a dark cross (Fig. 4(e)) due to the structure shown in Fig. 4b, i.e., two surface defects known as boojums. This is because of the anchoring condition change at the particle surface by UV light irradiation; homeotropic to planar. After termination the irradiation, a Saturn ring perpendicular to the rubbing direction (Fig. 4(f)) was observed by the anchoring change from planar to homeotropic again.

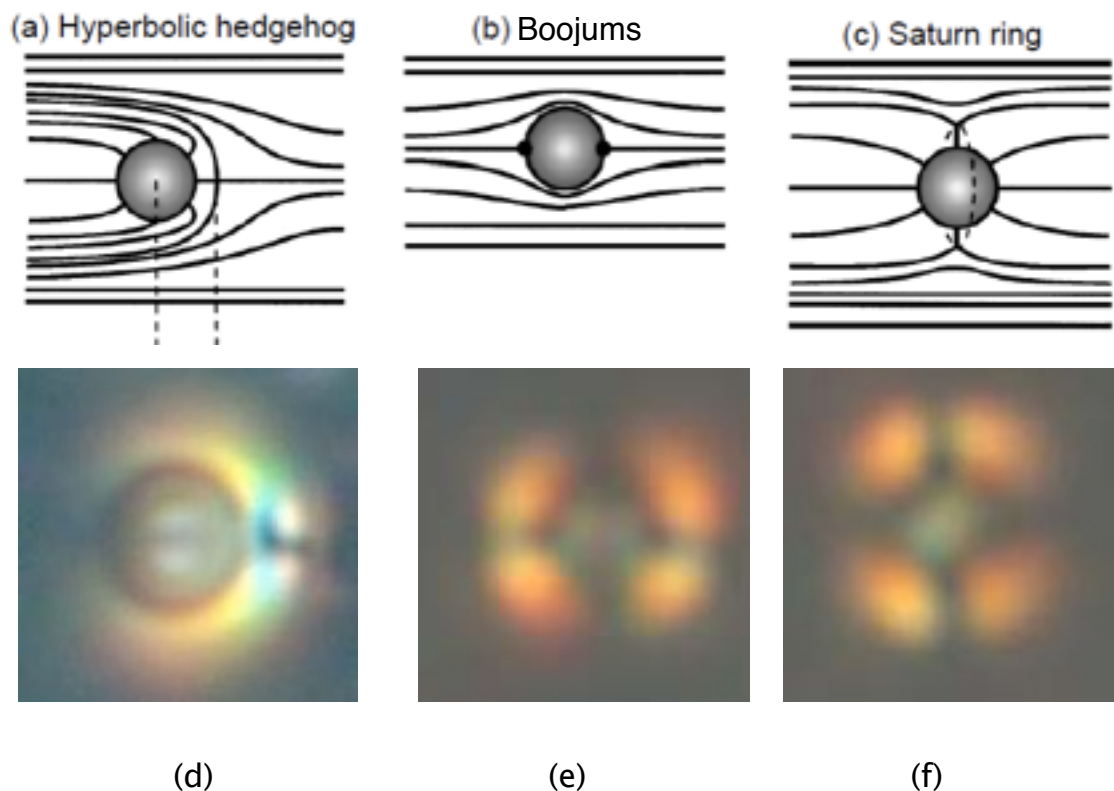


Fig. 4: Defect structures of liquid crystal around a microparticle, (a) hyperbolic hedgehog, (b) boojams, and (c) Saturn ring. Observation of a microparticle in uniform 5CB field, (d) before irradiation, homeotropic anchoring, (b) during UV irradiation, and (c) after UV irradiation. The structure changes are due to the surface anchoring condition changes, homeotropic–planar–homeotropic.

In this way, we showed the usefulness of the azo–dendrimer for manipulating the surface anchoring condition by light irradiation. The advantages of this technique are (a) no need of surface pre–treatment of micro–particles, (b) possible observation of dynamic process of defect structure change due to surface anchoring condition change. We will apply this technique to broader systems such as banana smectics (3), micro–rod (4), and multi–particle system (5). In the system (3) such as SmCP (B2) phase, the phase appears as spherical domains with conical smectic layers (onion structure) when it appears in the isotropic phase. It is interesting to see how the interface orientation influences the structure. In the system (4), we have already observed the defect structures, and even some dynamics such as translation and rotation. In the system (5), it is known that different kinds of 2D lattice structures such as quadrupolar nematic colloidal crystals using aligned Saturn ring defects and dipolar ones using hyperbolic hedgehog defects can be formed.⁸ In such structures, the surface is always homeotropically treated. It is interesting to see what happens in the structures when the surface anchoring condition is

changed from homeotropic to planar. Hopefully, we will present the results in such systems in addition to those in the systems (1) and (2).

References:

- ¹K. Ichimura et al., *Langmuir*, 1988, **4**, 1214.
- ²K. Yonetake et al., *Macromolecules*, 1999, **32**, 6578.
- ³Y. Momoi et al., *J. Soc. Inf. Display*, 2012, **20**, 486.
- ⁴W. Li et al., *Macromolecules*, 2012, **45**, 6618.
- ⁵T. Ikeda et al., *Appl. Phys. Exp.*, 2013, **6**, 061701.
- ⁶G. Lee et al., *Part. Part. Syst. Charact.*, 2013, **30**, 847.
- ⁷P. Poulin and D. A. Weitz, *Phys. Rev. E*, 1998, **57**, 626.
- ⁸I. Musevic et al., *Science*, 2006, **313**, 954.

Compensation of smectic layer contraction in carbosilane ‘de Vries’-type liquid crystals

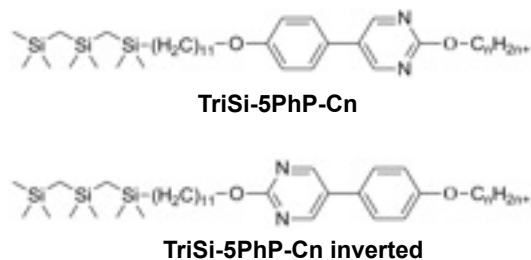
Andreas Bogner^{a,*}, Chris Schubert^b, Sonja Dieterich^a, Robert P. Lemieux^b,
Frank Giesselmann^a

^a Institute of Physical Chemistry, University of Stuttgart, Pfaffenwaldring 55,
70569 Stuttgart, GERMANY.

^b Chemistry Department, Queen’s University, Kingston, Ontario, CANADA.

e-mail: andreas.bogner@ipc.uni-stuttgart.de

Typically, the phase transition from the orthogonal smectic A (SmA) into the tilted smectic C (SmC) phase is associated with a substantial shrinkage of the smectic layer thickness. In some rare cases however, smectic A – C transitions with little or no layer contraction in the SmC phase were observed. The essentially constant smectic layer spacing in these ‘de Vries’ smectics can only be understood if there is a mechanism which compensates the layer contraction due to the increasing director tilt angle θ . Possible explanations are temperature-dependent variations in the effective molecular length L_{eff} or the orientational order parameter S_2 which counteract the tilt-induced layer contraction.



X-ray diffraction experiments on SmC monodomains allow to measure the smectic layer spacing d , the orientational order parameter S_2 and the director tilt angle θ simultaneously in the same experiment¹ and thus provide a powerful tool to elucidate the nature of ‘de Vries’ smectics. So far, there are only four of these measurements reported in literature. All these measurements were done on carbosiloxane mesogens and they showed either temperature-dependent variations of L_{eff} while S_2 remained essentially constant¹ or vice versa². Thus, only the two borderline

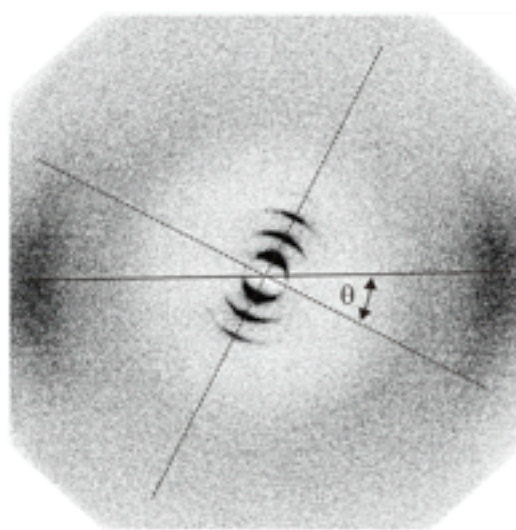


Fig. 1 Representative X-ray pattern from a SmC monodomain of TriSi-5PhP-C6.

cases have been observed till now.

We now investigated new carbosilane ‘de Vries’-type materials the structure of which is shown in Fig. 1. We obtained large monodomains by either cooling slowly from the isotropic phase and/or by measuring near the surface of the capillary both for the C6 and C8 homologue of the two series. Estimating the effective molecular length using^{2,3}

$$d(T) = \frac{1}{3} [S_2(T) + 2] L_{\text{eff}}(T) \cos \theta(T)$$

and the experimental $\theta(T)$, $S_2(T)$ and $d(T)$ data, we found an increase in L_{eff} and in S_2 at decreasing temperature in SmC. The contributions of these

mechanisms are shown in Fig. 2. The d values of the lower curve are calculated with temperature-dependent values for θ while L_{eff} and S_2 are kept constant, showing the pure effect of tilting on the layer spacing. Taking the temperature variation of S_2 also into account leads to the curve seen in the middle. Finally, if in addition the variation of L_{eff} is also included, the experimental values (upper curve) are reproduced.

This leads to the conclusion that in the case of carbosilane ‘de Vries’-type liquid crystals the layer contraction is indeed compensated by a combination of both mechanisms: an increase of orientational order (intermolecular ordering) and an increase in L_{eff} (intramolecular conformational ordering).

Financial support by the Deutsche Forschungsgemeinschaft in the NSF/DFG program “Materials World Network” (DFG Gi 243/6) is gratefully acknowledged.

¹ H. Yoon, D. M. Agra-Kooijman, K. Ayub, R. P. Lemieux, S. Kumar, Phys. Rev. Lett. 2011, **106**, 087801.

² D. Nonnenmacher, S. Jagiella, Q. Song, R. P. Lemieux, F. Giesselmann, ChemPhysChem, 2013, **14**, 2990–2995.

³ J. P. F. Lagerwall, M. D. Radcliffe, F. Giesselmann, Phys. Rev. E. 2002, **66**, 031703.

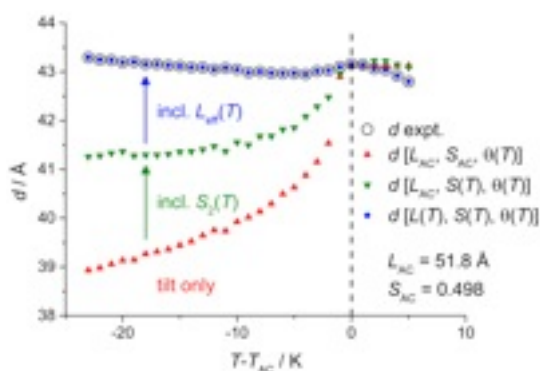


Fig. 2 Contributions of the increase in orientational order S_2 and in effective molecular length L_{eff} to the compensation of the tilt-induced layer contraction on cooling from SmA to SmC for TriSi-5PhP-C6.

Behaviour of complex polar structures in external field

P.V. Dolganov^{a*}, E.I. Kats^b, V.K. Dolganov^a

^a Institute of Solid State Physics RAS, 142432 Chernogolovka, Moscow Region, Russia

^b L.D. Landau Institute for Theoretical Physics RAS, 117940 GSP-1, Moscow, Russia

e-mail: pauldol@issp.ac.ru

In the last years essential progress was achieved in experimental and theoretical studies of polar liquid crystals. It was found that the realm of polar phases is sufficiently richer than presumed earlier. Apart from fundamental ferroelectric SmC^* and antiferroelectric SmC^*_A phases they include a number of subphases existing in a large number of materials in a relatively broad temperature range¹ (SmC^*_{d3} , SmC^*_{d4} , SmC^*_α) and microphases which at present have been observed in several (or even one) materials. Examples of these structures are phases with five-layer, six-layer, eight-layer and even ten-layer periodicity. Theory also has made a considerable step forward in the description of polar structures and their properties²⁻⁴. Moreover, some of the aforementioned phases were first predicted theoretically and then discovered experimentally. However, a number of questions remain open. The present report will focus on the behaviour of subphases in electric field and peculiarities of the phase transitions when frustrating interactions play a substantial role. Frustration is a phenomenon often occurring in condensed matter in particular in liquid crystals. Even when frustration itself does not induce new phases, its combination with electric field leads to unusual behaviour.

Frustration originating from long-range interlayer interactions² can critically change both the behaviour of the liquid crystal helical structure and transitions between different phases in electric field. It is well known that helical structure formed by chiral interaction transforms into a planar structure in electric field via helix unwinding. It takes place in cholesterics, ferroelectrics, antiferroelectrics, short-pitch SmC^*_α phase. If the helix is long with respect to interlayer spacing, unwinding occurs continuously. In short-pitch structures, unwinding occurs in a step-by-step manner⁵. Essentially differently happens the transformation into the planar structure when frustration is dominant in the formation of the helix. Such a situation may occur in the SmC^*_α phase. Calculations show⁶ that in electric field the simple helix is transformed into a structure with a sequence of left-hand and right-hand rotations. With field the amplitude of rotation

decreases and the transition into the planar structure occurs without unwinding.

Frustration also leads to anomalous transitions between different structures in electric field. Such a field-induced transition can occur both with structures existing without field and sufficiently new ones. An example of such behaviour is a transition from the antiferroelectric to the ferroelectric phase. It can occur via different ferroelectric structures which do not form without field. Another finding is that frustration can dramatically modify the behaviour of the first order antiferroelectric-paraelectric transition in electric field. Theory predicts that a single transition transforms into a staircase of intermediate states which are not observed in absence of the field. Polarization of the intermediate phases decreases with temperature in a stepwise manner.

The reported study was supported in part by RFBR, projects No. 12-02-33124, 13-02-00120 and 14-02-01130.

¹ We name commensurate smectic phases following the notation where the number in the index denotes the periodicity of the unit cell.

² M. Čepič, B. Žekš. Phys. Rev. Lett. 2001, **87**, 085501.

³ P.V. Dolganov, V.M. Zhilin, V.K. Dolganov, E.I. Kats. Phys. Rev. E. 2003, **67**, 041716.

⁴ A.V. Emelyanenko, M. Osipov. Phys. Rev. E. 2003, **68**, 051703.

⁵ B. Rovšek, M. Čepič, B. Žekš. Phys. Rev. E. 2004, **70**, 041706.

⁶ P.V. Dolganov, V.M. Zhilin. Phys. Rev. E. 2013, **87**, 062505.

Ferroelectric liquid crystalline nanocolloids: Effect of harvested nanoparticles on electro-optic and material parameters of FLC

R. K. Shukla¹ and W. Haase^{1*}

¹Eduard-Zintl-Institute of Inorganic and Physical Chemistry, Technical University Darmstadt, Petersenstr. 20, D-64287 Darmstadt, Germany.

*Corresponding author: E-mail: haase@chemie.tu-darmstadt.de

Collective ordered assemblies of nano metric objects dispersed in fluids are recognized as nanocolloids. In this context, anisotropic liquid crystals (LC) are a promising host media for such colloidal assemblies; they not only prompt anisotropic long-range interaction forces to accomplish oriented self-assembly, even also facilitates control of the inter-particle forces. Fast switching response, lower operational voltage, large optical contrast and orientational memory effect are the potential factors those distinguish the ferroelectric liquid mesogens from others. Nano materials with distinct physicochemical properties and shape anisotropy (spheres and rods) were employed for the fabrication of ferroelectric liquid crystal (FLC) nanocolloid.¹⁻³ In the recent past solid-state ferroelectric nanoparticles BaTiO₃ based nanocolloids were also reported.⁴⁻⁶ However, the persistence of the ferroelectricity at lower particle size in these publications remained the controversial issue. To deal with the ferroelectricity on the sub nanometre scale milling and harvesting processes have been investigated and recently reported.⁷ Very recently, harvested BaTiO₃ (9 nm, 12nm, 15nm, 26nm) dispersed FLCs (with different spontaneous polarizations) nanocolloids has been investigated. This report also highlighting the size dependence of harvested ferroelectric particles and strong modification in the switching response of the FLC.⁸

In the class of solid ferroelectrics, lithium niobate (LiNbO₃) could be the centre of interest for colloidal suspension due to its fascinating non linear optical properties.⁹ On the common properties platform one could expect the integration of solid-state ferroelectric LiNbO₃ and ferroelectric LC in a colloidal suspension may have enhanced properties. For the present study ferroelectric nanoparticles of LiNbO₃ (average size \approx 25 nm) capped with 1 wt. % oleic acid was used as the dopant material, while Phenylpyrimidines based ferroelectric liquid crystal mixture was employed

as a matrix for the nanocolloid preparation. In typical procedure, oleic acid capped LiNbO_3 nanoparticles were first dissolved in heptane followed by the sonication till the solution was visibly homogenous. Varying amount of homogenous solution containing 0.01, 0.05 and 0.10 wt% harvested nanoparticles were dispersed in FLC matrix to forms nanocolloids. The colloidal solution were filled in the planar cell of thickness $\approx 1.5 \mu\text{m}$ and studied at room and elevated temperature for electro-optic and dielectric behaviour. The details about the experimental setups and characterization techniques are given in the Ref. 3. About $\approx 40\%$ reduction in the switching time τ for nanocolloid with a higher concentration of harvested LiNbO_3 nanoparticles (0.10wt %) is observed as compared to the non doped FLC at 30°C as evident from the Fig. 1(a). Spontaneous polarization of nanocolloids also found to be decreased at the expense of increasing harvested LiNbO_3 nanoparticles concentration in the FLC matrix [Fig.1 (b)]

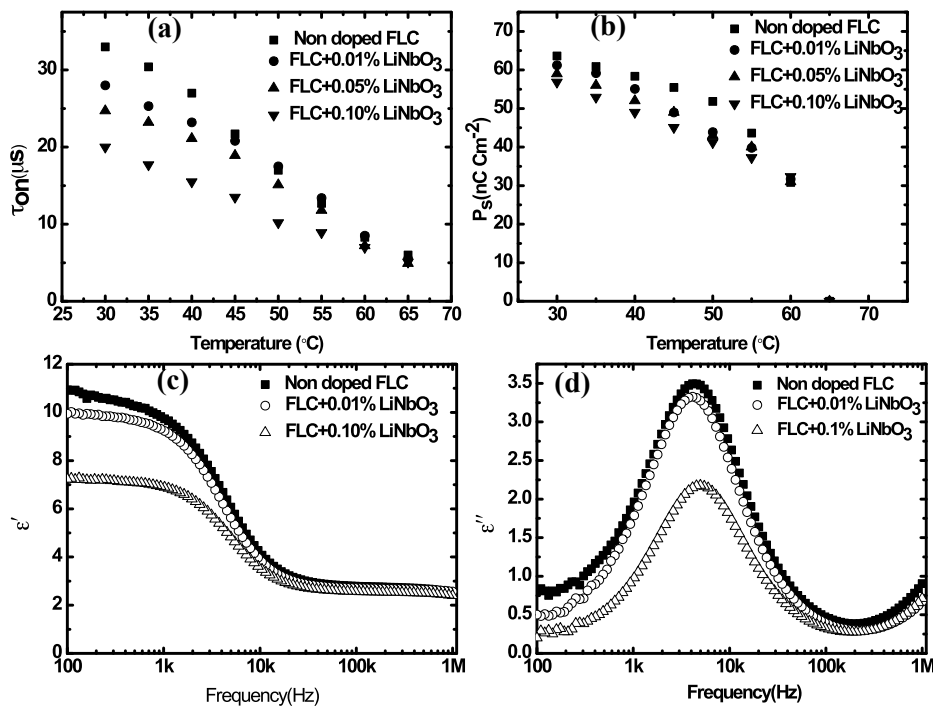


Fig.1. Temperature dependence of switching time τ_{on} (a) and spontaneous polarization P_s (b). Frequency dependent dielectric permittivity (c) and of absorption strength (d) of non doped FLC and nanocolloids.

Such behavior of τ could be explained considering ion capturing which forms a layer on the surface of particle and increase the l_{oc} compared to the l_{oc} of the non doped FLC, thus decreasing the switching time τ . While reduction in P_s is due the reason that harvested LiNbO_3 nanoparticles distort the polarization vector and follow the anti parallel correlation with FLC molecules. As far as dielectric parameters concern, addition of LiNbO_3 reduces the dielectric permittivity as well as the absorption strength of FLC. Dielectric parameters show the strong dependence on the concentration of the dopant particles. The observed behaviour

corresponds to the reduction of ionic impurities in nanocolloids resulted in the decrease of magnitude of ϵ' and ϵ'' under the influence of applied electric field. In a final remark, nanocolloid comprising 0.10 wt. % dopant may be the best candidate to date for applications in the nano electronic devices due to its faster switching response. Furthermore ferroelectric LiNbO₃ nanoparticles may be employed as a beneficial dopant in FLC for further studies of nonlinear optical response.

We acknowledge receiving the harvested nanoparticles from D.E. Evans and C. Liebig, Air force Lab.

- 1 T. Hegmann, H. Qi and V. M. Marx, *J. Inorg. Organomet. Polym. Mater.*, 2007, **17**, 483.
- 2 Y. A. Garbovskiy and A. V. Glushchenko, *Solid State Physics*, 2011, **62**,1.
- 3 F. V. Podgornov, A. V. Ryzhkova and W. Haase, *Appl. Phys. Lett.*, 2010, **97**, 212903.
- 4 Mikulko, P. Arora, A. V. Glushchenko, A. Lapanik and W. Haase, *Europhys. Lett.*, 2009, **87**, 27009-1.
- 5 H. H. Liang, Y. Z. Xiao, F. J. Hsh, C. C. Wu and J. Y. Lee, *Liq.Cryst.*, 2010, **37**, 255.
- 6 P. Ganguly, A. Kumar, S. Tripathi, D. Haranath, and A. M. Biradar, *Appl. Phys. Lett.*, 2013,**102**, 222902.
- 7 S. A. Basun, G. Cook, V. Y. Reshetnyak, A. V. Glushchenko, D. R. Evans, *Phys. Rev. B*, 2011, **84**, 024105.
- 8 A. Rudzki, D.R. Evans, G. Cook, and W. Haase *Appl. Opt.*, 2013, **52**, 22.
- 9 E. Ouksova, D. Lysenko, S. Ksondzyk, L. Cseh, G. H. Mehl, V.Y. Reshetnyak, Y. Reznikov, *Mol. Cryst. Liq. Cryst.* 2011, **545**, 1347

Microfluidic droplet production in a nematic matrix under AC electric fields

V. S. R. Jampani, K. Peddireddy, S. H. Tan, J. C. Baret, S. Herminghaus and Ch. Bahr

Max Planck Institute for Dynamics and Self-Organization, Göttingen, Germany.

e-mail: venkata.jampani@ds.mpg.de

We demonstrate the control on size and frequency of the generation of water droplets in the continuous phase of a nematic liquid crystal (LC) using a flow focusing microfluidic chip under AC electric fields¹. Usual soft lithography techniques were used to create a flow focusing junction of a lateral width of 100 μm and a height of 40 μm in PDMS. For the application of an external AC field, we have used electrodes which are patterned at a distance of 35 μm from the flow channels using a microsolidics technique. We found that we could tune the droplet size significantly in a range from 120 μm to 20 μm by varying parameters such as frequency and voltage of the applied field and the volumetric flow ratio. The reason for the tunability with the electric field might be due to the re-orientation of the LC director at the aqueous/LC interface. Furthermore, the droplet generation frequency shows a non monotonic dependence on the applied field. Typical curves of the droplet production frequency as a function of the applied AC frequency at different volumetric flow ratios are shown in Figure 1. Our goal is to use these monodisperse aqueous droplets for the study of LC topological defects, elastic-distortion-mediated 2D and 3D aqueous droplet chains^{2,3} and 3D colloidal packings in liquid crystals⁴.

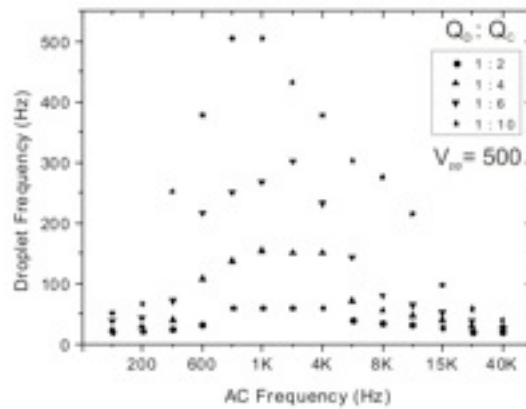


Fig 1. Droplet production frequency curves as function of the applied AC frequency at a fixed peak to peak voltage for different volumetric flow ratios of dispersed phase (Q_D , water) and continuous phase (Q_C , LC).

¹ S. H. Tan, B. Semin and J.-C. Baret, Lab Chip 2013, in press.

² P. Poulin, H. Stark, T.C. Lubensky and D. A. Weitz, Science 1997, **275**, 1770.

³ I. Musevic, M. Skarabot, U. Tkalec, M. Ravnik and S. Zumer, Science 2006, **313**, 954.

⁴ A. Nych, U. Ognysta, M. Skarabot, M. Ravnik, S. Zumer and I. Musevic, Nature Commun. 2013, **4**,1489.

Observation of Polarization in the Leaning Plane of a Bent-Core Molecular Compound

N. Chattham^{a,b}, M.-G. Tamba^a, H. Takezoe^{a,c}, R. Stannarius^a, E. Westphal^d,
C. Tschierske^d, A. Eremin ^{a,*}

^a Otto-von-Guericke-Universität Magdeburg, IEP/ANP, D-39106 Magdeburg, Germany

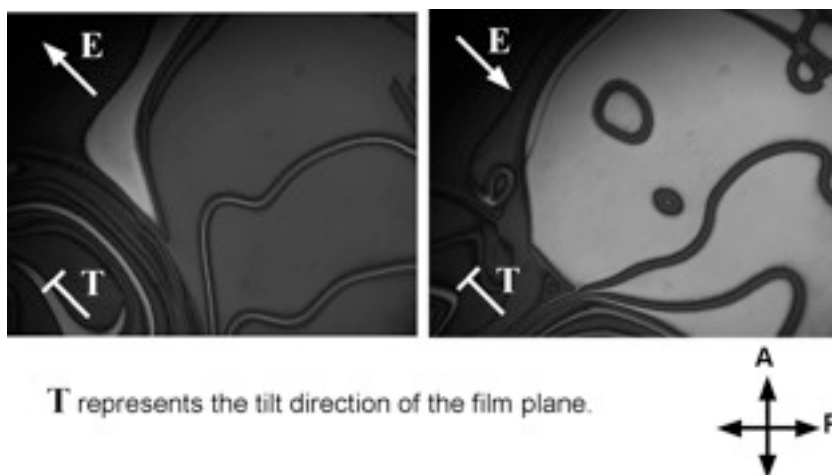
^b Department of Physics, Faculty of Science, Kasetsart University, Bangkok, 10900 Thailand

^c Department of Organic and Polymeric Materials, Tokyo Institute of Technology, Tokyo, 152-8552, Japan

^d Institute of Chemistry, Martin-Luther-University Halle-Wittenberg, D-06120 Halle, Germany

e-mail: alexey.eremin@ovgu.de

Bent-core molecules have been of interest to liquid crystal scientists for over decades. Designing molecules and identifying their phase structures provides much knowledge to understanding the complexity of molecular organization of these phase structures. In the conventional polar SmCP (B2) phase of bent-core mesogens, a tilt of molecules with respect to the layer normal occurs by the rotation about the bend direction, so that the spontaneous polarization is perpendicular to the tilt plane. In contrast, molecules lean within their bend plane in the SmC-leaning phase, where the polarization is in the leaning plane and deviates from the layer plane. Here we report a clear evidence of this structure, i.e., the polarization lying in the leaning plane. We show direct observations of the tilt in thick freely suspended films at inclined incidence under an in-plane electric field. Two photomicrographs in the figure below were taken under the application of two opposing electric fields, where the film is slightly tilted along the field direction.



T represents the tilt direction of the film plane.

A thick freely suspended film appearing dark and bright for opposite direction of electric field applied along the tilt direction of the film plane.

The photographs give different brightness (birefringence) indicating leaning angle increase or decrease, depending on the field direction. By tilting the film perpendicular to the electric field, no change in film brightness is observed. This observation reveals that the polarization direction is restricted to lie in the molecular (polarization) leaning plane. The induced polarization was also confirmed by second-harmonic generation (SHG) activity.

Yes, but what is the question?*

By

Pawel Pieranski
Laboratoire de Physique des Solides
Université Paris-Sud, Bât. 510
91405 Orsay, France

An unexpected phenomenon occurring in everyday life or in an experiment is like the answer “Yes” given by the Nature to a question, which remains to be found. Many of us have had one day the good luck to get this answer and to look subsequently for its meaning. We all know that, in particular, the discovery of liquid crystals was triggered by such a lucky event.



Photo: courtesy of Piotr Pieranski

In my talk I will quote and discuss other examples of serendipitous discoveries stemming from unexpected phenomena. Some of them are very striking and also easy to reproduce in “dreigroschen” experiments; I will not resist to the pleasure of showing them to You.

*Bernard Pivot, “Oui, mais quelle est la question?”, Editions Nil, 2012

Polymer stabilized short pitch chiral nematic liquid crystals: Electro-optics with interdigitated electrodes.

A. Lorenz^{a*}, D. J. Gardiner^b, S. M. Morris^{b,c}, T. D. Wilkinson^b

^a Berlin Institute of Technology, Dept. of Chemistry, Str. des 17. Juni 124, Berlin, Germany

^b Centre of Molecular Materials for Photonics and Electronics, Department of Engineering, University of Cambridge, 9 JJ Thomson Avenue, CB3 0FA, United Kingdom.

^c Department of Engineering Science, University of Oxford, Parks Road, Oxford, OX1 3PJ, United Kingdom

*e-mail: alexander.lorenz@online.ms

The electro-optic response of short-pitch polymer-stabilized chiral nematic liquid crystals was studied with interdigitated electrodes¹. The electro-optic response curves [Figure 1 (a)] were recorded and fitted with a model where both flexoelectric² and dielectric coupling could be considered in order to study their relative contributions.

Polymer stabilization was found to effectively suppress unwanted textural transitions of the chiral nematic LC especially near the electrodes. A device with a polymer content of 9% showed near ideal hysteresis [Figure 1 (b)] and fast response times < 300 μ s.

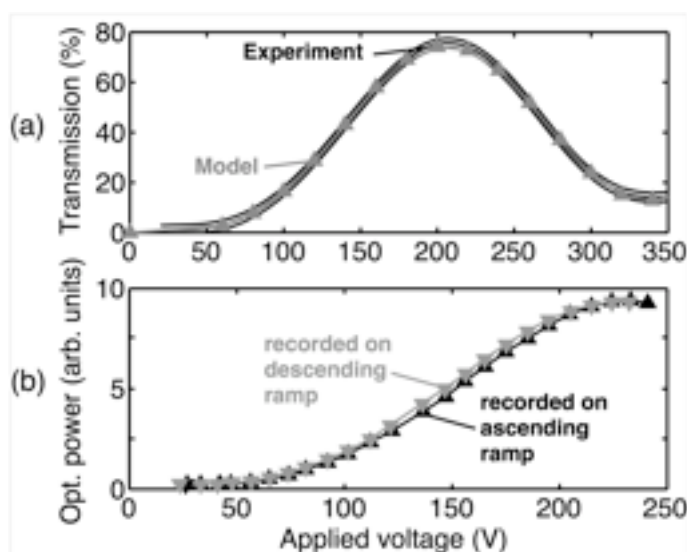


FIGURE 1: Transmission data recorded with monochromatic light on ascending voltage ramps (black double line); double line indicates 2s-experimental error obtained on analyzing several experimental runs. Additionally, modeled data is

shown. (b) Optical power vs. applied voltage recorded on ascending and subsequently descending voltage ramp.

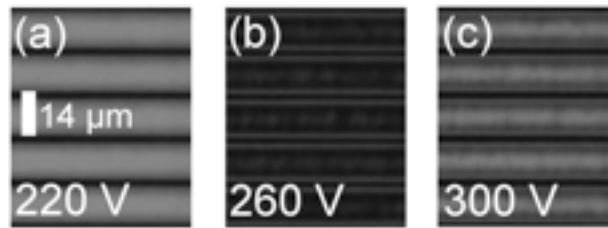


FIGURE 2: Microscopic images recorded with monochromatic light (589 nm) showing the same region of a polymer stabilized test cell at 220 V (a), 260 V (b), and 300 V (c).

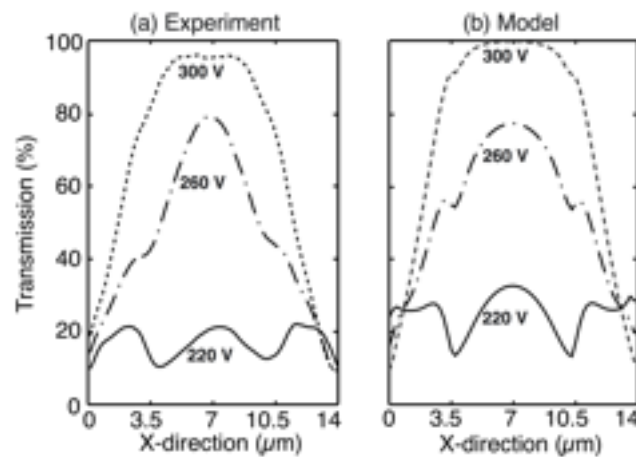


FIGURE 3: Estimated transmission profile of a polymer stabilized test cell and measured transmission profiles of such a test cell recorded with a 60x objective lens (experiment).

Polymer stabilized test cell were investigated with polarized optical microscopy. At various applied voltages, microscopic images (Figure 2) of the transmitted monochromatic light (589 nm wavelength) were recorded with a CCD camera. The imaging system was carefully calibrated and transmission profiles were extracted from the recorded image files [Figure 3 (a)]. Simulations of the inhomogeneous addressing electric fields were carried out and used to estimate the transmission [Figure 3(b)] in a theoretical approach based on Jones calculus, which was very useful to explain the experimental data.

In summary, it was found that the electro-optic response was mainly caused by the flexoelectro-optic effect at low voltages and by the Kerr effect at high voltages. The presented approach could also be very useful to investigate other fast electro-optic effects in LCs, such as the electro-optic response of polymer-stabilized blue phase LCs^{3,4}.

- ¹ A. Lorenz, D. J. Gardiner, S. M. Morris, F. Castles, M. M. Qasim, S. S. Choi, W. -S. Kim, H. J. Coles, T. D. Wilkinson, Appl. Phys. Lett. (submitted).
- ² F. Castles, S. M. Morris, and H. J. Coles, Phys. Rev. E. **80**, 1709 (2009).
- ³ H. Kikuchi, M. Yokota, Y. Hisakado, H. Yang, T. Kajiyama, Nature materials **1**, 64 (2002).
- ⁴ G. Nordendorf, A. Lorenz, A. Hoischen, J. Schmidtke, H. Kitzerow, D. Wilkes, M. Wittek, J. Appl. Phys. **114**, 173104 (2013).

Thermotropic Liquid Crystal Elastomer Micro-Actuators with Integrated Heating

Richard Rix^a, Sebastian Petsch^b, Bilal Khatri^b, Stefan Schuhlade^b, Hans Zappe^b and Rudolf Zentel^a

^a Institut of Organic Chemistry, University of Mainz, Germany

^b Gisela and Erwin Sick Chair of Micro-Optics, Department of Microsystems Engineering – IMTEK, University of Freiburg, Germany

Corresponding author: Richard Rix; rixr@uni-mainz.de

We present a thermal micro-actuator based on a liquid crystal elastomer (LCE) with an integrated, MEMS (micro-electro-mechanical systems) fabricated, deformable heater,. At the phase transition from the nematic to the isotropic phase at approximately 120°C the LCE shows a contraction of 28%. This concept uses for the first time MEMS fabricated deformable heaters embedded into LCEs for compact heaters. Figure 1a and b there shows a schematic cross-cut and a photograph of the complete actuator with the integrated heater.

LCEs are polymers which combine the mechanical properties of elastomers and the self-organization properties of liquid crystals.^[1] The mesogens are linked covalently to a crosslinked polymer network. Below the phase transition temperature to the isotropic phase the mesogens are in the nematic phase. The polymers to which they are bound to are in an elongated conformation. Above the phase transition temperature the mesogens are no longer aligned and the polymer chains contract into a random coiled state. The reversible mechanical actuation results from the back and forth transition between these two phases and is shown in Figure 1c.

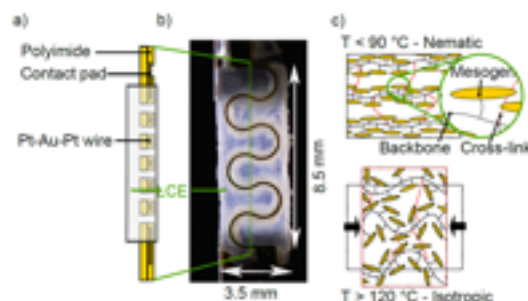


Figure 1: Illustration of the thermotropic actuator with integrated deformable wires. (a) Cross-sectional view of the system: deformable heaters with robust polyimide cladding are buried in the LCE. (b) Photograph of the completed

actuator. (c) Illustration of the liquid crystal elastomer actuation mechanism. At low temperatures the polymer chains are in the oriented state, imprinted by cross-linking. At the phase transition the mesogens lose their order and the polymer chains coil, leading to a macroscopic shape change.^[1]

The deformable micro-heater is built up from a robust polyimide cladding and metallic lines which results in a deformable wiring technology.^[3] The micro-heaters are wafer-level fabricated which offers high reproducibility, conductivity and reliability of the structures. On a spin-coated polyimide layer the metal lines (platinum/gold/platinum) are structured by evaporation (PVD, physical vapour deposition) and lift-off. A second layer of polyimide on top buries the metal structures. Finally the polyimide cladding is structured with reactive ion etching (RIE). The resulting micro-heater is shown in Figure 2.

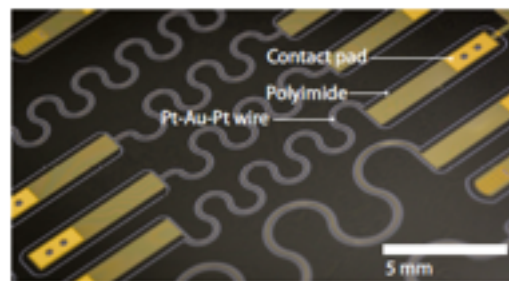


Figure 2: Photograph of the deformable thin film heaters embedded in polyimide on the handle wafer. ^[2]

Subsequently the completed micro-heater is embedded into the LCE. Therefore the microheater is placed in a PDMS mold which is heated to 95°C (Fig. 3a). At this temperature the liquid crystalline precursor is in the isotropic state. The precursor consists of the side on monomer (4'acryloyloxybutyl 2,5(4'butyloxybezoyloxy)benzoate,^[4] 10 mol% cross-linker and 1 mol% initiator. Slowly cooling the mold down under application of a magnetic field results in mesogens oriented parallel to the magnetic field (Fig. 3b). At a temperature of 60°C the liquid crystalline phase is polymerized to a cross-linked LCE (Fig. 3c). The demolded actuator contracts when heated over the phase transition temperature in the direction of the former magnetic field respectively the director (Fig. 3d). Compared to the previously published work of Spillmann et.al.^[5] this process is highly reproducible and reliable.

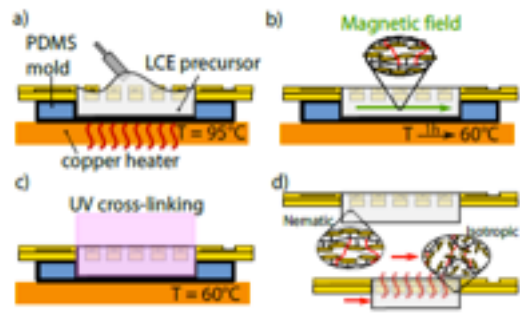


Figure 3: Schematic view of the fabrication of LCE actuators with buried heaters. (a) Pouring the LCE precursor in a preheated PDMS mold (95°C). (b) Let the mold slowly cool down to 60°C in presence of a magnetic field for orientation of liquid crystalline monomer. (c) Photopolymerization with UV light at 365 nm. (d) Heating the LCE above the phase transition temperature, results in a contraction along the orientation axis. [2]

The contraction of the actuator ((L x W x T) of 8.5 x 3.5x 0.5 mm³) and the passive relaxation for an applied electrical power of 320 mW and a load of approximately 2 g is shown in Figure 4. There are imaged different times in the heating and cooling cycle. From room temperature to its completely contracted state it takes 19.7 s. Relaxation is much faster as it takes only 5.6 s. Because of the low stiffness of the heating structure there is no measurable effect on the actuator efficiency. The measured contraction is 1.15 mm or 28%. The corresponding energy density was calculated with a value of 1.52 J/mm³.

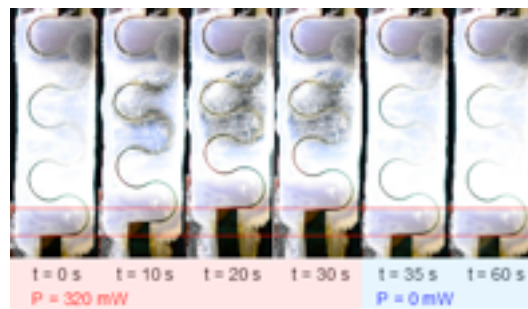


Figure 4: Photographs of the LCE micro-actor at different times of the contraction and relaxation cycle for 320 mW. Transparent regions in the LCE material indicate the phase transition to the isotropic phase. The deformation of the integrated heater is clearly visible. [2]

A novel thermotropic actuator with high work density and a large displacement has been presented. The MEMS fabricated deformable heater in combination with the LCE as an active material yield in a compact actuator and fast responding. The flexible conductors can be varied in design to fit into specific actuator designs and also could implement sensing elements for smart actuators.

References

- ¹ P. G. de Gennes, J. Prost, *The Physics of Liquid Crystals*, 2nd ed., ser. International Series of Monographs on Physics (83). Oxford: Clarendon Press, 1993.
- ² S. Petsch, R. Rix, P. Reith, B. Khatri, S. Schuhladden, D. Ruh, R. Zentel, H. Zappe, A Thermotropic Liquid Crystal Elastomer Micro-Actuator With Integrated Deformable Micro-Heater. *Micro Electro Mechanical Systems (MEMS)*, 2014 IEEE 27th International Conference on Jan. 26 2014 – Jan. 30 2014, San Francisco, CA, USA (in press).
- ³ R. Verplancke, F. Bossuyt, D. Cuypers, J. Vanfletern, *Journal of Micromechanics and Microengineering*, 2012, 22(1), p. 015002.
- ⁴ D. L. Thomsen, P. Keller, J. Naciri, R. Pink, H. Jeon, D. Shenoy, B. R. Ratna, *Macromolecules*, vol. 34(17), pp. 5868–5875, Aug. 2001.
- ⁵ C. M. Spillmann, J. Naciri, B. D. Martin, W. Farahat, H. Herr, B. R. Ratna, *Sensors and Actuators A: Physical*, 2007, 133(2), pp. 500–505.

~~Liquid Crystalline polymers networks as molecular imprinting materials~~

~~S. Bedjaoui^{a, b, c}, L. A. Bedjaoui^a, [N. Bouchiki^a](#), [U. Maschke^b](#)~~

~~^aLaboratoire de Recherche sur les Macromolécules, Faculté des Sciences de l'Université de Tlemcen, BP119, 13000 Tlemcen, Algeria~~

~~^bUnité Matériaux et Transformations (UMET), UMR CNRS 8207, Université Lille 1 – Sciences et Technologies, 59655 Villeneuve d'Ascq Cedex, France~~

~~^cDépartement des Sciences, Faculté des Sciences et Technologie, Université de Bechar, Algeria~~

~~E-mail: sofianeg1@yahoo.fr, ulrich.maschke@univ-lille1.fr~~

CANCELLED

the speaker did not show up

Preferential solubility effects of a commercial nematic LC blend towards Poly(methylphenylsiloxane)

F. Semdani^a, A. Bouriche^a, Y. Derouiche^{b,c}, T. Bouchaour^a, L. Bedjaoui^a, and U. Maschke^b

^aLaboratoire de Recherche sur les Macromolécules, Faculté des Sciences de l'Université de Tlemcen, BP119, 13000 Tlemcen, Algeria

^bUnité Matériaux et Transformations (UMET), UMR CNRS 8207, Université Lille 1 – Sciences et Technologies, 59655 Villeneuve d'Ascq Cedex, France

^c Laboratoire des dispositifs des micro-ondes et matériaux pour les énergies renouvelables, Faculté des Sciences et Technologies, Université Ziane Achour, 17000 Djelfa, Algeria.

e-mail: ulrich.maschke@univ-lille1.fr

Blends of the nematic liquid crystal (LC) E7 and linear polymethylphenylsiloxane (PMPS) with different molecular weights $M_w = 9600, 50000$ and 70900 g/mol were investigated by polarized optical microscopy (POM) and differential scanning calorimetry (DSC) techniques. This study was prompted by observations made recently by analyzing the phase diagrams of linear poly(siloxanes)/E7 [1]. It has revealed a remarkable increase of the nematic to isotropic transition temperature T_{NI} when polymer was added to the LC.

This behavior was attributed to the multicomponent nature of the LC which is made of four cyano substituted polyphenylenes. Indeed, different miscibilities of the LC components towards PMPS lead to changes of the LC composition in the droplets which in turn yield a different nematic-isotropic transition temperature.

The immediate consequence of these compositional changes was a shift in the nematic-isotropic transition temperature which increases with decreasing polymer concentration. This effect can be explained by the growing percentage of the higher molecular weight LCs in the droplets, compared to the other LC. Even a small compositional change of E7 involving 4-cyano-4''-n-pentyl-p-terphenyl leads to a pronounced effect on T_{NI} which can be easily detected experimentally by POM and DSC measurements.

The results obtained by POM and DSC were analysed using a combination of the Flory-Huggins [2] theory of isotropic mixing and the Maier-Saupe

[3] theory of nematic order. Changes in shape, distribution and size of nematic inclusions dispersed in the PMPS were highlighted by POM as a function of molecular weight, composition and temperature.

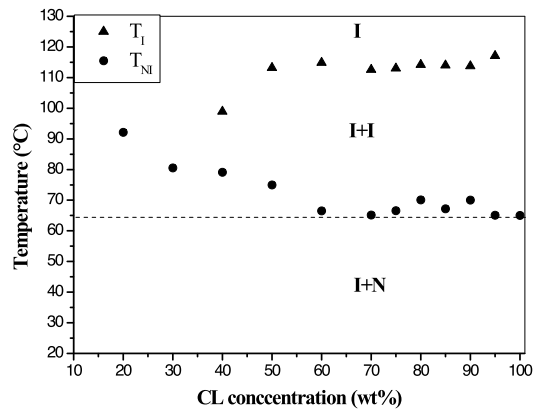


FIGURE. Experimental phase diagram of the PMPS70900/E7 system obtained by POM. The dashed line corresponds to the nematic–isotropic transition temperature of the pure LC E7. I stands for Isotropic, and N for nematic phases.

¹ M L. Bedjaoui–Alachaher, H. Bensaid, C. Gordin, U. Maschke, *Liquid Crystals* 2011, **38**, 1315.

² J.P. Flory, *Principles of Polymer Chemistry*. Ithaca: Cornell University Press 1965.

³ W. Maier, A. Saupe, *Z. Naturforschung* 1960, **15a**, 287.

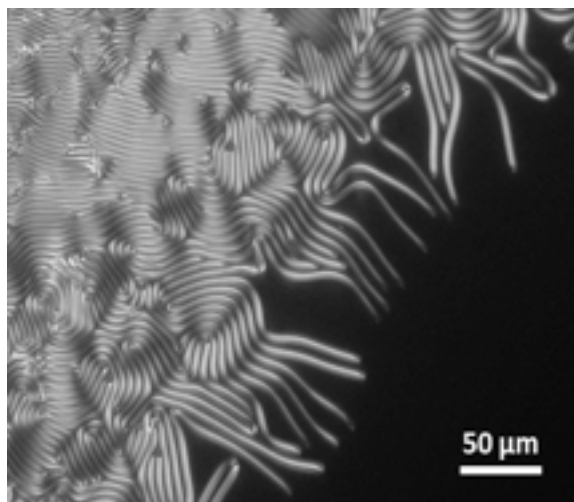
Solvent induced twist grain boundary phase in a lyotropic liquid crystal

Johanna R. Bruckner^a, Jan H. Porada^a, Frank Giesselmann^{a*}

^a Institute of Physical Chemistry, University of Stuttgart, Pfaffenwaldring 55, 70569 Stuttgart, Germany.

e-mail: f.giesselmann@ipc.uni-stuttgart.de

Only months after the theoretical prediction of the twist grain boundary phase (TGB) by Renn and Lubensky,¹ the TGBA* phase was experimentally observed by Goodby et. al in 1989.² Since then, new liquid crystalline materials that show this phase were found continuously. But so far, all of these compounds are thermotropic in nature, even though a lyotropic L_{12} -TGB phase was already described theoretically in 1997.³ In this work we now report the first observation of a solvent induced TGBA* analog phase.



Recently, we investigated a hybrid molecule that consists of a thermotropic phenylpyrimidine core and a lyotropic diol headgroup (Fig. 1) and showed that solutions of this surfactant in water or formamide, are able to form a lyotropic smectic C* analog phase.⁴ We now expanded the number of used solvents to N-methylformamide. The phase diagrams of this solvent / surfactant system were measured in heating and cooling. In the neat state the surfactant exhibits a monotropic cholesteric phase only. Apart from enantiotropic cholesteric and

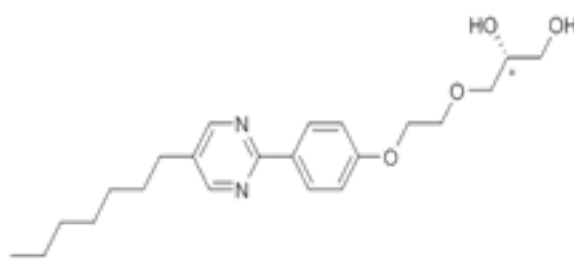


Fig. 1: Characteristic filament texture between crossed polarizers at the phase transition from the lamellar L_a phase to the solvent induced TGB phase (top) and chemical structure of the used surfactant (bottom).

lamellar L_{12} phases (smectic A* analog), the addition of N-methylformamide leads to the formation of several monotropic phases at low solvent concentrations, such as two columnar phases, a re-entrant

cholesteric phase and a lyotropic TGB phase. The existence of the latter two phases was not only proofed by texture observations (Fig. 1), but also by discontinuities in the pitch values and two-dimensional X-ray measurements of oriented samples. Even though the TGB phase occurs at very low solvent concentrations, it is still remarkable that this phase only exist in the presence of a solvent.

In conclusion, we showed that twist grain boundary phases can be induced by the addition of solvent in a lyotropic state. These results thus contribute to an enhanced and unified understanding of the often completely separately treated fields of lyotropic and thermotropic liquid crystals.

Financial support by the Deutsche Forschungsgemeinschaft (DFG Gi 243/4-3) and the Landesgraduiertenförderung Baden-Württemberg is gratefully acknowledged.

¹ S. R. Renn, T. C. Lubensky. *Phys. Rev. A.* 1988, **38(4)**, 2132.

² J. W. Goody, M. A. Waugh, S M. Stein, E. Chin, R. Pindak, J. S. Patel. *Nature.* 1989, **337**, 449.

³ R. D. Kamien, T. C. Lubensky. *J. Phys. II.* 1997, **1**, 157.

⁴ J. R. Bruckner, J. H. Porada, C. F. Dietrich, I. Dierking, F. Giesselmann. *Ange. Chem. Int. Ed.*. 2013, **52**, 8934.

Novel ionic liquid crystals designed from amino acids

M. M. Neidhardt^a and S. Laschat^a

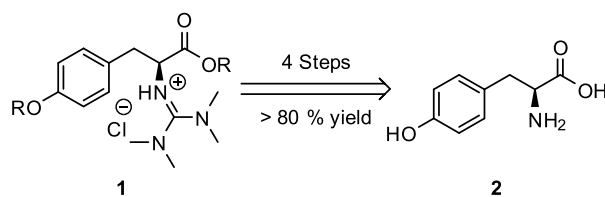
^a Institut für Organische Chemie, Universität Stuttgart, Stuttgart, Germany.

E-mail: manuel.neidhardt@oc.uni-stuttgart.de

The synthesis of ionic liquid crystals (ILCs), which are compounds combining both physical and chemical characteristics of liquid crystals (LCs) with ionic liquids (ILs) is of ever-increasing research interest in recent years. Such properties include the anisotropic physical properties of LCs, e.g. birefringence and orientational order, with the fluidity, low vapour pressure and ionic conductivity found in ILs. For this reason, they have potential to be used in a large range of applications.¹

Chiral ILCs are a further development to non-chiral ILCs and have been shown interest due to their promising application possibilities for chiral discrimination in NMR, stereoselective polymerisation, transport membranes for CO₂, chiral chromatography and asymmetric synthesis.² Due to the high cost of the starting materials and difficulties during the scale-up process in many synthetic processes, our aim is to use cheap building-blocks in combination with an effective synthetic route which leads to reduced-cost chiral ILCs. Amino acids from the chiral pool are ideal precursors for this purpose due to their good availability and their low expense.³

Based on this structural background and previous work in our group we were able to develop a new synthetic strategy, which uses naturally-occurring amino acids with a chiral stereocentre already incorporated, leading to chiral ILCs.



Scheme 1: Retrosynthesis of the chiral ILC 1 based on amino acid (L)-tyrosine 2.

The mesomorphic properties of the thus synthesised ILCs were studied by DSC, POM and XRay diffraction. Further investigations relating to the chirality of the ILCs were also carried out within this work.

¹ a) K. V. Axenov, S. Laschat. *Materials*. 2011, 4, 206. b) T. Kato, N. Mizoshita. *Angew. Chem. Int. Ed.* 2006, 45, 38. c) K. Binnemans. *Chem. Rev.* 2005, 105, 4148.

² a) P. Borowiecki, M. Milner-Krawczyk. *Eur. J. Org. Chem.* 2013, 712. b) S. Kasahara, E. Kamio. *Chem. Commun.* 2012, 48, 6903. c) M. Li, D. Bwambok, S. Fakayode in *Chiral Ionic Liquids in Chromatographic Separation and Spectroscopic Discrimination* (Ed. A. Berthod), Springer, Berlin, 2010, 289. d) S.-P. Luo, D.-Q. Xu. *Tetrahedron: Asymmetry*. 2006, 17, 2028. e) C. Baudequin, D. Brogeon. *Tetrahedron: Asymmetry* 2005, 16, 3921. f) D. Tsiourvas, C. M. Paleos. *Chem. Eur. J.* 2003, 9, 5250. g) P. Wasserscheid, A. Bosmann, C. Bolm. *Chem. Commun.* 2002, 200.

³ M.Mansueto, W. Frey, S. Laschat. *Chem. Eur. J.* 2013, 19, 16058.

Coalescence of Islands in Smectic Membranes

K. Harth^{a*}, Z. Nguyen^b, A. Goldfain^b, J. E. Maclennan^b, C. Park^b, M. Glaser^b,
N. Clark^b

^aInstitute of Experimental Physics, Otto-von-Guericke-University Magdeburg

^bLiquid Crystals Materials Research Center, University of Colorado, Boulder, USA

e-mail: Kirsten.Harth@ovgu.de

The coalescence dynamics of droplets of fluid and its reverse, the pinch-off, are interesting both from a theoretical and an experimental point of view: Mathematically, these events are connected to a change of topology, and a scaling and divergence of scales. The dynamics are important, e.g. in sintering or cloud formation. Experiments in three dimensions received a boost over the last decade. Interestingly, a breakdown of universal dynamics was found depending on fluid viscosities [1].

The problem of the coalescence of two infinitely long, viscous cylinders of identical diameter (which is the analogue of only two islands of identical diameter in an ideal 2D fluid) without surrounding fluid was solved analytically by Hopper [2]. The coalescence process is described in terms of a parameter $m \in [0,1]$. The shapes adopted throughout the process are inverse ellipses (see Figure 1), and the temporal evolution is obtained from an elliptic integral. The usual focus is the evolution of the bridge width of the coalesced region (at $y=0$). At short times, the scaling of the width of the bridge connecting the fluid domains is expected to be linear with a logarithmic correction.

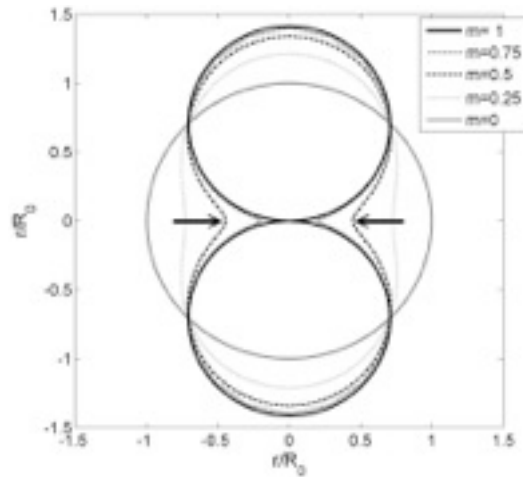


Figure 1: Inverse ellipses as shapes of the coalescing islands for different values of the parameter m . The bridge width w is measured at $y=0$.

In two dimensions, hydrodynamic behavior is altered such that the surrounding medium and the fluid domain size may play a dominant role. Free-standing smectic films represent an ideal model system to investigate rheology in two dimensions: Large stable fluid films of well-defined thickness are readily prepared. Basic predictions about thin film rheology were confirmed only recently [3]. Previous experiments used nematic domains on a Langmuir trough [4], so that the main dissipation is through the underlying fluid and not the membrane itself. Alternatively, the coalescence of an water droplet with the fluid surface was observed in the small gap between two glass plates [5], where the boundary conditions are significantly altered respective to Hopper's assumptions.

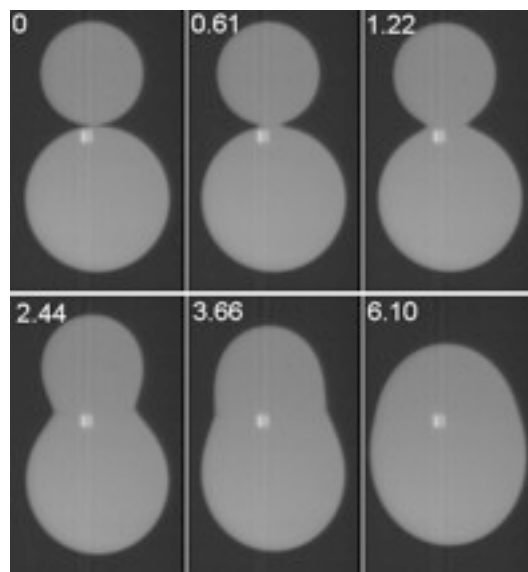


Figure 2: Snapshots during the coalescence of two equally thick islands (25 layers ≈ 78.5 nm) in a 8CB film of 5 layers (≈ 16 nm) thickness. Numbers give the time after initiation in ms. The initial diameters are ≈ 130 μm and ≈ 160 μm , respectively.

We prepare islands (regions with additional layers) in free-standing smectic films, and investigate their coalescence dynamics using high-speed video imaging. Some exemplary snapshots are shown in Figure 2. Different ratios of effective two-dimensional viscosities and densities are realized by varying the thickness of the islands and the background film. Surprisingly, our measurements of the bridge width in the early times do not agree with the theoretical predictions by Hopper [2] for the coalescence of two infinitely long viscous cylinders, see Figure 3. At late times, the merged island shows an unprecedented exponential shape relaxation, with dissipation occurring mainly through the membrane.

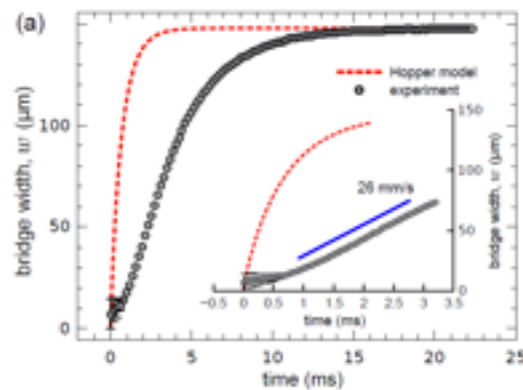


Figure 3: Measured bridge width w over time for the coalescence of a pair of equally thick islands of identical initial radii in comparison to the predictions of Hopper's model (dashed line). Initially, a linear increase of w is observed.

The deviations can have several reasons, where the main contributions are expected to occur due to a) the surrounding air, b) dissipation in the background film, which is not considered in the model, or c) reorganization of dislocations in smectic layer structure. The delay at very early times is attributed to the latter. Still assuming no background film viscosity, a simple analytical approach is given to explain the influence of the surrounding air. In a numerical calculation considering both islands and background film, we solve the full Navier–Stokes equations in 2D using a finite elements method on a moving mesh [6]. The analytical result is compared to and extended by these calculations. We conclude that the coalescence dynamics is dominated by the interplay between film and air flow, in both islands and surrounding film. Hydrodynamically, the process is at the crossover between 2D and 3D flow characteristics.

- ¹P. Doshi, et al., *Science* 2003, **302**, 1185; X. D. Shi, et al., *Science* 1994, **265**, 219.
- ²R. W. Hopper, *J. Am. Ceram. Soc.* 1993, **76**, 2947.
- ³Z. Nguyen et al., *Phys. Rev. Lett.* 2010, **105**, 268304; A. Eremin, et al., *Phys. Rev. Lett.* 2011, **107**, 268301.
- ⁴U. Delabre and A.-M. Cazabat, *Phys. Rev. Lett.* 2010, **104**, 227801.
- ⁵M. Yokota and K. Okumura, *PNAS* 2011, **108**, 6395.
- ⁶S. Ganesan and L. Tobiska, *Int. J. Numer. Methods Fluids* 2008, **57**, 119–38; S. Hysing, et al., *Int. J. Numer. Methods Fluids* 2009, **60**, 1259–88.

With an open attitude new doors open

Reflections on interdisciplinarity, knowledge sharing and the future of liquid crystal research and applications in Europe and in South Korea

Jan Lagerwall

University of Luxembourg, Physics & Materials Science Research Unit,
162 A, Avenue de la Faïencerie
L-1511 Luxembourg

e-mail: jan.lagerwall@lcsoftmatter.com

„Man hat mir wohl die Frage gestellt, ob sich kristallin-flüssige Substanzen technisch verwenden lassen? Ich sehe keine Möglichkeit dazu.“ This statement, now perhaps as famous in the liquid crystal community as it was wrong when Daniel Vorländer expressed it in 1924, is a brilliant reminder of how difficult it is to predict the application potential of scientific research results. Considering the immense success of liquid crystals in displays (LCDs), with the Korean electronics giants Samsung and LG today mass producing liquid crystal-based TV sets with jaw-dropping sizes and a situation where we have more LCDs than people on the planet, it seems almost inconceivable how Vorländer could have been so pessimistic. Yet, sadly, a sentiment that is not too different (replace “technisch verwenden lassen” with “außerhalb LCDs technisch verwenden lassen”) has been clearly present over the last several years in the liquid crystal community, as well as outside it among scientists and decision makers with influence over science. Many are those who have left the field or who avoided entering it because of self-named gurus claiming that “liquid crystal research has no future”.

I am deeply convinced that this attitude is as wrong today as Vorländer’s prediction was in 1924 and in my talk I will argue that one of the reasons for its prevalence is a tendency of isolation of the liquid crystal community (imposed by others as well as—to some extent—self-inflicted), in combination with an unfortunate widespread misconception that liquid crystals and displays are more or less synonymous. Very importantly, we must remember that applications are not necessary to motivate research. Liquid crystals constitute an incredibly rich class of materials with immense opportunities for stimulating scientific studies as well as numerous applications, also in areas totally different from displays or other electrooptic devices¹. But to expose these opportunities we need to

adopt an open attitude, both in terms of interest in other research areas and in sharing the understanding of liquid crystals and their potential.

I will use four examples from the research of my collaborators and myself (microfluidics-produced nematic elastomer shells for micropumps or cargo delivery vehicles²; the relevance of the balance between liquid crystalline ordering and gelation/glass formation for understanding structure formation in suspensions of cellulose nanocrystals³; wearable technology based on liquid crystal-functionalized polymer fibers⁴; controlled drug delivery exploiting the anisotropic diffusion properties of nematics) to highlight how an understanding of liquid crystals can provide new solutions to problems in diverse areas, with new application potential, as well as reinforce research and development pursued by scientists who currently have weak connection with the liquid crystal community, for instance in colloid science and chemical engineering communities.

¹ J.P.F. Lagerwall, and G. Scalia, *Curr. Appl. Phys.* 2012, **12**, 1387

² E.-K. Fleischmann, H.-L. Liang, N. Kapernaum, F. Giesselmann, J.P.F. Lagerwall, and R. Zentel, *Nat. Commun.* 2012, **3**, ARTN: 1178

³ J.P.F. Lagerwall, C. Schütz, M. Salajkova, J. Noh, J.H. Park, G. Scalia, and L. Bergström. *NPG Asia Mater.* 2014, **6**, e80.

⁴ D.K. Kim, M. Hwang, and J.P.F. Lagerwall. *J. Polym. Sci. B Polym. Phys.* 2013, **51**, 855

Group velocity dispersion in liquid crystal–filled photonic crystal fibers

M. Wahle and H.–S. Kitzerow,

Department of Chemistry, University of Paderborn, Warburger Str. 100, 33100
Paderborn, Germany

e–mail: markus.wahle@upb.de

Introduction

Photonic crystal fibers (PCFs) are a relatively new type of optical fibers in which light is confined by a micro–structured cladding¹ while the guiding in standard optical fibers (SIFs) is based on a refractive index difference between core and cladding. One kind of this type of fibers are solid core PCFs (Fig. 1) which are made of periodically arranged air inclusions embedded in a silica surrounding. These fibers exhibit a broadband transmission similar to SIFs. However, solid core PCFs only support a single mode over a broad wavelength range.

Filling the inclusions with a nematic liquid crystal limits the transmission to certain wavelength windows. Each of these windows is expected to have a unique group velocity dispersion. This has already been shown to be true for all–solid PCFs where the inclusions are made off high index glasses². The group velocities and the dispersion determine the velocity and the change in shape of a pulse travelling through a fiber. Consequently, this is an important factor for applications where the response to a pulse has to be known. Furthermore, the group velocity dispersion is of great importance for frequency conversion e. g. parametric down conversion, where a phase matching condition has to be fulfilled for efficient operation.

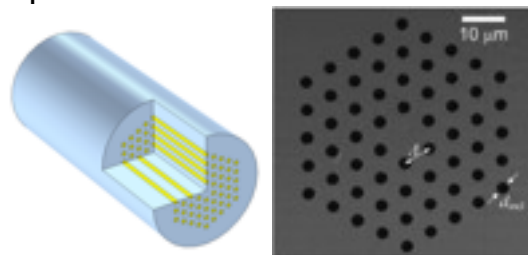


Fig. 1. (left) 3D schematic of a solid core photonic crystal fiber. (right) SEM image of a LMA8, where Λ denotes the inclusion–to–inclusion distance and d_{incl} the inclusion diameter.

Liquid crystal–infiltrated photonic crystal fibers

Photonic crystal fibers can in general be considered as a 2D photonic crystal, where a defect has been introduced to form a core, in which light can be confined along the invariant direction. PCFs with low index inclusions, i.e. lower than the refractive index of the surrounding, guide light by modified total internal reflection, which is very similar to the guiding mechanism of standard step index fibers. For this purpose, an effective refractive index for the cladding is introduced which, is equal to the fundamental space filling mode of the corresponding infinite photonic crystal cladding. Similar to SIFs, this type of PCFs shows high broad band transmission.

However, the use of high index glasses or the infiltration of air inclusion with high index liquid like liquid crystals (LCs) lead to loss variations in the transmission spectrum (Fig. 2). In this case, the mTIR approach does not work. The high index inclusions may be seen as an array of waveguides. Thus, light coupled into the core can couple to the modes of the surrounding cladding³. Consequently, light can only be guided efficiently in wavelength regions where no matching cladding modes exist. In the language of photonic crystals, this corresponds to regions with a complete photonic band gap. Therefore, this type of fibers are called photonic band gap fibers (PBGFs).

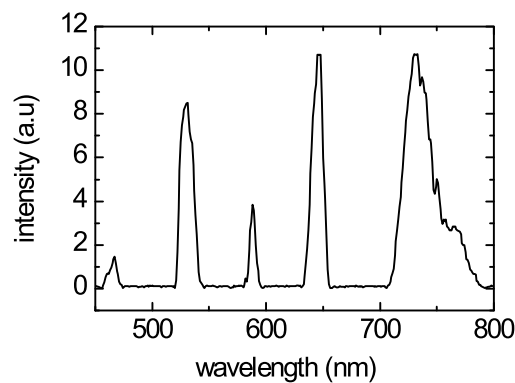


Fig. 2. Transmission spectrum of a PCF filled with liquid crystal.

The use of liquid crystals instead of high index glasses offers large tuning possibilities due to modification of the director configuration inside the inclusions. The influence of alignment agents on the director configuration in circular capillaries is well known, e. g. planar alignment leads to a uniaxial director field while homeotropic alignment can result in different director configurations⁴. This has strong influence on the cladding modes and thus on the transmission. Additionally, tuning of the director field is possible by applying external electric or magnetic fields perpendicular to the fiber axis. This has been utilized for designing LC–

PCF-based in-line polarizers⁵ as the band structures for light polarized perpendicular and parallel to the external field are different.

Group velocity and dispersion

Optical pulses consist of different frequencies unlike monochromatic plane waves. The shorter the pulse, the broader the frequency spectrum. This is the reason why the phase velocity v_{ph} does not describe the speed at which a pulse travels. Thus, the group velocity $v_g = \partial\omega / \partial\beta = (\partial\beta / \partial\omega)^{-1}$ is introduced, where ω denotes the angular frequency and β the propagation constant of the mode confined to a waveguide. It describes the velocity of the pulse envelope. The group velocity is a first order effect as the first derivative of β is used. Waveguide characteristics have a strong effect on the group velocity. Second order effects, namely the group velocity dispersion $GVD = \partial^2\beta / \partial\omega^2$, lead to symmetric changes of the pulse shape around the peak. Higher order effects lead to chirping of the pulse, a deformation which is not symmetric around the central frequency.

Experiments

The PCFs used in this study are commercially available large mode area fibers (LMA8, NKT photonics) with a typical length of 20 cm. In order to control the alignment inside the inclusions of the PCFs, a photoalignment agent (ROLIC) based on polyvinylcinnamate (PVCi) is used. A solution of 2% PVCi in cyclopentanone is filled into the inclusion and consequently extracted by using a nitrogen flow at a pressure of approximately 3 bar. A film of the solution resides on the inner surface. The fibers are dried for 30 min at 135°C and are then photopolymerized with a UV-source with 10 W/cm² for 500 s. Finally, the prepared PCFs are infiltrated with the liquid crystal.

The group delay is determined by use of a Mach-Zehnder-type interferometer (Fig. 3). A supercontinuum source (NKT SuperK compact) is used to investigate the visible and the near infrared (450–1600nm) spectral region. A grating monochromator is used to create monochromatic pulses. The pulses are splitted by a 50/50 non-polarizing broadband beamsplitter. On one side, the pulses are coupled into the fiber under test. The other side serves as the delay path with a variable path length. Both paths are reunited at a second beam splitter and the intensity is measured with a Si-photo diode for the visible range and an InGaAs-photo diode for the near-infrared, respectively. By varying the delay path, interferograms can be recorded. The differences in group delay T can be calculated from the change of the peak position Δ by $T = 2\Delta/c_0$, where c_0 is the speed of light. The dispersion D is then found by $D = -L^{-1}dT/d\lambda$, where

L denotes the fiber length and λ the wavelength. This is done by fitting a Sellmeier-like equation to the group delay.

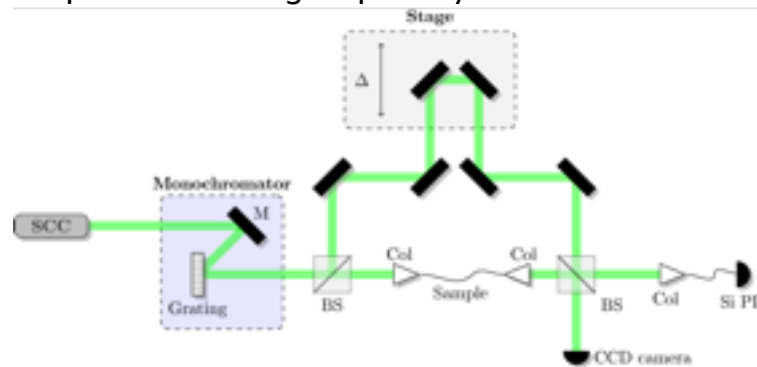


Fig. 3: Schematic of a Mach-Zehnder type interferometer. Mirror M, collimator Col, beamsplitter BS, silicon photo diode Si PD.

Results

Figure 4 (top) shows the transmission spectrum of a LMA8 fiber with uniaxial alignment filled with LC E7; two intensity windows are observed. At the bottom, the dispersion (black solid line) and the delay (measurements: black circles, Sellmeier fit: blue dashed line) are displayed. As expected, every transmission window exhibits a unique group delay which has a minimum at the far wavelength edge. The dispersion shows a zero dispersion wavelength (ZDW) for each window as well. This is unusual, as standard optical fibers and also mTIR photonic crystal fibers typically have only one ZDW in the visible to the near infrared wavelength range. It needs to be emphasized that the strong bending of the dispersion occurs at the edges of the transmission window. This is a result of coupling of the core mode to the cladding modes, which influences the properties of the guided mode including group velocity and dispersion. This effect is most pronounced at the edges as the highest interaction is to be found at the limit, where the modes become no longer guided. This also leads to confinement loss at the edges.

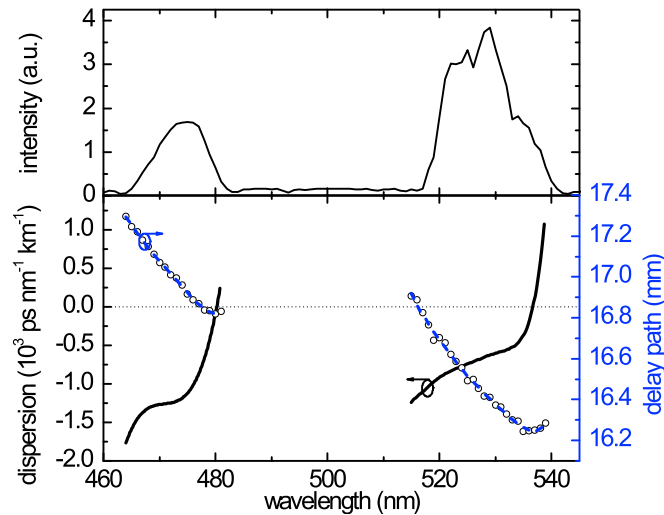


Fig. 4. Result: Measurements on a LMA8 fiber with uniaxial configuration filled with E7. (top) Transmission spectrum. (bottom) Group delay (open circles) and the corresponding fit (dashed blue line) and the dispersion (solid black line) calculated from the fit.

Conclusion

The windowed transmission of liquid crystal-filled photonic crystal fibers on the first glance seem to be a disadvantage compared to PCFs with low index inclusions. But in fact, the resulting unusual properties offer interesting possibilities for pulse shaping and phase matching⁶ due to strong bending of the group delay and dispersion close to the edges of the transmission windows.

Acknowledgements

The support by the German Research Foundation (GRK1464) is gratefully acknowledged.

- 1 P. St. J. Russell. *J. Lightwave Technol.* 2006, **24**, 4729.
- 2 F. Luan, P. St. J. Russell, et al. *Opt. Lett.* 2004, **29**, 2369.
- 3 T. A. Birks, G. J. Pearce and D. M. Bird. *Opt. Express.* 2006, **14**, 9483.
- 4 S. V. Burylov. *JETP* 1997, **85**, 873.
- 5 A. Lorenz, R. Schuhmann and H. S. Kitzerow. *Appl. Opt.* 2010, **49**, 3846.
- 6 Ch. Silberhorn. Private communication, 2012.

Design and investigation of liquid crystal superlattice forming gold nanoparticles – a route to plasmonic metamaterials

C. H. Yu¹, B. J. Tang¹, C. Schubert¹, M. G. Tamba¹, C. Welch¹, O. Amos¹, X. B. Zeng², X. Mang², F. Liu², G. Ungar², J. Dintinger³, T. Scharf³, G. H. Mehl¹

1 Department of Chemistry, University of Hull, Hull, HU6 7RX, UK;

g.h.mehl@hull.ac.uk

2 Department of Materials Science and Engineering, University of Sheffield, UK

3 Optics and Photonics Technology Laboratory, EPFL, Neuchâtel, Switzerland

Metallic nanoparticles (NPs), in most cases gold (Au) NPs, are currently exploited in a wide range of applications which rely on their plasmonic resonances^[1], ranging from molecular biosensing^[2] to solar energy conversion^[3] or cancer phototherapy^[4]. Forming dense arrangements of such resonant structures allows the creation of artificial composites, termed metamaterials^[5]. They are an attractive new class of materials, as they promise to generate synergistic materials properties unavailable to their constituents. Most current realisations of metamaterials rely on top-down techniques, excellent for the design of planar materials, bottom-up approaches based on the self-assembly of metal NPs permit potentially the easy generation of bulk meta materials. Here the use of liquid crystal systems is very promising, as they allow for the control of assembly by appropriate molecular design.^[6] Critical design parameters are here the control of the LC phase, the size of the NPs and the addressing of the two dimensional (2D) and three dimensional (3D) self assembly of the NPs. Important is not only to generate LC-NP nanocomposites synthetically but also to address the density of NPs and their spatial assembly in the compositions.

In this context work on small spherical Au NPs, functionalized with nematogenic groups which form 2D and 3D self-assembly structures is useful. Important features to be controlled are NP size, and the number and type of the organic content, especially that of the number and size of the mesogenic groups. ^[7]

Means of controlling the size of the NPs via a range of synthetic approaches will be presented ^[8] and the correlation of phase structures, phase transition temperatures and 2D and 3D packing of the Au NPs with the size and size distribution of the particles and the size and number of the mesogens attached to the particles will be discussed. Based on these

results the design and investigation of a LC-NP nanocomposite with plasmonic metamaterial properties will be presented.^[9]

- [1] U. Kreibig, M. Vollmer, Optical properties of metal clusters, Springer, **1995**.
- [2] J. N. Anker, W. P. Hall, O. Lyandres, N. C. Shah, J. Zhao, R. P. Van Duyne, Nature Mater. **2008**, 7, 442.
- [3] H. A. Atwater, A. Polman, Nature Mater. **2010**, 9, 205.
- [4] S. Lal, S. E. Clare, N. J. Halas, Acc. Chem. Res. **2008**, 41, 1842.
- [5] Y. Liu, X. Zhang, Chem. Soc. Rev. **2011**, 40, 2494; W. Cai, V. Shalaev, Optical Metamaterials Fundamentals and Applications Introduction, Springer, **2010**.
- [6] L. Cseh, G. H. Mehl, J. Am. Chem. Soc. **2006**, 128, 13376; M. Wojcik, W. Lewandowski, J. Matraszek, J. Mieczkowski, J. Borysiuk, D. Pocięcha, E. Gorecka, Angew. Chem. Int. Ed. **2009**; M. Draper, I. M. Saez, S. J. Cowling, P. Gai, B. Heinrich, B. Donnio, D. Guillon, J. W. Goodby, Adv. Funct. Mater. **2011**, 21, 1260.
- [7] X. Zeng, F. Liu, A. G. Fowler, G. Ungar, L. Cseh, G. H. Mehl, J. E. Macdonald, Adv. Mater. **2009**, 21, 1746; X. Mang, X. Zeng, B. Tang, F. Liu, G. Ungar, R. Zhang, L. Cseh, G. H. Mehl, J. Mater. Chem. **2012**, 22, 11101.
- [8] C. H. Yu, C. P. J. Schubert, C. Welch, B. J. Tang, M. G. Tamba, G. H. Mehl, J. Am. Chem. Soc. **2012**, 134, 5076.
- [9] J. Dintinger, B. J. Tang, X. Zeng, F. Liu, T. Kienzler, G. H. Mehl, G. Ungar, C. Rockstuhl, T. Scharf, Adv. Mater. **2013**, 25, 1999–2004.

Cytoskeletal pattern formation: Self organization of topology

A.R. Bausch

Lehrstuhl für Biophysik (E27), TU München
James-Franck-Strasse D-85747
Garching, Germany

Email: abausch@ph.tum.de

Living cells rely on the self organization mechanisms of cytoskeleton to adapt to their requirements. Especially in processes such as cell division, intracellular transport or cellular motility the controlled self assembly to well defined structures, which still allow a dynamic reorganization on different time scales are of outstanding importance. Thereby, the intricate interplay of cytoskeletal filaments, crosslinking proteins, molecular motors and topology play a central role. One important and promising strategy to identify the underlying governing principles is to quantify the physical process in model systems mimicking the functional units of living cells. Here I will present first an in vitro minimal model systems consisting of actin filaments and myosin II exhibiting collective long range order and dynamics and second a model system consisting of microtubules and kinesin, which is encapsulated into lipid vesicles and shows a rich shape fluctuations. I will discuss how a balance of local force exertion, crosslinking, hydrodynamics and topology affect the evolving dynamic structures.

Two dimensional X-ray diffraction patterns of liquid crystalline Gay-Berne phases: reliability of orientational order parameters

F. Jenz^a, S. Jagiella^a, M. Glaser^b, F. Giesselmann^{a*}

^a Department of Physical Chemistry, University of Stuttgart, Pfaffenwaldring 55, 70569 Stuttgart.

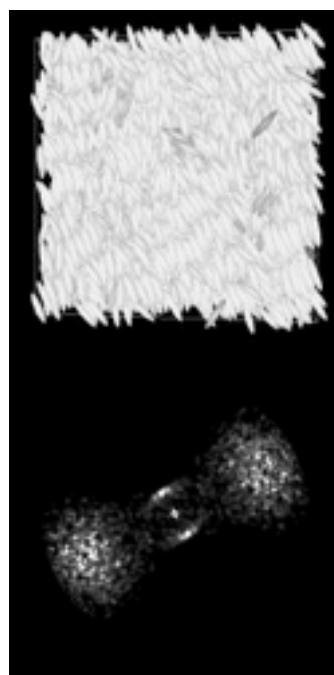
^b Department of Physics, University of Colorado, 390 UCB, Boulder, CO 80309-0390.

e-mail: f.jenz@ipc.uni-stuttgart.de

The orientational order parameter S_2 is the most relevant quantity to describe the quality of long-range orientation ordering inherent to all liquid crystal phases. There are several approaches to experimentally measure this order parameter of liquid crystalline phases but every method includes substantial simplifications and assumptions. We now present a simulation-based approach to elucidate the reliability of the methods by Leadbetter et al.¹ and Davidson et al.² to determine the orientational order parameter S_2 from 2D X-ray experiments.

We set up molecular dynamics (MD) simulations using the Gay-Berne potential which gave us isotropic, nematic, smectic A, smectic B and crystalline phases. S_2 was then calculated from the simulation results by diagonalization of the order tensor and obtained as the largest eigenvalue.³ A grid representation of the electron density of the rod-like molecules was calculated. The electron density was transformed to reciprocal space by 3D Fourier transform. 2D diffraction patterns were obtained by clipping out a 2D slice from the calculated reciprocal space.

After generating 2D diffraction patterns of the simulation results, we were able to apply the method of Davidson et al. on these patterns to



Top: Simulated SmA phase of 8000 Gay-Berne particles with aspect ratios of 1:1:5. S_2 calculated by diagonalization of the order tensor is 0.8.

Bottom: Calculated 2D X-ray diffraction pattern corresponding to the simulated SmA phase. S_2 calculated via the evaluation method of

obtain S_2 once again. The orientational order parameters evaluated via the method of Davidson et al. are in good agreement with the order parameters obtained directly from the simulated phase by diagonalization of the order tensor over the complete range of the simulated liquid crystalline phases. Nevertheless, there is a small deviation of less than 0.05 which can be explained by the non-perfect translational order in liquid crystals.⁴ These results confirm the validity of liquid crystal orientational order parameters obtained from X-ray diffraction by the Davidson-type analysis.

¹ A.J. Leadbetter, E.K. Norris. *Mol. Phys.* 1979, **38-3**, 669.

² P. Davidson, D. Petermann, A.M. Levelut. *J. Phys. II* 1995, **5**, 113-131.

³ C. Zannoni. *Computer Simulations*, in *The Molecular Physics of Liquid Crystals* 1979, 191.

⁴ M. A. Osipov, B. I. Ostrovskii, *Cryst. Rev.*, **3**, 113-156 (1992).

Unidirectional laning and migrating cluster crystals in confined active systems

Andreas M. Menzel^{a,b,*}, Hartmut Löwen^a, Takao Ohta^{b,c}

^a Institut für Theoretische Physik II: Weiche Materie, Heinrich–Heine–Universität
Düsseldorf, D–40225 Düsseldorf, Germany.

^b Department of Physics, Kyoto University, Kyoto 606–8502, Japan.

^c Department of Physics, Graduate School of Science, The University of Tokyo,
Tokyo 113–0033, Japan.

*e-mail: menzel@thphy.uni-duesseldorf.de

Without exaggeration, we can say that the study of active systems and the collective behavior of self-propelled particles is a booming field. Several recent reviews give an overview on the subjects under consideration in this context^{1–4}.

The study of active systems has a lot of its foundations in the field of liquid crystals. From a macroscopic point of view, the hydrodynamic-like equations describing coherent active motion appear as an extension of the ones for liquid crystals in the passive case^{5–7}. We use the same order parameters to describe collective motion as we use for liquid crystals, i.e. the polar order parameter vector and the nematic order parameter tensor^{8,9}. And the particle–particle interactions, from which order emerges, can be of similar steric origin when we consider for example elongated rod-like constituents that are self-propelled^{8,10}.

In the present contribution, we operate on the very point of intersection between the classical concept of describing liquid crystals on the mesoscale and characterizing collective motion in active systems on the particle level. Our basis is the famous Vicsek model¹¹.

Here, self-propelled particles are treated in a very simple reductionist approach. As a major simplification, the particles always self-propel with the same speed. Their migration direction changes by orientational noise and by interaction with other particles. This interaction is simplified to effective interaction rules, which mimic for example steric particle–particle interactions that lead to alignment. In the field of conventional liquid crystals, we measure the order of the molecule orientations. Here, we use the same formalism, but measure the order of the propulsion directions. High degrees of polar order indicate collective motion, with all particles on average propelling into the same direction.

Most interestingly, the Vicsek model predicts a transition from disordered motion to a highly ordered state of coherent collective motion. This transition occurs with increasing particle density or decreasing strength of orientational noise. Various experimental results are available, in which this scenario was qualitatively observed^{12,13}.

In its original version, the particles in the Vicsek model are assumed as point-like without repulsive interactions between them, and the systems were considered as infinite with periodic boundary conditions. The particles abruptly change their migration directions in response to their nearest neighbors: they average over the migration directions in a closer spherical environment around themselves in each time step, and abruptly set their own migration direction equal to the resulting average.

We here relax these rigid conditions¹⁴. First, a step-wise version of adjusting the migration directions is chosen. Secondly, the particles suffer from repulsive interactions when they come too close, which bounds the particle density and avoids a collapse to unrealistically high density spots. And finally, we confine the system between hard boundaries, a necessary ingredient for most experimental set-ups. In combination, these modifications lead to qualitatively new effects not observed before that we will briefly outline in the following¹⁴.

The system is confined in a long channel between two parallel repulsive walls as shown in the figures by the gray bars. Furthermore, if two particles come too close, they feel a repulsive interaction that reorients their migration directions away from each other. This bounds the local particle density. If the total particle density is low, the particles form swarms that are guided to propel along the channel. With increasing particle density, the particles more and more fill the whole channel and form a collectively migrating cloud of relatively homogeneous density. This picture changes qualitatively when we further increase the particle density. We find the spontaneous emergence of spatial patterns that have not been observed before.

First, stable lanes appear in the form of elongated high-density layers between the channel boundaries. An example of this smectic-like density distribution is given by Fig. 1. Laning has been observed before in self-propelled particle systems^{10,15,16}, but the situation here is qualitatively different. Previously, it was found that the particles in neighboring lanes propel into opposite directions. In contrast to the previous studies^{10,15,16}, however, we here

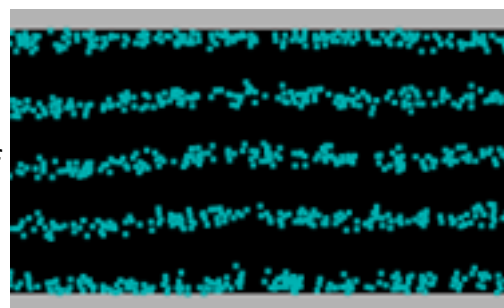


Fig. 1: Example for a state of unidirectional laning. All particles collectively propel to the left. The distance between the top and bottom confining walls (gray bars) determines the number of lanes. Only a fraction of the channel is shown in the horizontal direction.

find that all particles within all lanes on average propel into the same direction along the lane extension. We therefore introduced the term unidirectional laning to characterize this state. Furthermore, there is a finitely sized gap region between the lanes. Again, this is very different from the laning scenarios previously observed.

We analyzed the situation and identified the mechanism of formation behind these lanes. It will be explained in detail in the presentation. In short, an “overreaction” takes place when particles try to align their migration direction with respect to their nearer environment. When a particle from one lane tries to enter the gap region, its velocity has been misaligned with the average of all other particles in its environment. Otherwise it would have stayed within the lane with its velocity aligned along the lane direction. Having entered the gap, it now detects not only the particles in the lane that it tries to escape from, but also particles in the lane behind the gap. This increase in detected particles leads to an “overreaction” in the velocity alignment. The new velocity is oriented not parallel to the lanes, but back towards the lane of escape. In effect, a backscattering into the lane occurs.

If we still further increase the total particle density, the density modulation does not only take place perpendicularly to the channel direction. Now also the density along the channel direction is modulated. We obtain lines of particle clusters as illustrated in Fig. 2. Globally, these particle clusters are arranged in a hexagonal way. All particles in all clusters on average migrate into the same direction so that we obtain a collectively migrating cluster crystal.

We have observed resting cluster crystals in a previous study of deformable self-propelled particles¹⁶. Furthermore, we recently proposed a density-field approach to active crystals¹⁷. In the latter picture, high-density regions can characterize a single active particle, but also clusters of active particles. Increasing the active drive, we observed a transition of the resting structure to a collectively migrating texture similar to the one depicted in Fig. 2. However, here the structures emerge spontaneously, whereas in our previous investigation the formation of crystalline textures was put in by hand through a corresponding chemical potential. We will outline this connection to our previous studies in the presentation.

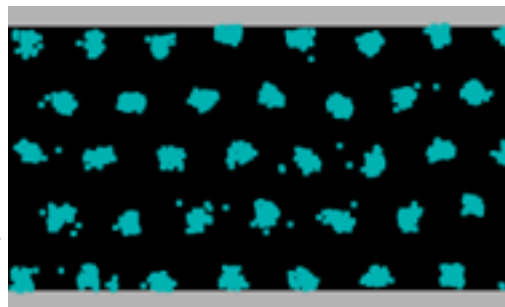


Fig. 2: Example for a collectively traveling cluster crystal composed of self-propelled particles. The whole structure collectively migrates to the left. Again, the distance between the top and bottom confining walls (gray bars) determines the number of cluster lines. Only a fraction of the channel is shown in the horizontal direction.

In general, we observe that the number of lanes and cluster lines increases with the channel thickness. It will be explained in more detail that the distance between the lanes is related to the interaction range for the mechanism of velocity alignment. For the effect to occur and the ordered patterns to emerge, it is essential to allow for a stepwise alignment of the velocity direction of each particle. This means that the velocity alignment does not occur abruptly as in the original version of the Vicsek model, but it can take several time steps until it is completed. However, a discrete nature of the time evolution in successive steps is maintained. This is a reasonable assumption when comparing to real systems, if we think for example of animals, insects, or vibrated granular particles that move by discrete steps or hops.

Finally, for very high particle densities, the system does not find a single global migration direction any more. It rather turns to a chaotic state with repeated changes of the migration direction, reflections of particle clouds between the walls, collisions of particle clouds, and even inversions of their migration directions along the channel. A “phase diagram” will be presented as a function of the total particle density and the channel width showing where the different states can be found.

In summary, we present a modified version of the famous Vicsek model. The local particle density is bounded by repulsive interactions between the self-propelling particles, and the system is confined between repulsive walls. In contrast to the original version of the Vicsek model, the adjustment of the migration direction with respect to the surrounding particles does not occur abruptly but can take several time steps, allowing for an “overreaction” in the velocity alignment. As a result, new states of collective motion spontaneously emerge that have not been observed before. They show regular spatial patterns in the form of unidirectional laning or collectively migrating cluster crystals. A comparison with previously observed states of collective motion is made. Our assumptions of bounded particle density, the presence of confining walls, as well as the stepwise velocity alignment seem reasonable from an experimental point of view. Thus we expect that our predictions can actually be observed in real experimental systems.

¹ S. Ramaswamy. *Annu. Rev. Condens. Matter Phys.* 2010, **1**, 323.

² M. E. Cates. *Rep. Prog. Phys.* 2012, **75**, 042601.

³ P. Romanczuk, M. Bär, W. Ebeling, B. Lindner, L. Schimansky-Geier. *Eur. Phys. J. E – Special Topics.* 2012, **202**, 1.

⁴ M. C. Marchetti, J. F. Joanny, S. Ramaswamy, T. B. Liverpool, J. Prost, M. Rao, R. A. Simha. *Rev. Mod. Phys.* 2013, **85**, 1143.

⁵ J. Toner, Y. Tu. *Phys. Rev. Lett.* 1995, **75**, 4326.

⁶ J. Toner, Y. Tu. *Phys. Rev. E.* 1998, **58**, 4828.

⁷ J. Toner, Y. Tu, S. Ramaswamy. *Ann. Phys. New York.* 2005, **318**, 170.

- ⁸ A. Baskaran, M. C. Marchetti. Phys. Rev. Lett. 2008, **101**, 268101.
- ⁹ A. M. Menzel. Phys. Rev. E. 2012, **85**, 021912.
- ¹⁰ H. H. Wensink, H. Löwen. J. Phys.: Condens. Mat. 2012, **24**, 464130.
- ¹¹ T. Vicsek, A. Czirók, E. Ben-Jacob, I. Cohen, O. Shochet. Phys. Rev. Lett. 1995, **75**, 1226.
- ¹² I. S. Aranson, A. Sokolov, J. O. Kessler, R. E. Goldstein. Phys. Rev. E. 2007, **75**, 040901.
- ¹³ J. Deseigne, S. Léonard, O. Dauchot, H. Chaté. Soft Matter. 2012, **8**, 5629.
- ¹⁴ A. M. Menzel. J. Phys.: Condens. Matter. 2013, **25**, 505103.
- ¹⁵ S. R. McCandlish, A. Baskaran, M. F. Hagan. Soft Matter. 2012, **8**, 2527.
- ¹⁶ A. M. Menzel, T. Ohta. Europhys. Lett. 2012, **99**, 58001.
- ¹⁷ A. M. Menzel, H. Löwen. Phys. Rev. Lett. 2013, **110**, 055702.

Synthesis and liquid crystalline properties of new azobenzene based bent-core liquid crystals

M. Alaasar,^{a,b} M. Prehm,^a A. Eremin,^c G.-M. Tamba^c and C. Tschierske^a

^a Institute of Chemistry, Martin-Luther-University Halle-Wittenberg, Kurt-Mothes Str. 2, 06120 Halle, Germany

^b Department of Chemistry, Faculty of Science, Cairo University, P.O. 12613 - Giza, Egypt

^c Institute of Experimental Physics, University Magdeburg, Universitätsplatz 2, 39106 Magdeburg, Germany

Presenting author; E-mail: M_Alaasar@yahoo.com

Bent-core liquid crystals (BCLCs) incorporating azo (-N=N-) linkages are very versatile materials due to their photochromic effects in addition to their high birefringence, providing access to potential new multifunctional materials where polar response can be modulated by light. Introduction of lateral substituents represent one of the most important ways to modify the mesomorphic properties of bent-core molecules. Recently we have reported the first examples of bent-core molecule shown in Fig. 1 (X = CN, Z = -N=N-), forming a uniformly tilted polar SmC phase with randomized polar direction (SmC_sP_R phase) in addition to nematic and different polar smectic phases [1,2]. Moreover, we have reported other examples of BCLCs based on 4-iodorescinol (X = I, Z = -N=N-) which show a new type of dark conglomerate phase (DC) [3].

Herein we report the synthesis and the liquid crystalline properties of new laterally substituted bent-core materials (X = Br, CH₃, CN, Y = F, H) possessing azo groups in only one or in both of the side wings and having various terminal chain lengths (n = 6 - 20). The mesomorphic behaviour of these materials has been investigated with polarising microscopy, DSC, XRD, electro optical studies and additional methods. Based on the lateral substitution and/or length of the terminal chains new phase sequences were observed.

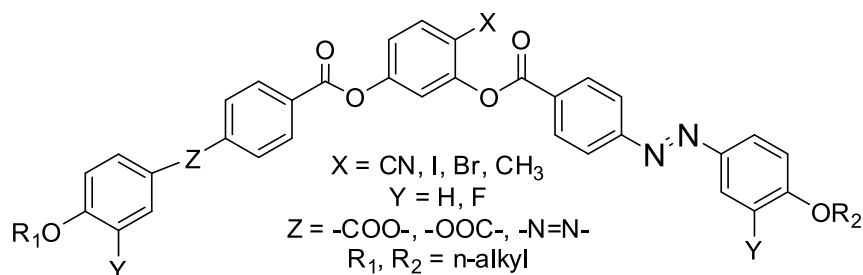


Figure 1. Chemical structure of compounds under discussion.

Acknowledgement

M. Alaasar is grateful to the Alexander von Humboldt Foundation for the research fellowship at Martin–Luther University, Halle (Saale), Germany.

References:

- ¹ M. Alaasar, M. Prehm, M. Nagaraj, J. K. Vij and C. Tschierske, *Adv. Mater.* 2013, **25**, 2186.
- ² M. Alaasar, M. Prehm, K. May, A. Eremin and C. Tschierske, *Adv. Funct. Mater.* 2013, DOI: 10.1002/adfm.201302295.
- ³ M. Alaasar, M. Prehm and C. Tschierske, *Chem.Comm.* 2013, **49**, 1106.

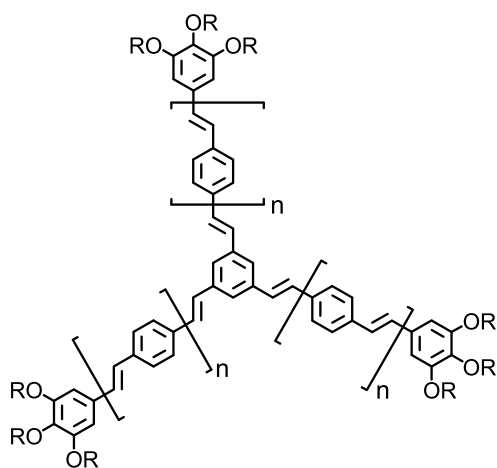
Shape-Persistent, Star-Shaped Host-Guest Supermesogens

M. Lehmann, P. Maier, B. Fröhlich¹ and M. Hügel

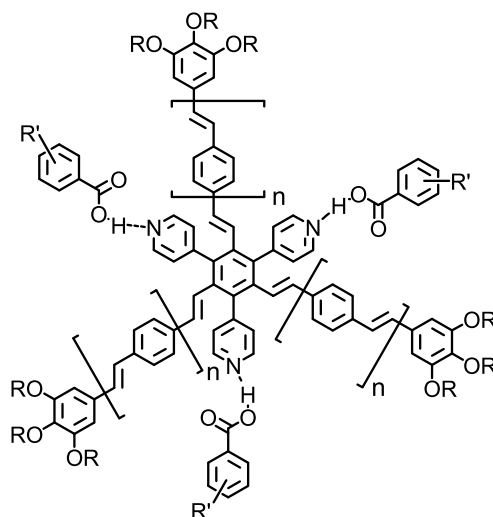
Institute of Organic Chemistry, University of Würzburg, Am Hubland, D-97074 Würzburg.

e-mail: matthias.lehmann@uni-wuerzburg.de

Star-shaped mesogens are non-conventional liquid crystalline compounds composed of linear arms symmetrically attached to a multifunctional core. [1] The void between the arms increases with increasing arm length and has to be compensated during the self-assembly process. Most of the molecules are flexible and fold to improve space-filling and nanosegregation. Shape-persistent molecules can form mesophases without considerable spacial rearrangement of the molecular scaffold. For stilbenoid structures **1** the free space is filled by translation and rotation about the centre of the column and without loss of the overall star morphology.[2] These parent compounds self-organise in Col_h mesophases. It is very attractive to fill such free space with guests, which may covalently or supramolecularly attached to the arms or the core. The latter has been realised earlier in semi-flexible melamine derivatives. In such star-shaped mesogens which may be considered as endoreceptors only one guest could be included,[3] whereas three arms could be attached when a melamine core with an alkyl chain or only one mesogenic arm was used to form a supermesogen by an exorecognition process.[4] The acceptance of three guest molecules in an endoreceptor may be possible for shape-persistent stars with extended arm structures **2**. With this strategy, alternately positioned functional units along a nanostructured column will become feasible, which is of high interest for organic electronics.



1a-c
(n = 1-)



2a,b
(n = 0,1)

The present contribution will show the preparation of the hexa-substituted benzene derivatives **2**. Their supramolecular and mesomorphic properties will be discussed based on polarised optical microscopy, differential scanning calorimetry and X-ray diffraction.

References

- [1] M. Lehmann, *Star-shaped Mesogens in Handbook of Liquid Crystals*, 2nd edition, (eds. J. W. Goodby, P. J. Collings, T. Kato, C. Tschierske, H. Gleeson, P. Raynes, Wiley-VCH, Weinheim (2013).
- [2] M. Lehmann, N. Rumpf, M. Hügel, publication in preparation.
- [3] A. Kohlmeier, D. Janietz, *Liq. Cryst.* **34**, 289-294 (2007).
- [4] J. Barberá, L. Puig, P. Romero, J.-L. Serrano, T. Sierra, *J. Am. Chem. Soc.* **128**, 4487-4492 (2006).

Investigation of dimeric systems with a nematic – nematic phase transition

M.-G. Tamba^{*}, A. Kohlmeier, G. H. Mehl

Department of Chemistry, University of Hull, Hull HU6 7RX, UK

e-mail: maria-gabriela.tamba@ovgu.de

Several hydrocarbon linked mesogenic dimers are known to exhibit an additional nematic phase (N_x) below a conventional uniaxial nematic phase (N). The appearance of such nematic – nematic phase transitions separated by either a first or a second order phase transition has been reported for dimeric mesogens containing 4-cyanobiphenyl units and 2', 3'-difluoroterphenyls units.¹ The correlation between molecular structure and the nematic – nematic phase transitions ($N-N_x$) is not yet well understood. Nematic – nematic transitions are in thermotropic liquid crystals associated in most cases with the formation of a columnar structure in the low temperature nematic phase^{2,3} or the onset of cluster formation⁴ or with folding processes of polymer chains,⁵ though the formation of the twist-bend or heliconical structures⁷ or chiral domain formation has been discussed too.⁶⁻⁹

Here we will report on symmetric and non-symmetric materials and we will compare positive and negative $\Delta\epsilon$ mesogens with non-symmetric systems containing mesogens of different type and $\Delta\epsilon$ and of mixtures thereof. The synthesis of these dimeric materials, as well as the characterisation of these systems by POM, DSC and detailed XRD studies for pure substances and in selected mixtures will be described. The results will be compared with earlier work and a model for the self-assembly behaviour of the mesogens in both nematic phases will be discussed.

A considerable effort was dedicated to investigate the phase behaviour of the dimer series **CB_Cn_CB** (see Fig. 1) derived from cyanobiphenyl units with a spacer consisting of a flexible alkyl chain. For these materials in the low temperature nematic N_x phase either k_{11} or k_{22} have a negative value.^{1a} Crucially for these systems the nematic – nematic transition cannot be explained easily in terms of a frustrated arrangement, as has been discussed earlier for many low molar mass systems. Considering thus the theoretical importance of systems which interconvert directly between two distinct nematic phases and the importance for the understanding of such transitions and potentially for the design of materials which form a biaxial nematic phase we decided to explore this question further. Fundamental

parameters which affect the nematic – nematic phase transition for dimeric systems are: a) length of hydrocarbon spacers linking the two mesogens, b) possibly absence of ether linkages, c) occurrence of a drastic odd–even effect.

A systematic investigation of these dimers with a spacer length n varying between 6 and 12 methylene units was performed. All compounds exhibit exclusively nematic LC phase behaviour (see Fig. 1). An odd–even effect was observed on varying the spacer length between $n = 6, 7, 8, 9, \dots, 12$. The even – spacers members ($n = 6, 8, 10, 12$) exhibit only a nematic phase, whereas the odd – spacers dimers **CB_C n _CB** ($n = 7, 9, 11$) exhibit two nematic phases, which can be clearly distinguished by their textures and by differential scanning calorimetry. Interestingly, we could observe the second nematic phase, the N_x phase only for the odd–membered dimers.

In order to establish a correlation of the transition temperatures with the number of methylene units, n , in the flexible spacer, the N – I transition temperatures were compared (Fig. 1b). There is a clear alternation of the clearing temperatures with increasing the number of methylene units in the flexible spacer, where the even members exhibit the higher values. With increasing the spacer lengths this alternating effect is decreasing. The dimers with the shorter spacer length exhibit the highest transition temperature. It is remarkable that on extending the spacer from $n = 6$ for **CB_C6_CB** (with the shortest spacer length) to $n = 12$ for the dimer **CB_C12_CB** (with the longest spacer length), the clearing temperature is decreasing by about 72 °C. For the odd–numbered dimers, a very small increase of the N–I transition temperatures on increasing the spacer length from 116 °C ($n = 7$) to 125 °C ($n = 11$) occurs. Looking at the N – N_x transitions, which exist only for the odd–numbered dimers, one can observe a small rise of the transition temperatures on increasing spacer length from 104 °C ($n = 7$) to 108 °C ($n = 9$).

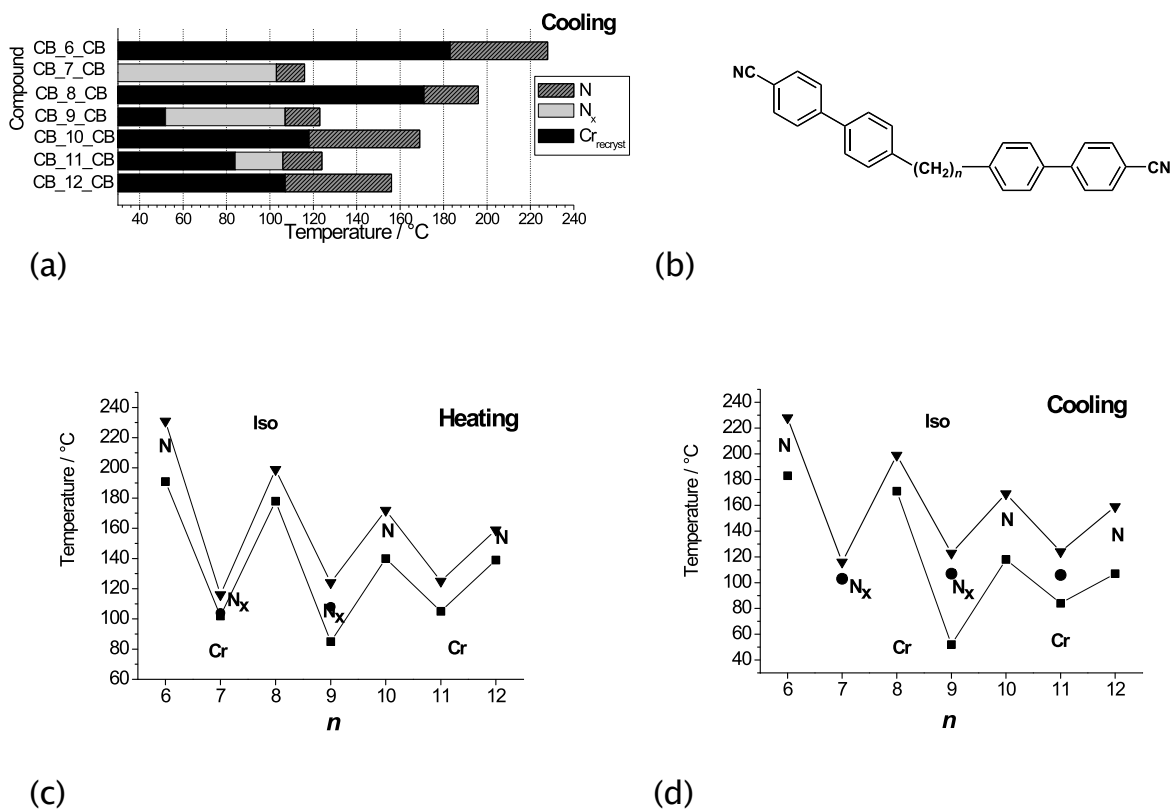
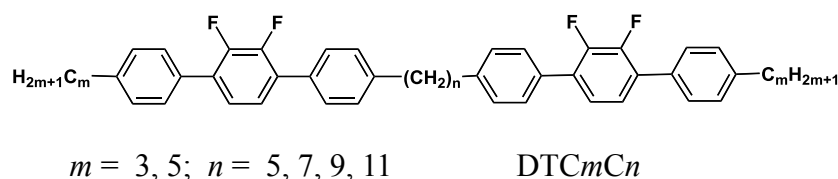


Figure 1: (a) The homologues dimeric mesogens **CB_nCB** derived from cyanobiphenyl units ($n = 6, 7, 8, 9 \dots 12$); (b-d) dependence of transition temperatures on the number of methylene units, n , in the flexible spacer for dimers **CB_nCB**; transition temperatures were taken from (b,d) the first DSC cooling scans (10 Kmin^{-1}), and (c) the first DSC heating scans (10 Kmin^{-1}).

The nematic–nematic (N – N_x) dimorphism was reported recently too for a series of homologues dimeric mesogens **DTCmCn** with a completely different mesogenic architecture. The dimers **DTCmCn** are derived from 2',3'-difluoroterphenyls units connected via flexible alkyl chains, n is the spacer length varying between 5, 7, 9, and resp. 11 methylene units (see Fig. 2). m represents the number of carbons in the terminal chain ($m = 3, 5$). The 2',3'-difluoroterphenyls are an example of classical negative dielectric anisotropy $\Delta\epsilon$ liquid crystals. Despite the obvious chemical differences between the cyanobiphenyl dimers **CB_nCB** and the dimers **DTCmCn**, at different phase transitions temperatures, and even with different signs of dielectric anisotropy $\Delta\epsilon$ (positive for the dimers **CB_nCB** and negative for the dimers **DTCmCn**), these materials exhibit two nematic phases with a N – N_x transition, suggesting a characteristic feature of the self-assembly of molecules. On POM investigations a clear difference in between the two phases could be observed, similar to the series **CB_nCB**. For all of these materials the change in the optical textures is obvious, sharp, and occurs at a well-defined temperature.

Remarkably, for both these bimesogenic dimer series a nematic phase with well-defined periodic patterns due to at least one of the elastic constants (K_{11} or K_{22}) being negative could be detected.^{1a} All these mesogenic dimers exhibits N – N_x phase sequences, with the exception of dimer **DTC5C5**, which presents no liquid crystalline behaviour.

Remarkable, for the dimer **DTC5C9** the POM studies and the calorimetric investigations evidenced the existence of a N – N_x – N_{x2} phase sequence. On POM investigations a clear difference in between the two high temperature phases could be observed for the phase transition N to N_x on cooling. At the phase transition N_x to N_{x2} however there are no significant changes in the textural features of the two mesophases. The high-temperature phase could be easily identified as a nematic phase by its characteristic texture (see Fig. 90 a). At the phase transition to the N_x phase an oily streaks patterns accompanied by a partially homeotropically aligned regions, or as a fine structured rope texture and / or fan-like texture develops (see Fig. 90 b,c), which doesn't change much on cooling to the N_{x2} phase. This N_{x2} phase exhibits textural and structural features similar to the low-temperature N_x phase found for the homologues of series **CB_Cn_CB** and **DTCmCn**.



Compound	m	n	Transitions temperatures [°C]
DTC3C11	3	11	Cr 97.8 N_x 114.1 N 181.5 I
DTC5C5	5	5	Cr 213.5 I
DTC5C7	5	7	Cr 99.5 N_x 128.1 N 156.9 I
DTC5C9	5	9	Cr 95.5 (N_{x2} 81.1) N_x 120.3 N 165.3 I
DTC5C11	5	11	Cr 98.3 N_x 128.0 N 167.7 I

Figure 2: The series of homologues dimeric mesogens **DTCmCn** derived from 2', 3'-difluoroterphenyls units connected via flexible alkyl chains (spacer length $n = 5, 7, 9, 11$). Transition temperatures of **DTCmCn** were taken from the first DSC heating scan (10 Kmin^{-1})

A non-symmetric novel dimer **CB_C9_Terph** with a 4-cyanobiphenyl unit connected through a flexible hydrocarbon spacer containing nine methylene units to a 2',3'-difluoroterphenyl unit (see Figure 3) was thus synthesised to explore the effect of the modulation of symmetry and dielectric anisotropy. A systematic investigation of the binary mixtures of

the positive $\Delta\epsilon$ material **5CB** with negative $\Delta\epsilon$ mesogen **MCT5** were conducted prior in order to investigate if the presence of a strong calorimetric signal is dependent on the dielectric anisotropy of the materials. This study revealed that additional layer - structured mesophases are induced in the mixed phase region of this binary monomeric systems, i.e. a new SmA phase could be found.

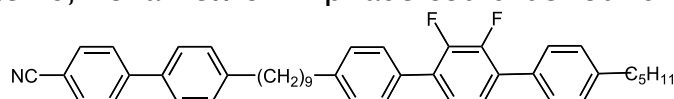


Figure 3: The non-symmetric dimer **CB_C9_Terph** containing a 4-cyanobiphenyl unit and a 2',3'-difluoroterphenyl unit.

The mesophases of the dimer **CB_C9_Terph** were characterized by their optical textures, calorimetric studies and by X-ray investigations. No additional layer - structured mesophases were found, i.e. two nematic phases could be detected. Thus the phase behaviour of the novel dimer **CB_C9_Terph** is different from that of monomer binary mixtures. These two nematic phases show the same interesting textural and structural features as the nematic phases found in the pure odd-spacered dimers **CB_Cn_CB** and the dimers **DTCmCn**.

References:

- ¹ (a) V. P. Panov, M. Nagaraj, J. K. Vij, A. Kohlmeier, M.-G. Tamba, R. A. Lewis, G. H. Mehl, *Phys. Rev. Lett.* 2010, **105**, 167801; (b) V. P. Panov et al., *Appl. Phys. Lett.* 2011, **99**, 261903; (c) V. P. Panov et al. *Appl. Phys. Lett.* 2012 **101**, 234106; (d) E. Burnell, et al., *Chem. Phys. Lett.* 2012, **552**, 44; (e) S. P. Tripathi et al., *Phys. Rev. E.*, 2011, **84**, 041707. (e) R. Balachandran et al., *Liq. Cryst.* 2013, DOI: 10.1080/02678292.2013.765973.
- ² P. H. J. Kouwer, W. F. Jager, W. J. Mijs, S. J. Picken, *Macromolecules* 2000, **33**, 4336.
- ³ M. W. Schroeder, S. Diele, G. Pelzl, U. Dunemann, H. Kresse, W. Weissflog, *J. Mater. Chem.* 2003, **13**, 1877.
- ⁴ C. Keith, A. Lehmann, U. Baumeister, M. Prehm and C. Tschierke, *Soft Matter* 2010, **6**, 1704.
- ⁵ G. Ungar, V. Percec, M. Zuber, *Macromolecules* 1992, **25**, 75.
- ⁶ (a) M. Cestari et al., *Phys Rev E* 2011, **84**, 031704; (b) L. Beguin et al. *J. Phys. Chem. B*, 2012, **116**, 7940; (c) J. W. Emsley et al. *Phys Rev. E.* 2013, **87**, 040501.
- ⁷ V. Borshch, Y.-K. Kim, J. Xiang, M. Gao, A. Jáklí, V. P. Panov, J. K. Vij, C. T. Imrie, M. G. Tamba, G. H. Mehl, O.D. Lavrentovich, *Nature Communications*, 2013, **4**, 2635.
- ⁸ D. Chen, J. H. Porada, J. B. Hooper, A. Klitnick, Y. Shen, M. R. Tuchband, E. Korblova, D. Bedrov, D. M. Walba, M. A. Glaser, J. E. Maclennan, N. A. Clark, *Proc. Natl. Acad. Sci.* 2013, **110**, 15931.
- ⁹ A. Hoffmann, A. G. Vanakaras, A. Kohlmeier A, G. H. Mehl, 2014; Arxiv: 1401.5445

Poster Presentations

Switching between the resonance modes of split ring resonators

Bernhard Atorf^{a,c*}, Holger Mühlenbernd^{b,c}, Mulda Muldarisnur^{b,c}, Thomas Zentgraf,^{b,c} and Heinz Kitzrow^{a,c}

^a Department of Chemistry, Faculty of Science, University of Paderborn, Warburger Str. 100, 33098 Paderborn, Germany

^b Department of Physics, Faculty of Science, University of Paderborn, Warburger Str. 100, 33098 Paderborn, Germany

^c Center for Optoelectronics and Photonics Paderborn, University of Paderborn, Warburger Str. 100, 33098 Paderborn

e-mail: Bernhard.Atorf@uni-paderborn.de

Metamaterials are effective media showing extremely unusual macroscopic material properties. Liquid crystals can be used to develop cells with tunable transmission. A recent publication^[1] demonstrated switching between the resonance modes of split ring resonators (SRR) by means of a twisted nematic (TN) liquid crystal (LC). To achieve the twisted nematic structure, a metasurface was used as an alignment layer. Another recent publication^[2] shows that also other plasmonic structures may be used to achieve uniaxial alignment. However, switching times of about 1 s^[1] present an obstacle for useful applications. To solve this issue we study different ways to improve the switching times:

- 1.) with a TN cell separated from the metasurface,
- 2.) with a Fredericks cell with uniformly aligned nematic LC acting as a retarder with switchable retardation and
- 3.) with a ferroelectric liquid crystal (FLC) acting as a retarder with switchable optical axis^[3].

When the sample is illuminated with linearly polarized light [Stokes vector $S_0 = (1, 1, 0, 0)^T$], the light transmitted through the TN cell (case 1) is described by $S = (1, -1, 0, 0)^T$, while the light transmitted through a uniformly aligned LC (case 2 and 3) is described by^[4]

$$S = \begin{pmatrix} 1 \\ \cos^2(2\varphi) + \sin^2(2\varphi)\cos\delta \\ \cos(2\varphi)\sin(2\varphi)(1 - \cos\delta) \\ \sin(2\varphi)\sin\delta \end{pmatrix}$$

where φ corresponds to the azimuthal direction of the optical axis and $\delta = 2\pi\Delta nd/\lambda$ to the retardation of the LC cell. We envisage switching between $\delta(0V) = \pi$ and $\delta(10V) \approx 0$ at $\varphi = 45^\circ$ for the uniformly aligned nematic LC and switching between $\varphi = 0^\circ$ and $\varphi = 45^\circ$ at $\delta = \pi = \text{const}$ for the FLC.

Preliminary studies indicate the following results.

- 1.) A TN-cell separated from the metasurface is applicable to switch between the resonance modes^[5].
- 2.) The results from a Fredericks cell separated from the metasurface is shown in Fig. 1. A switching between the resonance modes close to each other is possible and the wavelength dependence of the retardation is negligible.
- 3.) For FLC applications, we propose the structure shown in Fig. 2, which is subject to ongoing investigations.

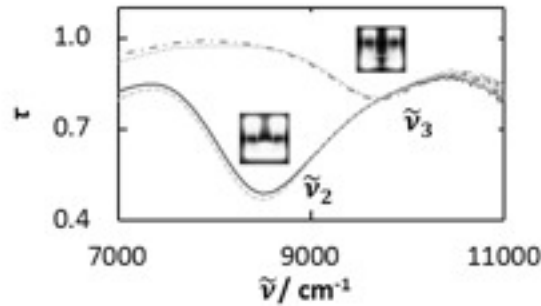


Fig. 1: SRR substrate placed on top of a Frederick's cell, which fulfills a retardation of π . Solid line and dashed-dotted line represent x-polarized radiation without and with an applied voltage, respectively. Dashed line and dotted line represent y-polarized radiation without and with an applied voltage, respectively.

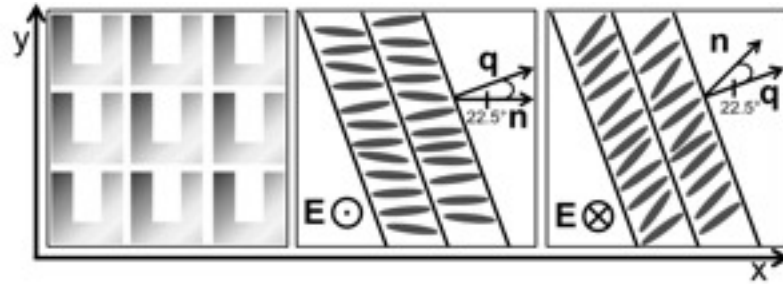


Fig. 2: Schematic illustration for the use of an FLC cell as a $(\lambda/2)$ -waveplate in combination with SRRs. The sample is illuminated with linearly polarized radiation. In one stable state the director \mathbf{n} should be orientated along the x or y-axis in the other state at an azimuthal angle of 45° .

¹ M. Decker, C. Kremers, A. Minovich, I. Staude, A. E. Miroshnichenko, D. Chigrin, D. N. Neshev, C. Jagadish, and Y. S. Kivshar. *Optics Express*. 2013, **21**(7), 8879

² O. Buchnev, J. Y. Ou, M. Kaczmarke, N.I. Zheludev, and V. A. Fedotov. *Optics Express*. 2013, **21**(2), 1633

³ S. T. Lagerwall, "Ferroelectric and Antiferroelectric Liquid Crystals", Wiley-VCH, Weinheim, 1999

⁴ W. A. Shurcliff, "Polarized Light", Harvard University Press, Cambridge, 1962

⁵ B. Atorf, H. Mühlenberd, M. Muldarisnur, T. Zentgraf, and H. Kitzrow. *ChemPhysChem*. in press

Phase separation effect on polymer/liquid crystal systems including nano-sized diamond particles

Malika ELOUALI^{a,b}, Frédéric DUBOIS^c, Sofiane BEDJAOUI^{a,d}, Boucif ABBAR^e, Ulrich MASCHKE^a

^a Unité Matériaux et Transformations (UMET), –CNRS UMR 8207–Bâtiment C6, Université Lille 1 – Sciences et Technologies, 59655 Villeneuve d’Ascq Cedex, France

^b Faculté des Sciences, Université de Mascara, 29000 Mascara, Algeria

^c Unité de Dynamique et Structure des Matériaux Moléculaires (UDSMM), Université du Littoral – Côte d’Opale, 62228 Calais, France

^d Département des Sciences, Faculté des Sciences et Technologie, Université de Bechar, Algeria.

^e Laboratoire de Modélisation et Simulation en Sciences des Matériaux, Université Djillali Liabes, Sidi Bel Abbès, Algeria

e-mail: ulrich.maschke@univ-lille1.fr

In this work, we study the influence of nano-sized diamond particles on physical (morphological, thermophysical, electro-optical, dielectric) properties of polymer/liquid crystal (LC) systems. These materials are elaborated by separation phase processes photoinduced by UV light, using the nematic LC 5CB and the E7 mixture. A thiolene prepolymer composition called NoA65 and tripropylene glycol diacrylate (TPGDA) are employed as monomers. The weight concentration of diamond nanoparticles varies between 0 and 1%.

Already a small quantity of diamond nanoparticles strongly influences thermophysical and electro-optical properties of the polymer/LC materials. For example, the presence of diamond leads to a reduction of both polymer glass transition and nematic–isotropic transition temperatures, and to an increase of switching voltages as well as to a decrease of the optical transmittance. The obtained results are explained by morphological observations, and notably by aggregation of nanoparticles for concentrations higher than 0.25%.

These materials are also studied by linear dielectric spectroscopy at room temperature in the frequency range from 20Hz to 1MHz. A strong decrease of the ionic conductivity of the monomer/LC mixtures is observed. On the contrary, the characteristics (relaxation frequency, dielectric strength) of observed relaxation modes (alpha-relaxation, Maxwell–Wagner effect) in polymer/liquid crystal systems vary only slightly with addition of diamond nanoparticles.

- ¹ L. Dolgov, O. Yaroshchuk, L. Qiu. *Mol. Cryst. Liq. Cryst.* 2007, **468**, 335.
- ² L. Méchernène, L. Benkhaled, D. Benaissa, U. Maschke. *Opt. Mat.* 2009, **31**, 632.
- ³ F. Z. Elouali, O. Yaroshchuk, U. Maschke. *Mol. Cryst. Liq. Cryst.* 2010, **526**, 1.

Optical transmission relaxation processes of polymer/liquid crystal blends

Z. Hadjou Belaid^{a,b}, L. Méchernène^b, A. Berrayah^b, S. Bedjaoui^{b,c}, U. Maschke^a

^a Unité Matériaux et Transformations (UMET), UMR 8207, Bâtiment C6, Université Lille1-Sciences et Technologies, France

^b Laboratoire de Recherche sur les Macromolécules, Université de Tlemcen, Algeria

e-mail: ulrich.maschke@univ-lille1.fr

The phase separation kinetics of selected monomer/liquid crystal (LC) blends has been studied by measuring the optical transmission relaxation as function of time, covering the period of exposure to UV-light and the following relaxation processes of the irradiated samples. These systems that are in the form of thin films containing LC microdroplets dispersed in a polymer matrix, were elaborated in situ by polymerization induced phase separation under ultraviolet (UV) radiation.

Binary systems composed of diacrylate monomers, Tripropylene glycol diacrylate (TPGDA) and polypropylene glycol diacrylate with two different molecular weights (500 and 900g/mol), and an eutectic nematic LC E7, were used as starting materials in the process of polymerization/crosslinking, in order to understand and quantify the kinetics of phase separation which greatly control the morphology of LC domains and the structure of the polymer matrix. The morphology of these systems was observed by polarized light optical microscopy provided with a heating stage allowing the knowledge of the nematic-isotropic transition temperatures.

The results obtained showed three domains of the optical transmission relaxation: a short time relaxation process which decays within a few seconds, characterized by the formation of LC droplets, an unexpected intermediate period where transmission was found to enhance due probably to a thermal effect, followed by a long lasting relaxation process which takes a few minutes to decay completely just after removing irradiation [1,2].

- ¹ Z. Hadjou Belaid, L. Méchernène, U. Maschke. *Molecular Crystals and Liquid Crystals*. 2009, **502**, 29.
- ² Z. Hadjou Belaid, L. Méchernène, U. Maschke. *Molecular Crystals and Liquid Crystals*. 2011, **554**, 157.

Polymer/Liquid Crystal networks : Correlation between morphologies and electrical, optical and electro-optical properties

Yazid Derouiche^{a,b,c}, Mohamed Bouchakour^a, Kaolian Koynov^b, Frédéric Dubois^d, Ulrich Maschke^a

^a Unité Matériaux et Transformations (UMET), UMR 8207-CNRS, Bâtiment C6, Université Lille 1 – Sciences et Technologies, 59655 Villeneuve d'Ascq Cedex, France.

^b Max-Planck Institute of Polymer Research, Postfach 3148, 55021 Mainz, Germany.

^c Laboratoire des dispositifs des micro-ondes et matériaux pour les énergies renouvelables, Faculté des Sciences et Technologies, Université Ziane Achour, 17000 Djelfa, Algeria.

^d Unité de Dynamique et Structure des Matériaux Moléculaires (UDSMM), Université du Littoral – Côte d'Opale, 62228 Calais, France

e-mail: ulrich.maschke@univ-lille1.fr

The purpose of the work is to compare the effect of the sample morphology of polymer/liquid crystal (LC) systems on thermophysical, electro-optical and dielectric properties. These materials were elaborated using the nematic LC mixture E7 but with three acrylic monomers. These difunctional monomers possess the same chemical structure but differ by their chain lengths. The corresponding PDLC materials were obtained by phase separation processes photoinduced by UV light.

The obtained PDLC films can be obtained with desired morphologies presenting controlled LC domain sizes, according to the used monomer, which were observed by using polarized optical microscopy. These results were correlated with the electro-optical responses and dielectric properties of these systems. The ordinary refractive index of E7 and the refractive index of the acrylic polymers are favourably close, so that the corresponding polymer/LC films become fully transparent in the field-on state.

The VTF (Vogel-Tamman-Fulcher), Arrhenius models and the new compensated Arrhenius model allow to describe the effect of conductivity of monomer/LC systems. The dielectric response of PDLC systems underlines alpha-relaxation. Its characteristics depend on polymer chain length and are correlated with the glass transition temperatures of the polymers.

- ¹ Y. Derouiche, K. Koynov, F. Dubois, R. Douali, C. Legrand, U. Maschke. *Mol. Cryst. Liq. Cryst.* 2012, **561**, 124.
- ² P. K. Rai, M. M. Denn, B. Khusid. *Langmuir*. 2006, **22**, 2528.
- ³ T-I. Yang, P. Kofinas. *Polymer*. 2007, **48**, 791.

Polymer Dispersed Liquid Crystal Systems : Electron Beam and UV-light induced polymerization/crosslinking processes

M. Bouchakour^{a,b,c}, Y. Derouiche^{a,b}, B. Djelita^{a,b,d}, C. Beyens^a, F. Riahi^c, S. Bouzid-Laghaa^d, L. Méchernène^e, and U. Maschke^a

^aUnité Matériaux et Transformations (UMET), UMR 8207-CNRS, Bâtiment C6, Université Lille 1 – Sciences et Technologies, 59655 Villeneuve d'Ascq Cedex, France.

^bFaculty of Sciences and Technology, University of Ziane Achour, 17000 Djelfa, Algeria.

^cLaboratoire d'élaboration et préparation des mélanges polymériques multiphasiques, Faculty of Sciences, University of Setif 1, 19000 Setif, Algeria.

^dLaboratoire Environnement, Eau, Géomécanique et Ouvrages (LEEGO), Université des Sciences et de la Technologie Houari Boumediene, USTHB, Algeria.

^eLaboratoire de Recherche sur les Macromolécules, Faculté des Sciences de l'Université de Tlemcen, BP119, 13000 Tlemcen, Algeria.

e-mail: ulrich.maschke@univ-lille1.fr

This contribution focuses on a detailed investigation of polymerization/crosslinking processes, either induced by a powerful UV radiation, or by electron beam exposure of tripropyleneglycoldiacrylate (TPGDA) and polypropyleneglycoldiacrylate (PPGDA) monomers of molecular weights 300 and 800g/mol. They differ from each other by the length of the spacer between the two reactive double bonds. The nematic liquid crystal (LC) E7 exhibits a broad nematic temperature range (-60 to 60°C). The comparison was focused mainly on the phase diagrams before polymerization, kinetics of polymerization by Fourier Transform InfraRed spectroscopy, morphology by polarized optical microscopy and scanning electron microscopy, thermal properties by differential scanning calorimetry and electro-optical properties of the obtained PDLC films.

From studies of the phase diagrams, it was shown that 60wt.% of E7 represents the limit of solubility for the PPGDA800 / E7 mixture at 20°C. From the kinetics of polymerization, remarkable differences between the two monomers were found towards the method of polymerization employed. Larger LC domains were obtained for PPGDA800 / 60wt.% E7 which confirms the longer distance between adjacent crosslinking points compared to the TPGDA system. Studies of the electro-optical responses of various PDLC systems exhibited noticeable changes between UV-cured and analogous Electron Beam (EB)-cured samples. It was found that

threshold and saturation voltages were considerably increased in the case of UV-cured systems. Other results involving electro-optical characteristics such as the contrast ratio, which was higher for EB-cured systems, confirm the higher quality of EB-cured systems.

- [1] U. Maschke, X. Coqueret, M. Benmouna. *Macromol. Rapid Commun.* 2002, **23**, 170.
- [2] L. Méchernène, L. Benkhaled, D. Benaissa, U. Maschke, *Optical Materials*. 2009, **31**, 632.
- [3] Y. Derouiche, S. A. K. Ghefir, F. Dubois, R. Douali, C. Legrand, M. Azzaz, U. Maschke, *I. R. E. Phy.* 2010, **4**, 3.

Structure and order parameters of an antiferroelectric liquid crystal with exceptionally high director tilt angle

Friederike Knecht^a, Alberto Sánchez–Castillo^a, Per Rudquist^b and Frank Giesselmann^{a*}

^a Institute of Physical Chemistry, University of Stuttgart, Pfaffenwaldring 55, 70569 Stuttgart, Germany

^b Department of Microtechnology and Nanoscience, Chalmers University of Technology, Gothenburg, Sweden

e–mail: f.giesselmann@ipc.uni-stuttgart.de

Antiferroelectric liquid crystals (AFLCs) with an optical tilt angle close to 45° are known as orthoconic AFLCs. Due to their anticlinic structure with 45° tilt, the antiferroelectric SmC_a^* phase appears optically isotropic in the direction normal to the tilt plane. Orthoconic materials are thus most interesting for solving the dark state problem of AFLC–based display devices.¹ However, the molecular origin of their exceptionally high tilt angle is still unclear. We now investigated the well–known orthoconic AFLC 1F6B² by means of polarized micro–Raman spectroscopy, which enables to selectively probe the tilt and the orientational order parameters of the aromatic molecular core³. The comparison of the Raman results with corresponding results from X–ray scattering and optical tilt measurements gives an insight into the specific contribution of the molecular core to the optical tilt and order parameters of the entire phase.

A major advantage of the micro–Raman technique is that the incoming laser beam, focussed down to a few microns diameter, allows to locally probe the tilt and the order parameters, e.g. inside a single, well–aligned domain. Temperature dependent measurements on 1F6B were carried out without and with an electric field applied, which transforms the anticlinic SmC_a^* structure into the synclinic state with an uniform tilt direction of the mesogens. For each selected combination of temperature and field, the

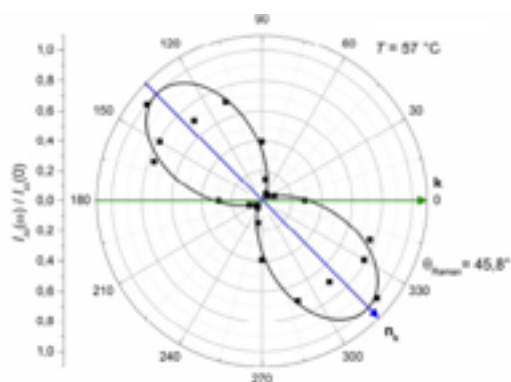


Fig.1: Polar plot of a polarized Raman results in the synclinic state of the antiferroelectric phase with layer normal \mathbf{k} and direction of the aromatic core \mathbf{n}_k (temperature: 57°C , electric field: $5.5 \text{ V}/\mu\text{m}$).

intensities at the stretching mode frequency of the aromatic cores I_{yz} and I_{zz} between crossed and parallel polarizers, respectively, are recorded as a function of the sample orientation and analyzed according to the procedures described in ¹. An example of normalized and fitted results, obtained in the synclitic state of the SmC_a* phase of 1F6B at 57°C is shown in Figure 1, where the molecular aromatic cores are on average tilted by 45.8° with respect to the smectic layer normal.

Overall we find for 1F6B that the tilt of the aromatic cores comes very close or even exceeds the optical tilt angle of about 45°, whereas the X-ray tilt – including contributions from the less-polarizable alkyl tails – is about 10° smaller than these tilt measures. At the same time the orientational order parameter of the cores has exceptional high values of almost 0.8. Even in the high-temperature smectic A* phase the order parameter of the cores is in the absence of an electric field about 20% higher than the order parameter of the entire molecules as revealed by 2D X-ray diffraction. These experimental observations clearly confirm that the aromatic cores have substantially higher tilt and orientational order than the other molecular segments and thus mainly contribute to the exceptional high optical tilt of orthoconic AFLCs. In conclusion, the structure and interactions of the molecular aromatic cores seem to be the key for the understanding and the rational design of new orthoconic AFLC materials.

¹ K. Dhare et al., Appl. Phys. Lett. 2000, **76**, 3528.

² W. Piecek et al., Mol. Cryst. Liq. Cryst. 2005, **436**, 149.

³ A. Sanchez-Castillo, M. Osipov and F. Giesselmann, Phys. Rev. E 2010, **81**, 021707.

Emissive cholesteric films: Dye depletion, dye diffusion and helix distortion

Jürgen Schmidtke and Heinz–Siegfried Kitzerow

Faculty of Science, University of Paderborn

e–mail: Juergen.schmidtke@upb.de

During the past decade, photonic band edge lasers based on dye–doped cholesteric liquid crystals (CLCs) have attracted considerable interest as self–assembled, coherent, tunable light sources. Currently, bleaching of the laser dye limits performance. Typical emission energies (a few μJ) and pulse rates (~ 10 Hz) are not sufficient for many applications in telecommunications, sensing, or displays. A thorough understanding of the dynamics of dye depletion and diffusion in optically excited LC films is a prerequisite for optimizing the performance of liquid crystal lasers. To this end, we performed time–dependent fluorescence measurements on dye–doped cholesteric films under high–power continuous–wave excitation.

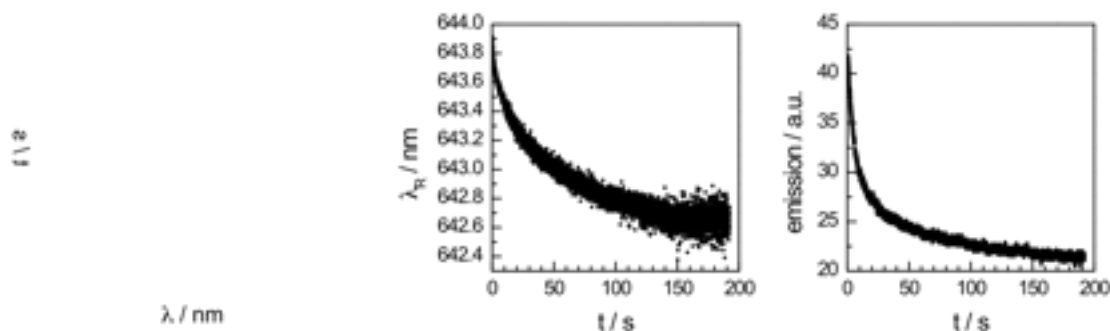


Fig. 1. Sample measurement: Evolution of emission spectrum (left; excitation is switched on at $t = 0$), time–dependent shift of long–wavelength band edge resonance (middle), and decay of integrated emission intensity (right).

Dye–doped cholesteric films were excited by a continuous wave laser, and the transient evolution of the emission spectrum was investigated (Fig. 1). Fluorescent guest molecules are sensitive probes of the photonic properties of the cholesteric film, with sharp emission peaks marking the band edge resonances available for the generation of laser emission. After switching on the pump laser, there is a fast jump of the band edge resonances, followed by continuous further drift of the emission peaks

away from their initial wavelengths. This can be explained by the local heating of the film and the associated changes of the refractive indices; comparison with temperature–dependent optical transmission measurements allows us to translate the observed shift of the emission peaks into the local temperature change of the sample (which can reach several K).

The time–dependent integrated emission intensity shows a rapid initial drop, followed by a slow further decline. The higher the pump intensity, the larger the initial drop and the lower the quantum yield of the film. The intensity–dependent reduction of emission efficiency can be explained by the bleaching of the dye at the pump spot. Neither local temperature nor emission intensity reaches any equilibrium value even for long excitation periods. The pump spot acts as a sink for the dye dissolved in the LC, and recovery can only happen by diffusion of dye from the surrounding area. The film area affected by the drain of the dye grows over time, and therefore replenishment of the dye at the position of the pump spot becomes less and less effective. The experimentally found time–dependence of emission intensity shows fair agreement with simulations (based on the numerical solution of the 2d diffusion equation including a localized sink).

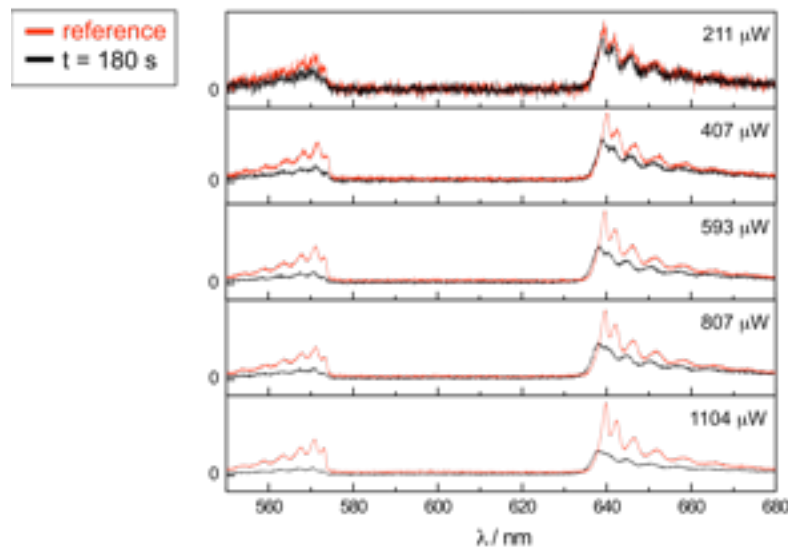


Fig. 2. Comparison of undisturbed emission (reference spectra obtained at low excitation power) with emission after 180 s of high–power cw excitation (excitation powers are indicated in the figure).

Analysis of the emission spectra shows a time–dependent deterioration of the quality of the band edge resonances. Increasing either pump intensity or dye concentration, the periodicity of the photonic medium formed by the CLC becomes more and more disturbed (Fig. 2). We attribute this to a non–uniform heating of the CLC along the film normal, resulting in a distortion of the cholesteric helix (pitch gradient).

Investigations on structural and dielectric dynamics of non-aqueous lyotropic mesophases

R.K. Shukla^{a,b*} W. Haase^b and K.K. Raina^a

^aMaterials Research Laboratory, School of Physics and Materials Science, Thapar University, Patiala –147004, India

^bEduard-Zintl-Institute of Inorganic and Physical Chemistry, Technical University Darmstadt, Petersenstr. 20, D-64287 Darmstadt, Germany.

*Corresponding author: E-mail: ravishukla82@gmail.com

Lyotropic liquid crystals (LLC) are the self assembled phases of amphiphiles in an aqueous and non-aqueous media. Architecture and dynamics of these self assembled phases are important due to their interfacial properties. Aqueous micellar and lyotropic phases of anionic, cationic, nonionic and zwitterionic amphiphiles are well studied and documented in literature.^{1, 2} Complementary to aqueous medium some non-aqueous solvents are also studied for the self assembly. Distinct spherical, cylindrical, rods like micelles of surfactants were reported in these solvents, however, only few reports highlight the liquid crystalline phases.²⁻³ These soft phases are extensively used for technological applications such as soft templating and drug delivery.¹⁻² Literature suggests that so far structural, thermal and rheological behaviors of these systems are discussed in detail²; while, reports are rare on the dielectric and molecular dynamics. Moreover, in the intact scenario, dielectric relaxation spectroscopy (DRS) emerges as a very sensitive tool to explicate molecular dynamics and the structural changes of soft materials because of its sensitivity to measure the orientation and fluctuation of all kind of dipole moments at low and higher frequency window. Reports on dielectric behaviour of lyotropic systems are rare.⁴ Recently, Chien et al.⁵ studied dielectric behaviour of chromonic lyotropic liquid crystals/isotropic fluids composite systems and hinted at the possibility of developing a high density electrolytic capacitor from these systems. Very recently, our group reported the dielectric study of lyotropic phases derived from binary mixtures of cetyl pyridinium chloride /ethylene glycol or formamide.⁶ The main focus of this study is to highlight the importance of the non-aqueous lyotropic phases and their dielectric dynamics. The main interest to prepare non-aqueous mesophases is attributed to the following prospective 1) stability of obtained mesophases up to higher temperature and with ageing effect; 2) grown phases could be used as a stable template for many inorganic material which are water sensitive. In this context, we employed anionic (sodium dodecylsulfate SDS), cationic (cetyltrimethylammonium bromide CTAB) and non-ionic (polyoxyethylene

20 sorbitan monolaurate Tween 20) amphiphiles and non-aqueous medium of ethylene glycol (EG) to prepare lyotropic phases.

Lyotropic mixtures are prepared via dissolving the appropriate amount of amphiphiles and solvent (10:90 wt/wt %) in three different glass vials. Acronyms used for three mixtures in this study are M1 (SDS: EG), M2 (CTAB: EG) and M3 (Tween20: EG). The homogenous mixing was achieved mechanically via using vortex rotar and thermally via several heating and cooling cycles in the temperature range of 30°C–100°C. The mesostructures of these mixtures are indexed via X-ray diffraction (XRD) and polarizing optical microscopy (POM) analysis, while, dynamical processes are proved by DRS. The details about experiments and characterization techniques are given in Ref.6.

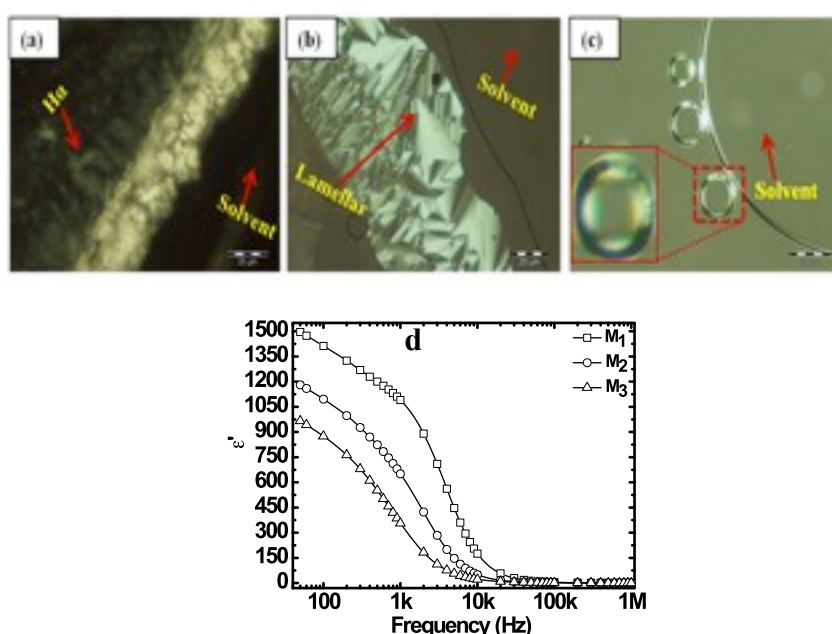


Fig. 1 (a) Texture patterns of lyotropic mixture M1 (SDS: EG) (b) M2 (CTAB: EG), (c) M3 (Tween 20: EG) (d) frequency dependent dielectric permittivity of three mixtures at 30°C.

Two dimensional hexagonal, lamellar and multiwall lamellar lyotropic mesophases are confirmed for three systems M1, M2 and M3 via XRD and POM measurements as shown in the Fig 1a–c. Self assembly and structure packing of these mesophases showed dependence on the chain length of the surfactant. Pronounced dispersion in the dielectric permittivity is noticed for three systems in the lower frequency window as evident from the Fig. 1d. Such behavior and large dispersion of permittivity could be attributed to the ionic and space charge polarization and concentration of ionic charges at the interface of lyotropic structures. The change in relaxation parameters of three systems can be understood considering the

size of the counter ion, bulkiness of hydrophobic chains and ordering of the mesophase. Good dielectric strength, lower loss and small relaxation time could present the application prospective of these systems for the charge storage devices.

We acknowledge Department of Science and Technology (DST), India for the financial support.

References

1. Neto F. A. M., Salinas S.R.A., Oxford University Press, New York, 2005.
2. Fong C., Le T., Drummond C. J., Chem. Soc. Rev., 2012, 41,1297.
3. Ray A., J. Am. Chem. Soc., 1969, 91, 6511.
4. Ishai P. B., Libster D., Aserin A., Garti N., Feldman Y., J. Phys. Chem. B, 2010, 114, 12785.
5. Chien L. C., Golovin A. B., Patent, 2008, US /0165472 A1, 1.
6. Shukla R. K., Raina K. K., Liq. Cryst. dx.doi.org/10.1080/02678292.2013.877602.

Dispersions of functionalized gold nanoparticles in nematic liquid crystals

M. Urbanski^{a*}, J. Mirzaei^b, T. Hegmann^{b,c}, H.-S. Kitzerow^a

^aUniversity of Paderborn, Warburger Str. 100, 33098 Paderborn, Germany.

^bUniversity of Manitoba, 144 Dysart Road, Winnipeg, MB, R2T 2N2, Canada.

^cLiquid Crystal Institute, 1425 University Esplanade, Kent (OH) 44242, USA.

e-mail: Martin.Urbanski@upb.de

Doping nematic liquid crystals with small amounts of organically functionalized gold nanoparticles (NPs) can significantly alter the electro-optic response of the nematic host. Some of the observable effects result from nanoparticles influencing the liquid crystal / substrate interface, while other effects are caused by nanoparticles in the bulk. The location of particles is strongly affected by the compatibility of organic ligand shell and nematic host. A high miscibility leads to well dispersed particles, a miscibility mismatch leads to an expulsion of particles from the nematic phase and a surface coverage of nanoparticles on the confining substrates. As nanoparticles residing on the substrates interfere with the initial alignment layers of electro-optic test cells, the electro-optic response of the dispersions strongly depends on the degree of surface coverage. In the present study, we show electro-optic results of three different gold NP / LC dispersions, where the NPs are primarily dispersed in the bulk, segregated at the interface or induce an intermediate state of surface coverage.

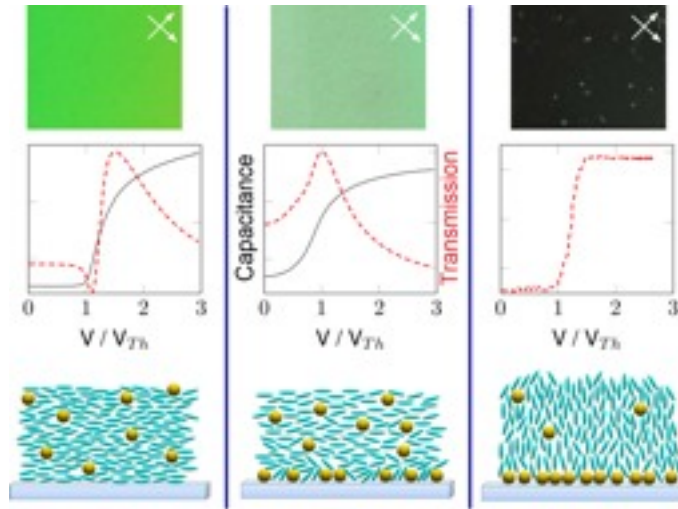


Figure 1: Illustration of three possible degrees of surface interactions of gold NPs. Left: No surface coverage of particles, the initial strong planar anchoring of molecules remains. Material parameters are easily accessible by experiment. Center: Slight surface coverage might affect the initial tilt angle and the anchoring strength. Material parameters cannot be derived directly from experiments, but numerical simulations and a fitting routine are required. Right: Strong surface coverage can induce homeotropic alignment by superimposing the initial planar alignment layers. No normal switching modes can be observed, but a reverse switching occurs at very low driving frequencies ($f=0.01$ Hz).

Examples for the three degrees of surface coverage:

No surface coverage

Dispersions featuring a good miscibility of ligand shell and nematic host show a high stability with no signs of agglomeration or particle precipitation. In this case of negligible surface coverage of nanoparticles, the initial alignment layers ensure strong boundary conditions with sufficiently small director tilt from the planar surface. A Fréedericksz-transition can be used to determine the threshold voltage $V_{th} = \pi \sqrt{K_{11}/\epsilon_0 \Delta\epsilon}$ and estimate the elastic and dielectric properties of the mixture.

For dispersions of **NP1** in **LC1** we found a decrease of threshold V_{th} and an increase of dielectric anisotropy $\Delta\epsilon$ compared to the pure host **LC1**. In conclusion, nanoparticle dispersions with a high miscibility of particles in the host may improve the electro-optic switching characteristic and therefore are promising candidates for the use in LC display applications [1].

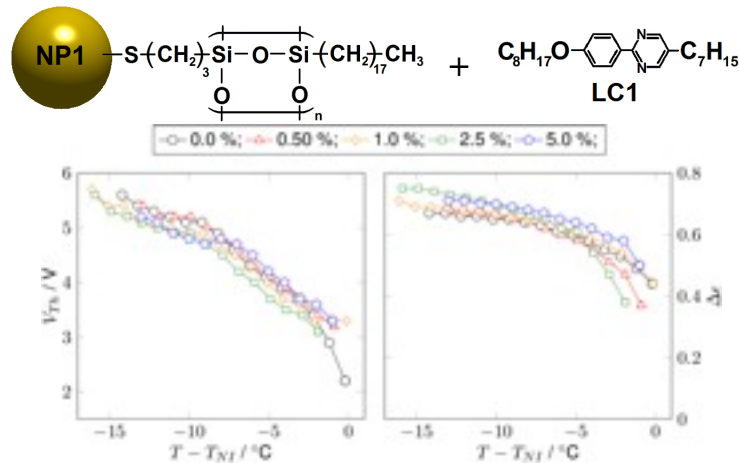


Figure 2: Plots of electro-optical data V_{th} (left) and $\Delta\epsilon$ (right) for **NP1** in **LC1**. For the dispersions shown here, nanoparticle doping clearly leads to a decrease of threshold voltage V_{th} and a slight increase of dielectric anisotropy $\Delta\epsilon$.

Intermediate surface coverage

An intermediate degree of surface coverage on the substrates may have an effect on the initial tilt angle θ_0 and the anchoring energy W , but is not sufficient to induce homeotropic alignment. In this case a Fréedericksz-transition still can be observed, but influences of tilt angle and weak boundary conditions have to be considered during data evaluation. Numerical simulations are needed to obtain the elastic and dielectric parameters of the dispersion.

For dispersions of **NP2** in **LC1** we found a temperature-dependent change of surface coverage. At low temperatures, the nanoparticles reside at the interfaces and induce high initial tilt angles, but do not affect the elastic constants of the host. At higher temperatures, a reversible movement of particles into the bulk occurs, whereas the influence of particles on the alignment layers vanishes. Instead, the nanoparticles decrease the elastic constants in the bulk of the dispersion compared to the pure host [2].

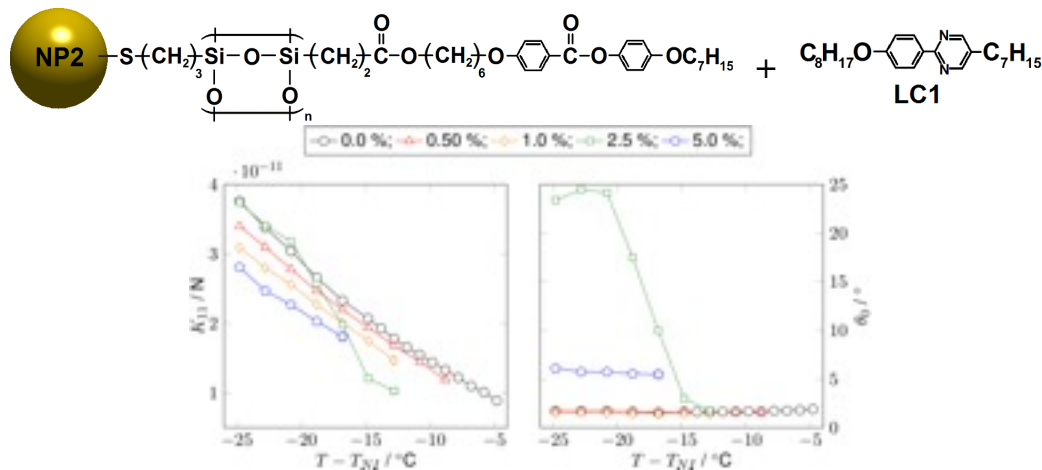


Figure 3: Plots of elastic constant K_{11} (left) and initial tilt angle θ_0 (right) obtained by numerical simulations for NP2 in LC1. For the dispersions containing 2.5 % (w) of NP2, a clear correlation between the decrease of elastic constant K_{11} and the increase of initial tilt angle θ_0 is found, indicating a temperature-induced movement of particles from the surface to the bulk.

Strong surface coverage

In the case of strong surface coverage, an alignment change from planar to homeotropic occurs. According to the explanation model established in literature and based on own experiments, this switching is caused by nanoparticles residing at the interfaces and superimposing the effects of the initial alignment layers. No Fréedericksz-like switching can be observed for liquid crystals with positive dielectric anisotropy and homeotropic alignment in test cells with opposing electrodes, where the electric field is perpendicular to the substrates.

For dispersions of NP3 in LC1, a reverse switching mode is found at very low frequencies, which corresponds to Williams-domains caused by electro-hydrodynamic instabilities [3].

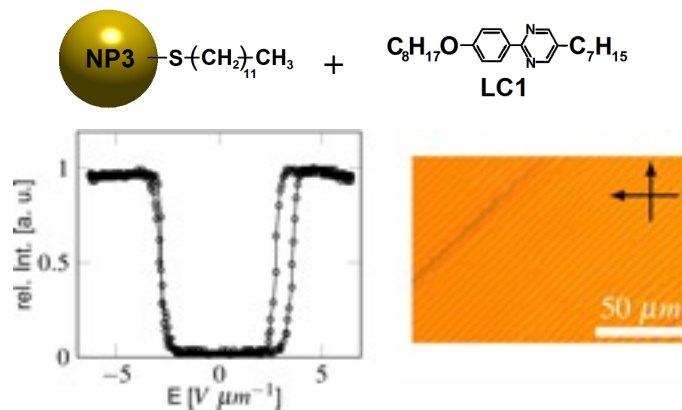


Figure 4: Left: Electro-optic response of a dispersion containing 5 % (w) of NP3 in LC1 at a frequency of 0.01 Hz. Right: POM image of the bright state showing convection rolls which could be identified as Williams- domains.

References

- ¹ J. Mirzaei, M. Urbanski, H.-S. Kitzerow, T. Hegmann. *Phil. Trans. R. Soc. A.* 2013, **371**, 20120256.
- ² M. Urbanski, J. Mirzaei, T. Hegmann, H.-S. Kitzerow. *ChemPhysChem.* 2014, (DOI: 10.1002/cphc.201301054).
- ³ M. Urbanski, B. Kinkead, H. Qi, T. Hegmann, H.-S. Kitzerow. *Nanoscale.* 2010, **2**, 1118–1121.

Dispersion of micro- and nanoparticles in a chromonic liquid crystal

Natalie Zimmermann^a, Gisela Jünnemann-Held^a, Peter Collings^{a,b}, and Heinz-S. Kitzerow^{a*}

^a Department of Chemistry, Faculty of Science, University of Paderborn, Warburger Str. 100, 33098 Paderborn, Germany.

^b Swarthmore College, 500 College Avenue, Swarthmore, PA 19081, USA.

e-mail: nati@mail.uni-paderborn.de

State-of-the-art methods of micro- and nanotechnology have made colloidal particles and nanoparticles with very different functionalities readily available. It is well-known that the presence of such particles can alter the properties of liquid crystals essentially – even if they add no specific property beyond their shape and surface interactions. In this contribution, we report on first attempts of dispersing colloidal particles and nanoparticles in chromonic liquid crystals made of Disodiumchromoglycat (DSCG dissolved in water) solutions. The phase diagram of this system shows a nematic phase (N) and a higher ordered phase (M), depending on concentration and temperature.

To investigate an example of colloidal particles, we studied poly(methyl methacrylate) [PMMA] with a particle diameter of 270–360 nm, synthesized by surfactant-free radical polymerization. Although the particles show very good solubility in water and are readily dispersed in the pristine liquid crystalline mixture, we observed that the particles are expelled from the mesophase on cooling, thereby forming aggregates in the isotropic phase in the biphasic temperature range. A nematic phase appearing next to the clearing temperature forms spherical or elliptical droplets, which grow together at lower temperatures thereby leading to randomly distributed clusters of colloidal particles (Fig. 1a). In contrast, the M phase growing from the isotropic phase forms parallel ribbons, separated by linear isotropic regions. Thus, the separation of colloidal particles results in the formation of parallel particle chains (Fig. 1b). This effect may be very useful for growing self-organized micro structures.

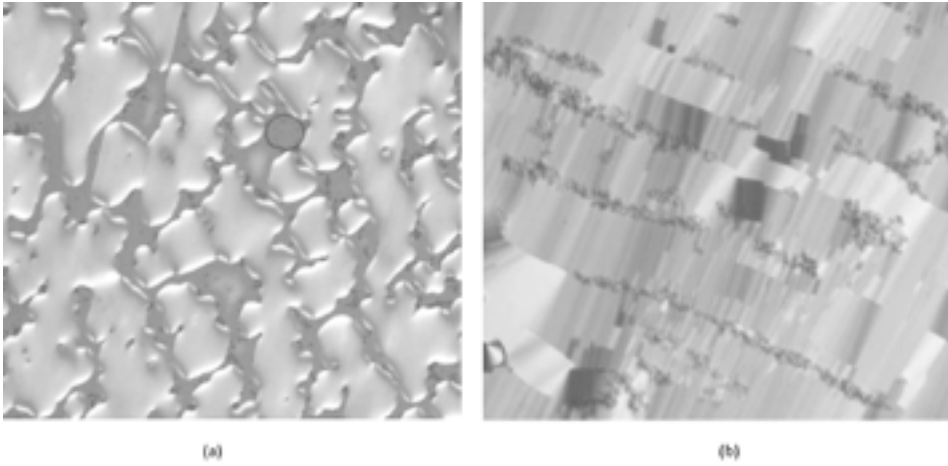


Figure 1. PMMA spheres in DSCG / water mixtures. (a) 15wt.-% DSCG (N phase), 25wt.-% DSCG (M phase)

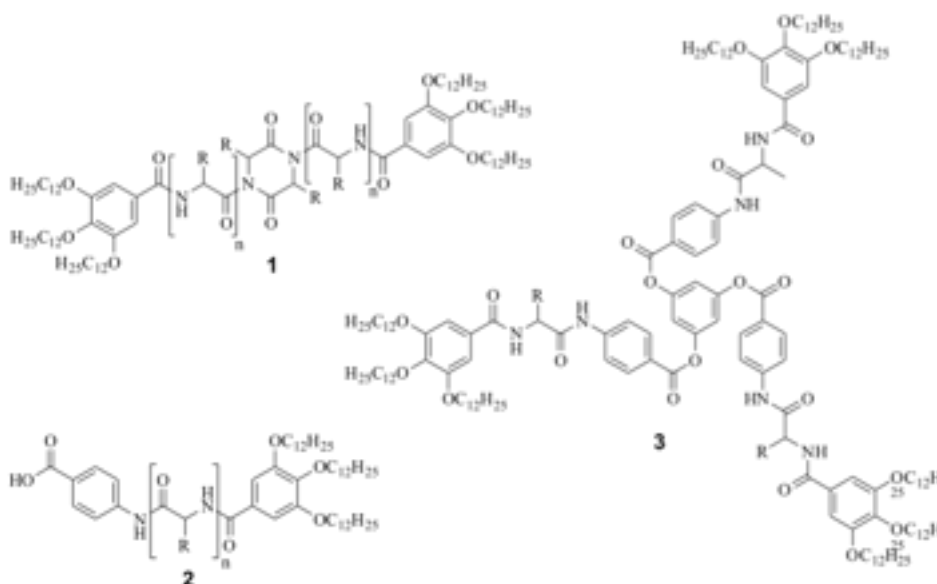
Recent advances in the synthesis of amino acid based arms and their conversion to C₃-symmetric star mesogens

Katrin Bahndorf and Matthias Lehmann

Institute of Organic Chemistry, University of Würzburg, Am Hubland, 97074
Würzburg, Germany

e-mail: katrin.bahndorf@uni-wuerzburg.de

The self-assembly of oligopeptides and proteins is essential for all processes of life and many of them organise also in oriented fluid matter, e.g. thermotropic or lyotropic liquid crystals.^[1] It is therefore attractive to synthesize linear oligopeptide arms by solid phase synthesis and linking them with the C-terminus to a nucleophilic core, such as phloroglucinol. The latter has been avoided owing to the risk of side reactions and racemisation – the resulting star mesogens in which the N-terminus of short peptide arms was attached to a trimesic acid core formed mesophases in solid state.^[2]



Indeed the coupling of the C-terminus to phloroglucinol is very challenging and in most reactions we could only isolate starting material, dimers such as molecule **1** and only in one lucky case the star could be obtained in very low yield. In order to avoid dimer formation and intramolecular side reaction when the carboxy group is activated^[3], the arm **2** was designed by solid state assisted synthesis. The conversion of acid **2** with phloroglucinol yields 50% of the star mesogen **3**. In this contribution we present this new synthetic strategy and the thermotropic properties of some parent oligopeptide stars.

¹ M. Lehmann and M. Jahr, *Comprehensive Nanoscience and Technology* 2011, **5**, 277–357.

² K. P. van den Hout, R. M. Rapun, J. Vekemans, *Chem. Eur. J.* 2007, **13**, 811–8123.

³ Ayman El-Faham and Fernando Albericio, *Chem. Rev.* 2011, **111**, 6557–6602.

Liquid crystalline guanidinium phenylalkoxybenzoates

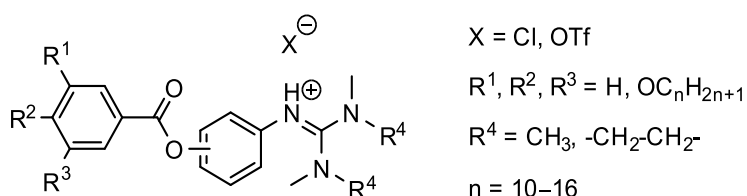
Johannes Christian Hänle^a, Martin Butschies^a, Sabine Laschat^{a*}

^a Institute for Organic Chemistry, University of Stuttgart, Stuttgart, Germany

e-mail: Sabine.Laschat@oc.uni-stuttgart.de

Guanidinium ionic liquids exhibit several interesting properties such as a low vapour pressure, high ionic conductivity, non-flammability and stability towards thermal or chemical strains. By attaching the soft guanidinium head group to anisotropic moieties one has access to beneficial properties of both: ionic liquids and liquid crystalline compounds. Many liquid crystalline imidazolium derivatives are known but only a few examples of thermotropic liquid crystals containing a guanidinium group exist.¹

A series of cyclic and acyclic guanidinium salts with one, two or three alkoxy chains (R^1 – R^3) bearing phenyl alkoxybenzoate cores have been synthesised and their mesomorphic properties were investigated by polarising optical microscopy (POM), differential scanning calorimetry (DSC) and powder X-ray diffraction experiments (small-angle and wide-angle X-ray scattering).²



It could be shown that the number of alkoxy chains is decisive for the observed mesophase. While the guanidinium chloride with one alkoxy chain showed a smectic A (SmA) phase, the anisotropic order is disturbed when the triflate anion is used. Derivatives with two alkoxy chains displayed SmA phases when using triflate anions, the corresponding chlorides showed columnar hexagonal (Col_h) phases. The triple chain guanidinium salts also showed Col_h phases. In order to get a better understanding of the mesophase type at a molecular level, XRD measurements were carried out. The investigations indicated columnar discs containing six or ten molecules for the chlorides with three or two alkyl chains. The single chain chlorides arranged probably in a bilayer structure.

All guanidinium chlorides had very high clearing points in the region of 200 °C. As indicated by DSC-curves and proven by thermogravimetric investigations of selected chloride derivatives, these compounds are close to a beginning thermal decomposition after heating up in the isotropic phase. Whereas the use of cyclic guanidinium head groups rather than acyclic ones had only a minor influence on the mesophase properties, melting points were significantly decreased by bent core units instead of their linear counterparts. Replacement of chloride counter ions by triflate lead to a further depression of the clearing points avoiding thermal decomposition and shifting the mesophase towards room temperature.

¹ K. V. Axenov, S. Laschat, *Materials*. 2011, **4** (1), 206–259.

² M. Butschies, J. C. Haenle, S. Tussetschläger, S. Laschat, *Liq. Cryst.* 2013, **40** (1), 52–71.

Photoresponsive ionic liquid crystals

Marc Harjung^a, Nadia Kapernaum^a, Eugen Wuckert^b, Sabine Laschat^b and Frank Gießelmann^{a*}

^a University of Stuttgart, Institute of Physical Chemistry D-70569 Stuttgart Germany.

^b University of Stuttgart, Institute of Organic Chemistry D-70569 Stuttgart Germany.

e-mail: f.giesselmann@ipc.uni-stuttgart.de

Ionic liquid crystals are a promising new class of materials which combine the unique properties of the ionic liquid "designer-solvents" with the anisotropic physical properties of conventional thermotropic liquid crystals. The systematic exploration of these long-range ordered fluid electrolytes is however still at the beginning. On the other hand photoresponsive liquid crystals based on azobenzene-moieties have been intensively investigated since the 1980s in the field of conventional non-ionic liquid crystals. We now synthesized a homologous series of six new ionic photoresponsive azobenzene-mesogens (see Fig. 1) in order to elucidate whether the behavior of photoresponsive materials differs in ionic liquid crystals from that in non-ionic liquid crystals.

The phase behavior of these mesogens was investigated by polarizing microscopy and X-ray diffraction. The translational order parameters of this smectic A phases turned out to be rather high, indicating a high degree of translational order in ionic smectics due to their ionic head group. The orientational order parameters were in the order of 0.5, independent of the chain length of the mesogens. The kinetics of the cis/trans reversion of these mesogens was then analyzed in two different reaction media: water, as an example for an isotropic medium, and C₁₂MIMBr (1dodecyl-3-methylimidazolium bromide) as an example for an anisotropic ionic medium. The isomerization kinetics was analyzed by UV/VIS-spectroscopy at different temperatures and the activation energy was determined by the Arrhenius law. Surprisingly, smaller activation energy of the cis/trans isomerization was found in the isotropic solution than in the ordered

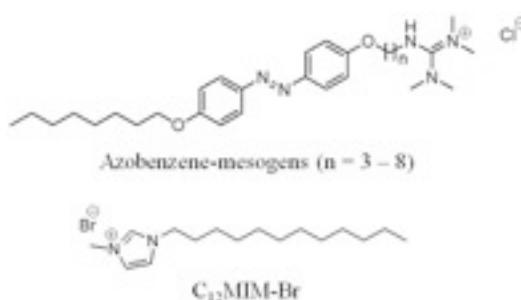


Fig.1: Chemical structure of the photoresponsive ionic mesogens (top) and the ionic liquid crystalline host phase (bottom).

liquid crystalline medium. This is probably due to the fact, that the molecular length of the photoresponsive mesogens is considerably larger than that of the ionic liquid crystalline host phase and thus does not fit well into the highly ordered smectic layers of the ionic host phase.

In conclusion we characterized a new systematic series of six ionic azobenzene-mesogens. The effect of different isotropic and anisotropic matrices on this homologues series of guest molecules could be shown and new knowledge about ionic liquid crystalline phases was achieved.

Star-shaped oligo-p-phenylenevinylene mesogens with fullerene guests

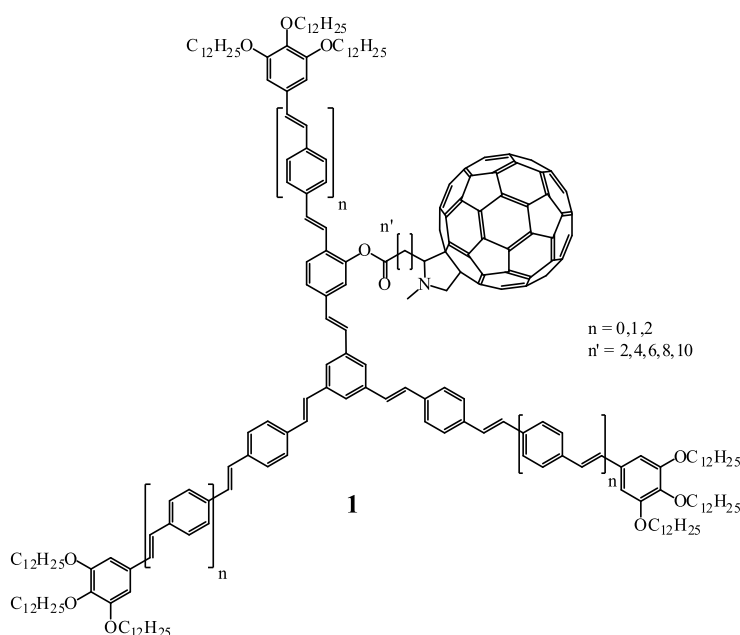
Markus Hugel, Matthias Lehmann*

Julius-Maximilians-Universitt, Am Hubland, 97072 Wrzburg, Germany.

e-mail: matthias.lehmann@uni-wuerzburg.de

Star-shaped oligo-p-phenylenevinylene (OPV) compounds with terminal alkoxy chains form columnar mesophases although space-filling is demanding.¹ The free space between the shape-persistent structure cannot be filled by folding as in star oligobenzoate mesogens, but instead by translational and rotational displacement along the columnar axis, combined with slight conformational adjustments about the single bonds of the OPV structure.² Molecular modeling suggests, that if these cavities are filled by a fulleropyrrolidine attached to the OPV scaffold via a flexible spacer, such as in star mesogen **1**, these compounds should accommodate in highly organised columnar stacks by nanosegregation of their different building blocks. Consequently, the self-assembly may result in defined donor-acceptor interfaces, which are crucial for efficient exciton dissociation in bulk heterojunction solar cells.^{3,4}

This contribution presents the successful preparation of the title compounds **1**. The materials properties are investigated by polarized optical microscopy, differential scanning calorimetry, X-ray diffraction, UV-Vis- and fluorescence spectroscopy.



- ¹ M. Lehmann et al., *Tetrahedron* 1999, 55, 13377–13394.
- ² M. Lehmann, *Star-shaped Mesogens in Handbook of Liquid Crystals*, 2nd edition (eds. J. W. Goodby, P. J. Collings, T. Kato, C. Tschierske, H. Gleeson, P. Raynes), Wiley-VCH, Weinheim, 2013.
- ³ C. W. Tang, *Appl. Phys. Lett.* 1986, 48, 183–185.
- ⁴ G. Yu et al., *Science* 1995, 270, 1789–1791.

Polyphilic Hydrogen-Bonded Complexes Bearing Oligoethyleneglycol and Semiperfluorinated Molecular Segments

Laura Vogel^a, Marko Prehm^b, Dietmar Janietz^{a*}, Carsten Tschierske^b

^a Fraunhofer Institut Angewandte Polymerforschung, Geiselbergstr. 69, 14476 Potsdam-Golm.

^b Martin-Luther-Universität Halle-Wittenberg, Institut für Organische Chemie, Kurt-Mothes-Str. 2, 06120 Halle (Saale).

e-mail: dietmar.janietz@iap.fraunhofer.de

Self-recognition of diamino-1,3,5-triazines with suitably modified complementary synthons offers a powerful approach towards tailoring thermotropic mesophase morphologies.^{1,2} Thus, hydrogen bond initiated heterodimerization with semiperfluorinated benzoic acids leads to columnar mesophases with various 2D lattice symmetries. The triazine component was designed such that it contains either lipophilic alkyl segments³ or that it provides additional partially fluorinated molecular blocks.⁴

We present here mesomorphic structure formation of the diamino-1,3,5-triazine **1** appended with a hydrophilic oligoethyleneglycol chain in equimolar mixtures with the semiperfluorinated benzoic acids **2-5**.

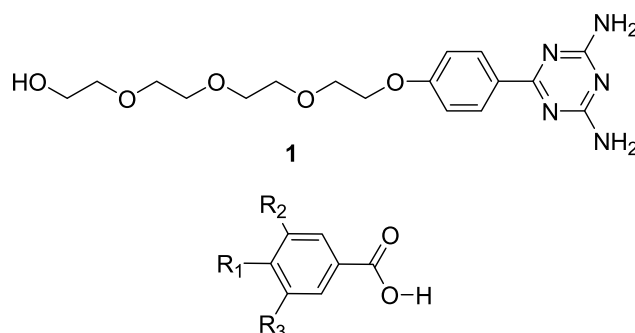


FIGURE 1. Chemical structure of the investigated compounds **1-5**.

The investigated 1:1 mixtures of the triazine **1** with the single chain carboxylic acids **2** show a direct transition to the isotropic liquid at temperatures quite different from the phase transition temperatures of the single components. While the SmC phases of the pure benzoic acids **2** disappear, the single melting transitions of **1/2** mixtures can be regarded as a hint that the aminotriazine **1** and the benzoic acids **2** do not act as

individual molecular species and association of the two components occurs.

Incorporation of at least a second partially fluorinated fragment into the acid component produces liquid crystallinity. The binary mixtures of the triazine **1** with the two-chain acids **3** display optical textures which point to columnar mesophases. However, so far the two-dimensional plane group could not be determined by X-ray because of the strong recrystallization tendency of the samples.

The textural features observed for the mixed systems with the two-chain and three-chain carboxylic acids **4** and **5**, respectively, are characteristic for hexagonal columnar mesophases. Noteworthy, association of the complementary molecular entities leads to mesophase induction for the non-liquid crystalline benzoic acids **4**. The X-ray diffraction pattern obtained for the mesophases of 1:1 mixtures **1/4** and **1/5** exhibit three sharp reflections in the small angle region and a diffuse halo in the wide angle regime. The position of the reflections of $1 : 1^{1/2} : 2$ prove the existence of columnar mesophases with hexagonal lattice symmetry.

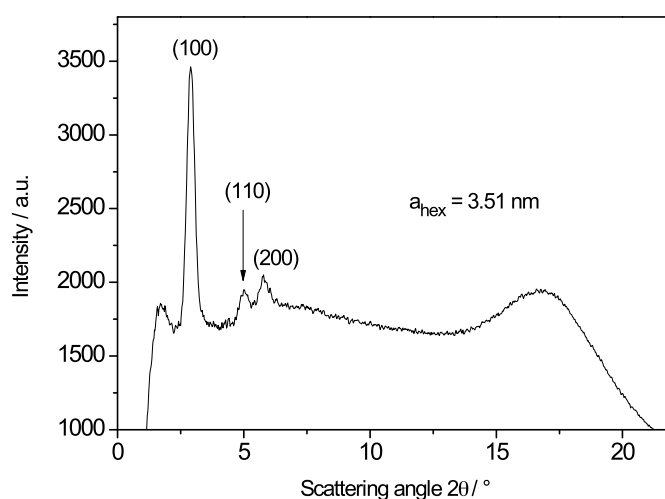


FIGURE 2. WAXS diffractogram of the 1:1 mixture **1/4**-[**4,6**].

Upon being heated, the birefringent mesophases of equimolar mixed systems **1/4** and **1/5** transform into a highly viscous optically isotropic phase. Even shearing does not induce any birefringence within the temperature range of this phase. DSC traces reveal an additional phase transition at more elevated temperatures, which is accompanied by a remarkable decrease in viscosity. These observations are a strong hint towards the existence of a cubic phase.

- ¹ A. Kohlmeier, L. Vogel, D. Janietz, *Soft Matter* 2013, **9**, 9476.
- ² D. Janietz, A. Kohlmeier, *Liq. Cryst.* 2009, **36**, 685.
- ³ A. Kohlmeier, D. Janietz, *Chem. Mater.* 2006, **18**, 59.
- ⁴ A. Kohlmeier, D. Janietz, *Chem. Eur. J.* 2010, **16**, 10453.

This work was supported by the BMBF-Initiative „Spitzenforschung und Innovation in den neuen Ländern“ within the cooperative project „Taschentuchlabor - Impulszentrum für Integrierte Bioanalyse“ (FKZ 03IS2201C).

Bent-shaped liquid crystals – Quantum chemical calculations or de novo synthesis?

Michal Kohout^{a*}, Jiří Tůma^a, Vladimíra Novotná^b, Jiří Svoboda^a

^a Department of Organic Chemistry, Institute of Chemical Technology Prague, Technická 5, CZ-166 28, Prague, Czech Republic

^b Institute of Physics, Academy of Sciences of the Czech Republic, Na Slovance 2, 18221, Prague 8, Czech Republic

e-mail: Michal.Kohout@vscht.cz

Since the discovery of their polar order and macroscopic chirality,^{1,2} the bent-shaped materials have gained considerable interest in the field of liquid crystals. The general structure of the bent-shaped materials, particularly, compounds with additional functionality such as light sensitive group, polymerizable unit etc. have been thoroughly studied and the findings were summarized in a number of reviews.³⁻⁵ However, a general rule for designing a material with specific properties has not been stated so far. Recently, we have focused on the synthesis of laterally substituted resorcinol-based compounds which comprise the missing pieces in the puzzle of bent-shaped liquid crystals with resorcinol as a central core, and compared their properties with compounds based on laterally substituted 3-hydroxybenzoic acid (**Fig. 1**).⁶ We studied the materials with optical polarizing microscopy, differential scanning calorimetry as well as x-ray diffraction and found a linking thread between the structure and physical properties of structurally related compounds. To find a key stone responsible for the similarities in the mesomorphic behaviour, we performed ab initio calculations for the selected representative of each series of compounds.

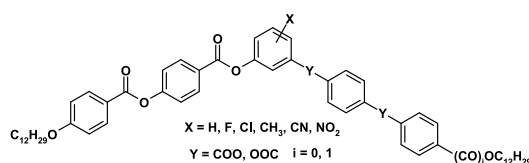


Figure 1 General structure of the studied materials

The results indicate that the mesomorphic properties of a new bent-shaped liquid crystal could be predicted on the basis of electron density distribution along the molecule. In this contribution we present features in the map of electrostatic potential which may be considered typical for materials forming a B₁ type of columnar phase (**Fig. 2**).



Figure 2 Electrostatic potential distribution along the conformer with minimum energy of a bent-shaped liquid crystal based on non-substituted 3-hydroxybenzoic acid.

Maps of electrostatic potential, similar to that shown in **Fig. 2**, were found for compounds with different substitution on the central core. All compounds with such electrostatic potential (electron density) distribution in the molecule exhibited a columnar mesophase of the B₁-type. In the contribution the influence of various structural elements on the overall electrostatic potential density and self-assembly ability of various compounds will also be discussed.

This work was supported by the Czech Science Foundation (projects No. 13-07397P and 13-14133S).

¹ T. Niori, T. Sekine, J. Watanabe, T. Furukawa, H. Takezoe. *J. Mater. Chem.* 1996, **6**, 1231.

² D. R. Link, G. Natale, R. Shao, J. E. Maclennan, N. A. Clark, E. Körblova, D. M. Walba. *Science* 1997, **278**, 1924.

³ R. A. Reddy, C. Tschierske. *J. Mater. Chem.* 2006, **16**, 907.

⁴ I. C. Pintre, J. L. Serrano, M. B. Ros, J. Martínez-Perdiguero, I. Alonso, J. Ortega, C. L. Folcia, J. Etxebarria, R. Alicante, B. Villacampa. *J. Mater. Chem.* 2010, **20**, 2965.

⁵ C. Tschierske. *Angew. Chem. Int. Ed.* 2013, **52**, 8828.

⁶ M. Kohout, V. Kozmík, M. Slabochová, J. Tůma, J. Svoboda, V. Novotná, D. Pocięcha. *Liq. Cryst.* **2014**, submitted.

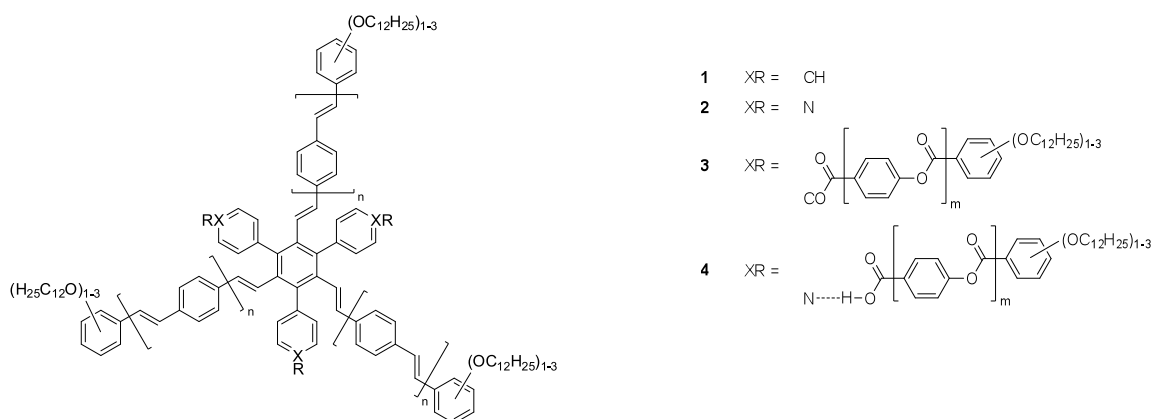
Star-shaped mesogens with a hexasubstituted C₃-symmetric benzene centre

Philipp Maier and Matthias Lehmann

Institute of Organic Chemistry, University of Würzburg, Am Hubland, D-97074 Würzburg.

e-mail: ph.maier@uni-wuerzburg.de

Liquid crystalline hexa-substituted, shape-persistent benzenes are sterically crowded star molecules for which in the majority of structures, the benzene centre is symmetrically linked with six identical arms.¹ Such mesogens form predominantly nematic phases, when the arms are connected via triple bonds to reduce the steric interaction. The synthesis of liquid crystalline C₃-symmetric benzenes with six arms is more challenging, but amplifies the possibility to control nanosegregation and functionality. In the few known examples three arms were connected by non-steric demanding triple bonds, and a second set of substituents consisting of aliphatic chains was attached via oxygen or amide functions which controlled the stacking behavior in columns.^{2,3}



In this contribution the preparation of new shape-persistent stars **1-4** is presented. They consist of three oligo(phenylenevinylene) arms and phenyl or pyridyl groups attached to a benzene core. Such structures allow incorporating additional extended arms either by covalent bonds, such as in mesogen **3**, or by hydrogen bonds (compound **4**). The structure-property-relationships of the new star mesogens are studied by polarizing optical microscopy, differential scanning calorimetry, X-ray diffraction, UV-Vis- and fluorescence spectroscopy.

References

- ¹ Review: H. Detert, M. Lehmann, H. Meier, *Materials* 2010, **3**, 3218–3330.
- ² M. L. Bushey, T.-Q. Nguyen, C. Nuckolls, *J. Am. Chem. Soc.* 2003, **125**, 8264–8269.
- ³ L. de Vega et al., *J. Org. Chem.* 2012, **77**, 10891–10896.

Shape-persistent V-shaped nematogens with cyclohexane units

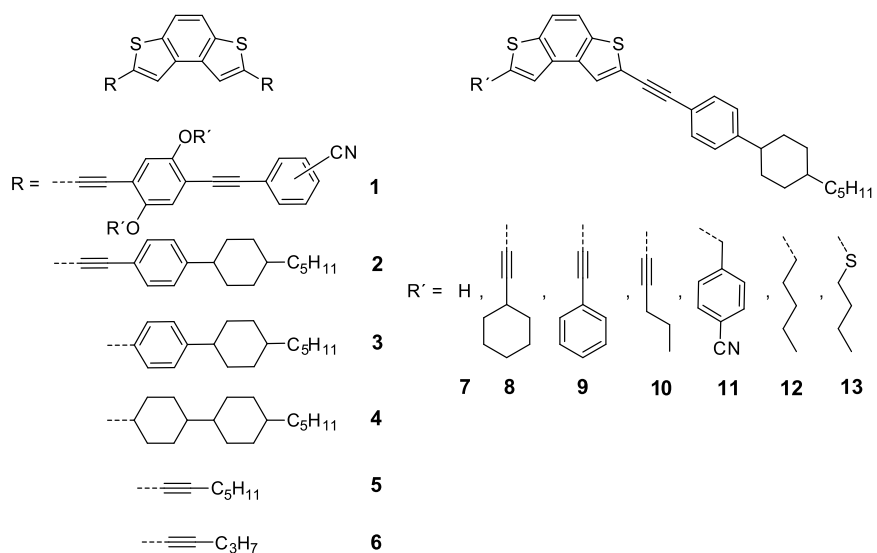
Stefan Maisch and Matthias Lehmann

Julius Maximilians-University of Würzburg

e-mail: stefan.maisch@uni-wuerzburg.de

V-shaped mesogens with a bending angle of 109.4° ,^[1] a planar, shape-persistent structure as well as a core dipole moment^[2] are proposed as a class of molecules with high potential towards the formation of a N_b -phase. Mesogen **1** with a benzo[1,2-b:4,3-b']dithiophene bending unit show a direct transition from the isotropic to a monotropic biaxial nematic phase. In order to stabilize the mesophase, lower the transition temperature and viscosity and to obtain colourless compounds, we exchanged phenylene ethynylene building blocks by cyclohexane units at different positions of the wings. Interestingly none of the symmetric compounds without lateral substitution with flexible chains (compound **2-6**) exhibit LC properties. Exclusively the hockey-stick mesogen **7** reveals a broad optical positive nematic mesophase, indicating the calamitic nature of the nematogen.

In the present contribution, the synthesis of compound **7** substituted by a number of different building blocks is shown. The thermotropic properties are investigated by optical microscopy, differential scanning calorimetry and X-ray scattering in order to determine to which degree the structure can be modified in order to lose the nematic properties. The nature of the nematic phases is studied by Conoscopy.



References

- [1] G.R. Luckhurst. *Thin solid films* 2001, **40**, 393.
- [2] M. Lehmann, J. Seltmann. *J. Org. Chem.* 2009, **5**, 73.
- [3] J. Seltmann, K. Müller, S. Klein, M. Lehmann. *Chem. Commun.* 2011, **47**, 6680.

Synthesis of Novel Liquid Crystal Materials for Ferroelectric Display

Rami Pashmeah^a, Mike Hird^a

^a Chemistry department, Hull University, Gottingham Road, Hull, HU6 7RX, UK.

e-mail: ram.rom.nano@gmail.com

Ferroelectric liquid crystal displays switch faster than conventional liquid crystal displays, and offer much higher resolution, and hence are suitable for microdisplay applications¹. Difluoroterphenyls² are well-recognised as excellent host materials for ferroelectric mixtures.

The synthesis of ortho difluoroterphenyls and ortho difluoroquarterphenyls with bulky terminal chains are detailed. The bulky terminal chain consists of a methoxy-4,4-dimethylpentyl group, a trimethylsilyl unit and a dimethylethyl group. All the final products will be evaluated for their mesomorphic properties and a wide range of other physical properties, and the most suitable compounds will be formulated into mixtures for evaluation in prototype microdisplays.

- 1- M. Walba, D.J. Dyer, X.H Chen, U. Muller, P Cobber, R. Shao, and N.A Clark, *Molecular Crystal and Liquid Crystal* 1996, **288**,83.
- 2- G. W. Gray, M. Hird, D. Lacey and K. J. Toyne, *J. Chem. Soc., Perkin Trans. 2*, 1989, 2041.

4-Cyanoresorcinol derived bent-core mesogens with different wing groups

M. Poppe¹, A. Lehmann¹, M. Prehm¹, G. Tamba², A. Eremin², C. Tschierske¹

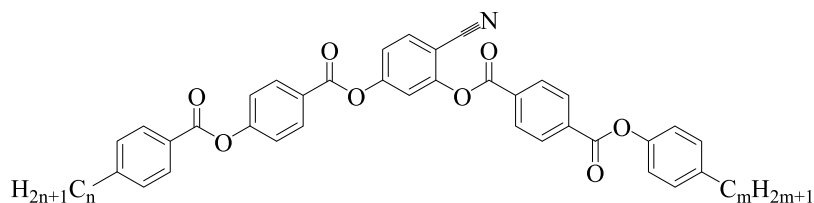
¹Institute of Chemistry, Martin-Luther-University Halle-Wittenberg, Kurt-Mothes-Str. 2, 06120 Halle, Germany

²Otto-von-Guericke-University Magdeburg, Universitätsplatz 2, 39016 Magdeburg, Germany

e-mail: marco.poppe@student.uni-halle.de

In contrast to the usually observed tilted polar LC phases of bent-core mesogens their non-tilted analogues are relatively rare [1]. Recently, non-tilted smectic phases, such as SmAP_A, [2,3] SmAP_R and SmAP_α, which arose significant interest, were proclaimed for 4-cyanoresorcinol based bent-core mesogens with two terephthalate wing groups [3].

Here we report the synthesis and investigation of a new series of non-symmetric 4-cyanoresorcinol based bent-core mesogens, combining two different types of wing groups at both sides; one is a phenyl benzoate (left side), the other a terephthalate wing (right side, see formula).



During the elongation of the terminal *n*-alkyl groups at both ends we observed a series of different LC phases and nearly a continuous transition from non-tilted to anticlinic and synclinic tilted polar smectic phases. The transition takes place when the terminal *n*-alkyl chains at both ends become $\geq C_{12}$, so that the contribution of the chains plays an important role.

While the transition from non-tilted (short *n*-alkyl chains) to tilted (long *n*-alkyl chains) smectic phases happens we found a new optically uniaxial, antiferroelectric switching and slightly tilted smectic phase (SmC_{xy}PA). This new phase was observed for compounds with medium chain length and arose special interest so that it was investigated in more detail.

References:

- [1] R. A. Reddy, C. Tschierske, *J. Mater. Chem.* 2006, **16**, 907; A. Eremin, A. Jakli, *Soft Matter* 2013, **9**, 615.
- [2] L. Kovalenko, M. W. Schröder, R. A. Reddy, S. Diele, G. Pelzl, W. Weissflog, *Liq. Cryst.* 2005, **32**, 857.
- [3] C. Keith, M. Prehm, Y. Panarin, J. Vij, C. Tschierske, *Chem. Comm.* 2010, **46**, 3702.; Y. P. Panarin, M. Nagaraj, S. Sreenilayam, J. K. Vij, A. Lehmann, C. Tschierske, *Phys. Rev. Lett.* 2011, **107**, 247801.

Bolapolyphiphiles with liquid crystalline and membrane modifying properties

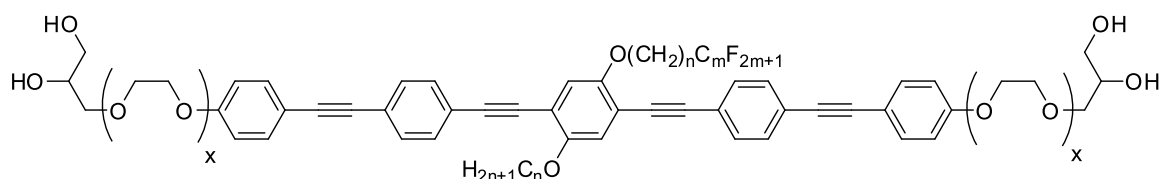
S. Poppe¹, H. Ebert¹, M. Prehm¹, S. Werner², K. Bacia², C. Tschierske¹

¹Institute of Chemistry, Martin-Luther-University Halle-Wittenberg, Kurt-Mothes-Str. 2, 06120 Halle

²ZIK HALOmem, Martin-Luther-University Halle-Wittenberg, 06120 Halle

e-mail: silvio.poppe@student.uni-halle.de

T-shaped and X-shaped bolapolyphiphiles form a series of complex thermotropic LC phases representing fluid honeycomb structures [1]. Recently, ternary and quarternary X-shaped bolaamphiphiles arose special interest because the complexity of their LC phases was further enhanced by formation of multi-color tiling patterns, where the space inside the honeycombs is filled by different materials [1]. As the length of the hydrophobic oligo(phenylene ethynylene) core fits well with the diameter of the lipophilic region of double layer lipid biomembranes (~3 nm) it was of interest to study the effects of these bolaamphiphiles on phospholipide model membranes. This requires molecules with enhanced solubility in aqueous systems. To this end novel ternary and quarternary X-shaped oligo(phenylene ethynylene) based bolapolyphiphiles with enlarged polar head groups and two equal or different lateral alkyl or semiperfluorinated alkyl chains were synthesized (see formula).



Depending on the length of the lateral and terminal chains the molecules shows different LC phases. These bolapolyphiles were incorporated into phospholipide membranes of giant unilamellar vesicles (GUVs) where they form a kind of raft domains with unique six-fold symmetric structure. The shape of these domains strongly depends on the head group structure. [2] Possible modes of organization of these molecules in the membranes are discussed and compared with the liquid crystalline self-assembly of the bulk materials.

References:

- [1] C. Tschierske, *Angew. Chem.* 2013, **125**, 8992–9047.
- [2] S. Werner, H. Ebert, A. Achilles, S. Poppe, B.-D. Lechner, A. Blume, K. Saalwächter, C. Tschierske, K. Bacia, *Angew. Chem.* submitted.

Design and synthesis of chiral liquid crystals with „de Vries-like“ mesomorphic behaviour

Anna Poryvai^a, Alexey Bubnov^b, Michal Kohout^{*a}, Vladimíra Novotná^b, Jiří Svoboda^a

^a Department of Organic Chemistry, Institute of Chemical Technology Prague, Technická 5, CZ-166 28, Prague, Czech Republic

^b Institute of Physics, Academy of Sciences of the Czech Republic, Na Slovance 2, 18221, Prague 8, Czech Republic

e-mail: Michal.Kohout@vscht.cz

Chiral smectics possessing the ferroelectric polar ordering are of high interest for their potential applicability in photonics and electro-optic devices.^{1,2} However, the majority of existing ferroelectric liquid crystals suffers from layer contraction at the transition from orthogonal smectic A* (SmA*) to tilted ferroelectric smectic C* (SmC*) phase. This layer contraction leads to chevron configuration of SmC* phase and formation of so-called “zig-zag” defects that drastically diminish the performance of a surface-stabilized LC devices.³ In early 70's the existence of the phase transition from the orthogonal to tilted smectic phase with no layer contraction was predicted theoretically.⁴ However, only in late 90's, utilizing ferroelectric and antiferroelectric liquid crystalline materials in electro-optical devices triggered an extensive search for smectics without or with at least very low (less than 4% of the smectic layer thickness) layer contraction⁵. Several groups have focused on design and synthesis of these, so-called “de Vries-type” materials. However, no rational design strategy has been proposed so far.

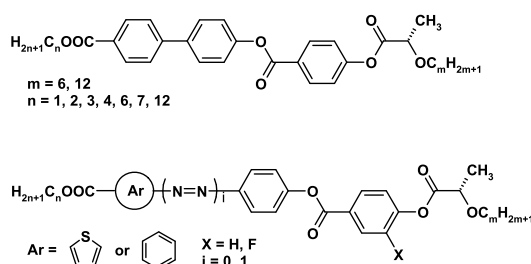


Figure 1 General structure of the studied materials⁶

Recently, we have described mesomorphic behaviour of series of lactic acid derivatives with one lactate group possessing nonchiral carboxylate chain which exhibited very small layer contraction.⁵ In this follow up study we decided to change the structure of the molecule by introducing a

lateral substituent, spacer between the aromatic units of the central core as well as by replacing phenyl ring with thiophene unit (Fig. 1).

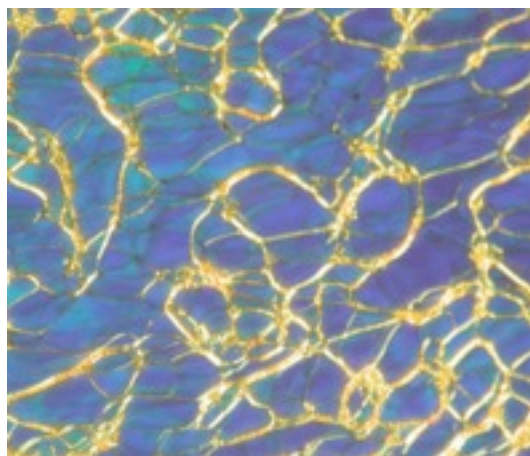


Figure 2 Texture of a homeotropic SmC* phase at 30 °C, image width 150 μm .

Properties of the new materials have been studied by optical polarizing microscopy, differential scanning calorimetry, small angle X-ray scattering and dielectric spectroscopy. The results indicate that every unit of the general structure (Fig. 1) plays an important role in the self-assembly of the molecules and thus mesophase formation. Replacing an aromatic ring with a thiophene unit in the molecular structure leads to formation of SmC* phase in a broad temperature range. Introduction of an azo spacer in the core of the liquid crystal induces formation of a chiral nematic phase, however, with higher transition temperatures. The influence of the length of terminal chains will be discussed as well.

This work was supported by the Czech Science Foundation (projects No. 13-07397P and P204/11/0723).

¹ J.P.F. Lagerwall, F. Giesselmann. *ChemPhysChem* 2006, **7**, 20–45.

² J.P.F. Lagerwall, G. Scalia. *Current Applied Physics* 2012, **12**, 1387–1412.

³ T. P. Rieker, N. A. Clark, G. S. Smith, D. S. Parmar, E. B. Sirota, C. R. Safinya. *Phys. Rev. Lett.* 1987, **59**, 2658–2661.

⁴ A. de Vries. *Mol. Cryst. Liq. Cryst.* 1977, **41**, 27–31.

⁵ Giesselmann F., Zugenmaier P., Dierking I., Lagerwall T. S., Stebler B., Kašpar M., Hamplová V., Glogarová M.: *Phys. Rev. E* 1999, **60**, 598.

⁶ M. Kohout, A. Bubnov, V. Novotná, J. Svoboda. 14th Int. Conf. on Ferroelectric Liq. Cryst. 2013, poster No. 31, Magdeburg, Germany.

Luminescent Discotic Liquid Crystals based on a Nitrogen-rich Core

Thorsten Rieth, Stefan Glang, Dorothee Borchmann, and Heiner Detert*

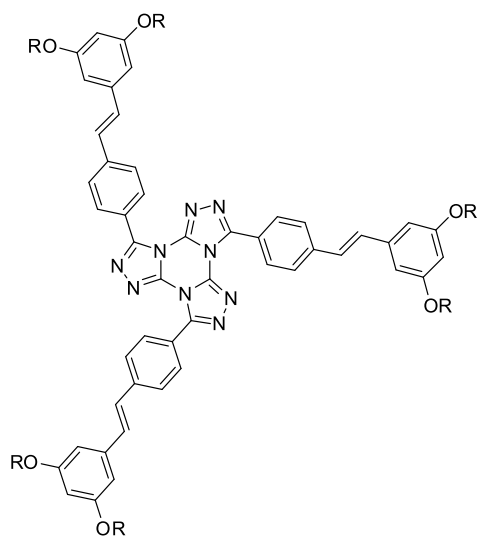
Institute of Organic Chemistry, Johannes Gutenberg–University Mainz,
Duesbergweg 10 - 14, D55099 Mainz, Germany, Fax: +49-(0)6131-39-25338

e-mail: detert@uni-mainz.de

Star-shaped planar aromatic polycycles containing nitrogen atoms, like hexaazatriphenylene and triazatruxene, deserve special attention as cores for discotic liquid crystals. Like their analogous polycyclic hydrocarbons, they are interesting for a variety of applications in organic electronics. The replacement of sp^2 -carbon atoms by nitrogen atoms does not change the structural characteristics, while the electronic properties can be modified largely, e. g. switching from p-type towards n-type semiconductors.¹

Recently, Gallardo² and we³ discovered the ability of the heterocyclic tristriazolotriazine (TTT) to be a suitable core for the formation of discotic liquid crystals. First reported by Huisgen⁴, the annulation of three triazoles to a central 1,3,5-triazine leads to three C_3 -symmetrical tristriazolotriazines

We report the synthesis, optical and thermal properties of a series of tristriazolotriazines with alkoxyphenyl groups and also their higher conjugated homologues bearing a stilbene moiety between the core and the lateral alkoxy groups. Triphenyl-TTTs with alkoxy side chains from hexyl to dodecyl form broad hexagonal columnar mesophases, this demonstrates that the tristriazolotriazine is an excellent core for discotic liquid crystals. The higher homologues are not mesomorphic or form LC phases with a different structure.



- ¹ S. Laschat, F. Giesselmann et al. *Angew. Chem.* 2007, 119, 4916
- ² R. Christiano, H. Gallardo, et al. *Chem. Commun.* 2008, 5134
- ³ S. Glang, H. Detert et al. *Proc. 36th German Topical Meeting Liquid Crystals*
a) 2008, 125 and b) 2010, 133
- ⁴ R. Huisgen, H.J. Sturm, M. Seidel. *Chem. Ber.* 1961, 94, 1555

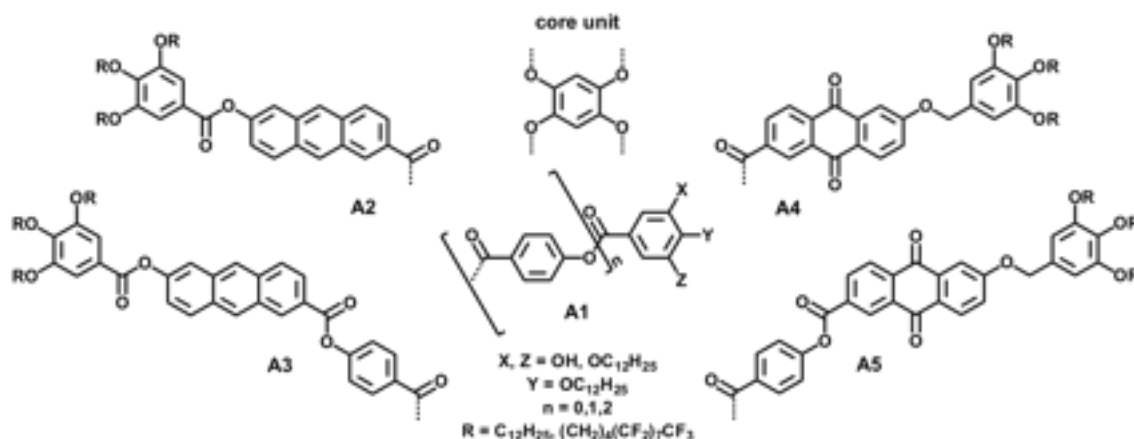
Synthesis and Properties of Differently Equipped Four-Armed Star-Shaped Mesogens

Sabine Roth*, Steffi Gloza, Matthias Lehmann

Julius-Maximilians-University of Würzburg.

e-mail: matthias.lehmann@uni-wuerzburg.de

Semiflexible star-shaped oligobenzoates with three arms (Hekates) are reported to fold and pack in a series of complex columnar and cubic mesophases driven by nanosegregation.^{1,2} Four-armed stars, for which only the parent systems are known,^{3,4} may behave differently due to the possibility of pair-wise nanosegregation of their arms. We recently investigated such mesogens (**A1**) containing four symmetrically linked oligobenzoate arms ($n = 0 - 2$) around the 1,2,4,5-tetrahydroxybenzene core. These materials form columnar and smectic phases depending on the number of alkoxy chains. The models suggest an indeed pair-wise folding of the arms in the columnar phase, which is of interest when chromophores (**A2–A5**) are incorporated.



In this contribution we present the synthesis of a variety of four-armed star-mesogens containing benzoate, anthraquinone and anthracene as repeating units with C_2 -symmetry (Figure). The thermotropic behavior is studied as a function of different, incompatible lateral chains which are also applied to separate donor and acceptor units. The achieved nanomorphology may be of interest for organic electronics. All compounds are characterised by polarised optical microscopy, differential scanning calorimetry, X-ray diffraction, UV-Vis absorption and fluorescence spectroscopy.

- ¹ M. Lehmann, M. Jahr, F. C. Grozema, R. D. Abellon, L. D. A. Siebbeles, M. Müller, *Adv. Mater.* **2008**, 20, 4414–4418.
- ² M. Lehmann, *Chem. Eur. J.* **2009**, 15, 3628–3651.
- ³ W. D. J. A. Norbert, J. W. Goodby, M. Hird, K. J. Toyne, *Mol. Cryst. Liq. Cryst.* **1995**, 260, 339–350.
- ⁴ S. Berg, V. Krone, H. Ringsdorf, U. Quotschalla, H. Paulus, *Liq. Cryst.* **1991**, 9, 151–163.

Oligomeric materials composed of bent-core and calamitic mesogenic units – mesomorphic and electro-optical properties

M.-G. Tamba^{*}, G. Pelz, U. Baumeister and W. Weissflog

Martin-Luther-University Halle-Wittenberg, Institute of Physical Chemistry,
D-06108 Halle, Von-Danckelmann-Platz 4, Germany

maria-gabriela.tamba@ovgu.de

Since 1996 when Niori et al.¹ reported on bent-core mesogens which are able to form smectic phases with polar order, these molecular systems have been extensively studied and represent a major subfield of thermotropic liquid crystals, different from the “classical” types such as calamitic and disc-like mesogens. Due to their particular design the molecules can be packed in the bent direction which leads to a long-range correlation of the lateral dipoles. Depending on the polar order correlation between adjacent layers, ferroelectric or antiferroelectric phases can be differentiated. From these smectic phases 2D phases (columnar phases) can also be derived which are considered to consist of layer fragments (broken layers). Such bent-core mesogens are able to form “calamitic phases”. These phases are of special interest due to unusual physical properties, e.g. biaxiality of uniaxial phases, special electroconvection patterns and high flexoelectricity of nematic phases.^{2, 3} There are different ways to design suitable molecules.⁴ One of these is a covalent linking of bent-core mesogenic units to calamitic moieties.^{5, 6} In order to investigate such compounds in more detail several series of non-symmetric dimers and symmetric trimers were synthesized. The liquid crystalline properties of the dimers (type **A**, see Fig. 1) and trimers (type **B** and **C**, see Fig. 1) strongly depend on the type and length of the aliphatic spacer, the length of terminal chains, the number of aromatic rings and the type and direction of connecting groups between the rings. To study the influence of the chemical structure on the mesophase behaviour, we have varied all these fragments. Five-, six- or seven-ring bent-core moieties are connected by spacer of different nature and length to different calamitic units containing one, two or three phenyl rings. On this way it is possible

to compare the behaviour of corresponding biphenyl, phenyl benzoate and azobenzene derivatives.

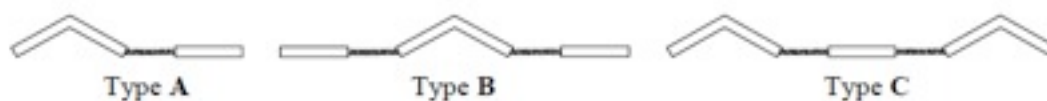


Fig. 1: Non-symmetric dimers type A and symmetric trimers type B and C.

Dimers type A

A representative example for the dimer type A containing the calamitic hexyloxybenzoyloxy-phenyl unit (dimer series A-1) together with the mesophase types and transition temperatures is given in Fig. 2. The compounds A-1 have a constant length of the alkyloxy chain attached to the bent-core unit ($n = 12$) and to the calamitic part ($p = 6$), however the length of the spacer (m) varies. All compounds exhibit liquid crystalline phases. The odd-numbered dimers exhibit exclusively columnar phases of different types. The even-numbered spacer lengths ($m = 6, 8, 10$) give rise to both nematic and columnar phases while for the longer member A-1j ($m = 12$) nematic and smectic (SmC_d) phases are observed. Thus, increasing spacer length appeared to promote smectic over columnar behaviour. The shortest member of the series, A-1a ($m = 2$), exhibits exclusively nematic behaviour. Interestingly, we could observe nematic phases only for the even-membered dimers.

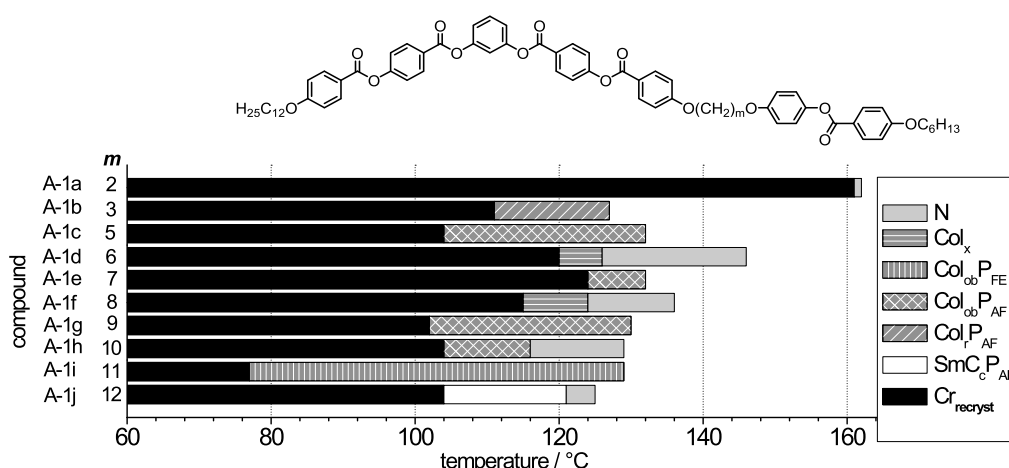


Fig. 2: Mesophase behaviour and transition temperatures (°C) of dimer series A-1, taken from the first DSC cooling scans.

In order to demonstrate the remarkable alternation effect, the dependence of the N – I, Col – I, Col – N and SmC_c – N transition temperatures on the number of methylene units, *m*, in the flexible spacer for the dimer series **A-1** is shown in Fig. 3.

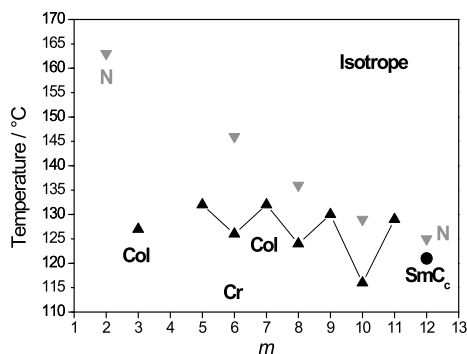


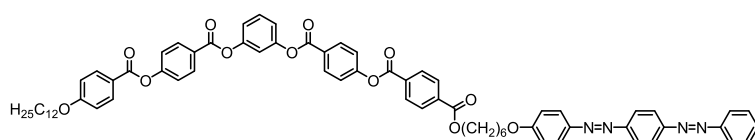
Fig. 3: Dependence of the transition temperatures on the number of methylene units, *m*, in the flexible spacer for the dimer series **A-1**; ▲ Col-I and Col-N transitions, ▼ N-I transitions and ● SmC_c-N transition; values are taken from the first cooling DSC scans.

The general tendency is a clear alternation of the isotropic – liquid crystal transition temperatures (which are not lined together in Fig. 3) with increasing number of methylene units in the flexible spacer, *m*, where the even members exhibit the higher values. A second type of alternation is attributed to the Col – I and Col – N transition temperatures (black line). Using this aspect the odd-numbered homologues show the higher transition temperatures. It seems that for the even members the increase of the number of methylene units in the spacer is associated with a continuous decrease of the N – Col transition temperatures. The alternation of the transition temperatures but also of the phase type in dependence of the spacer length is highly unusual, especially in the combination of nematic and columnar phases. On the other hand, looking at the N – I transition temperatures, which exist only for the even-numbered dimers, one can observe a monotone decrease on increasing the spacer length from 163 °C (*m* = 2) to 125 °C (*m* = 12). On applying a triangular-wave field above 15 V μ m⁻¹ almost all Col_{ob} phases of compounds **A-1** show an electro-optical switching with a current response indicating an antiferroelectric ground state, i.e. two polarization current peaks per half period were recorded. An exception is the Col_{ob} phase of compound **A-1i** which exhibits a ferroelectric switching process.

The values of the spontaneous polarization P_S was found to be for these Col_{ob} phases between 350–410 nC cm⁻². The P_S values increase on increasing the spacer length and on decreasing the temperature.

Interestingly, the application of an electric field on the SmC_c phase of compound **A-1j** leads to an electro-optical switching with a current response indicating an antiferroelectric ground state ($P_S = 300$ nC cm⁻²). Further studies of the influence of the spacer length in dimer series with different lengths of the terminal chains attached to the calamitic mesogenic unit and to the bent-core mesogenic unit prove nematic, columnar and/or various polar smectic phases and B₇' phases.

In order to study the influence of the chemical structure of the calamitic part on the mesophase behaviour a dimer series with azobenzene unit (dimer series **A-2**, see Fig. 4) was prepared.^{6b}



Cr 160 [66.41] (SmC_sP_{FE} 151 [0.13]) SmC_aP_{AF} 175 [29.05] I

Fig. 4: Example of a dimer type **A-2** containing azobenzene unit.

An exciting behaviour of the azobenzene compound **A-2c** (see Fig. 4 and Fig. 5) is the existence of a SmC_{synclinc} – SmC_{anticlinc} phase transition, which is characterized by a small transition enthalpy. The phase transition can be observed by POM due to typical turbulences between both smectic states, also reported for a comparable transition between two SmC phases of hockey-stick shaped mesogens.⁷ According to the defect lines observed by POM, the anticlinc SmC phase proved to be the high temperature phase. Electro-optical investigations indicated for the SmC_a phase the occurrence of two separate repolarization peaks in each half period of the applied triangular voltage field, which is characteristic for an antiferroelectric switching (SmC_aP_{AF} phase, $P_S = 700$ nC cm⁻²). The SmC_s phase exhibits a ferroelectric switching process (SmC_sP_{FE} phase, $P_S = 850$ nC cm⁻²). All dimers **A-2** exhibit smectic mesophases. The dependence of the transition temperatures and of the phase type on the number of carbon atoms in the flexible spacer m is given in Fig. 5.

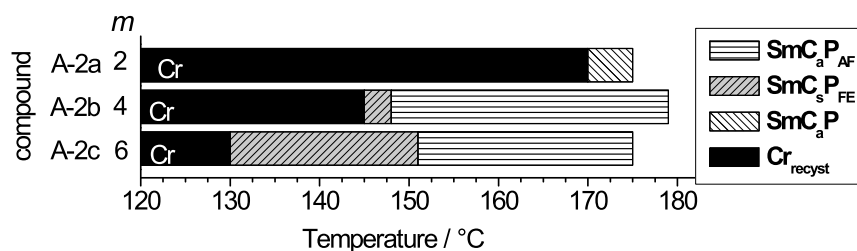


Fig. 5: Mesophase behaviour and transition temperatures (°C) of dimer series **A-2**.

Trimers type B

The trimers type **B** and **C** consist of molecules containing three mesogenic units joined by two flexible spacers. Several series of symmetric trimers **B** derived from resorcinol (trimer series **B-1**, see Fig. 6) and isophthalic acid (trimer series **B-2**) were synthesized. The two calamitic hexyloxybenzoyloxyphenyl units are attached to the terminal position of the bent-core unit by aliphatic spacer (*m*). The properties of these trimers were compared to those of the corresponding dimers and “monomers”.

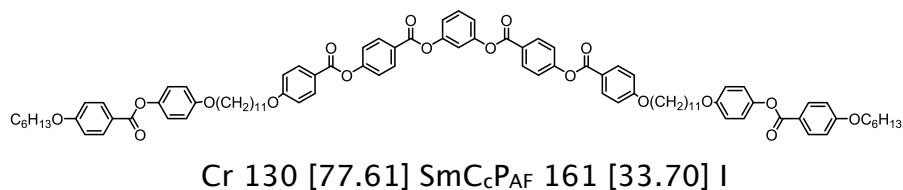


Fig. 6: Example of a trimer type **B-1** containing two calamitic hexyloxybenzoyloxyphenyl units.

Nearly all trimers **B** exhibit smectic mesophases. The transition temperatures exhibit an odd-even effect on increasing *m*. The even members show the higher values. The trimers derived from resorcinol (series **B-1**) exhibit additionally nematic phases for the even-membered compounds, similar to the corresponding dimers type **A-1**. Variation of the direction of the ester linking group (trimers of the series **B-2**), as well as introduction of two further aromatic rings in the bent-core mesogenic unit results in an enhancement of the clearing and melting point and in appearance of nematic phases.

Trimers type C

The inverse type of trimers (trimers type C) consists of two bent-core units and one calamitic moiety. Trimers containing biphenyl units (series C-1, $q = 1$, see Fig 6), phenyl units (series C-2, $q = 0$, see Fig 6) and azobenzene units (series C-3) were prepared. Different smectic phases have been observed. Electro-optical investigations give evidence for the antiferroelectric nature of these phases.

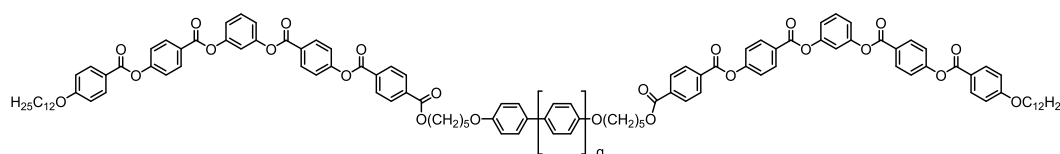


Fig. 7: Trimers type C-1 and C-2 containing biphenyl or phenyl units.

References

- ¹ T. Niori, F. Sekine, J. Watanabe, T. Furukawa and H. Takezoe, *J. Mater. Chem.* 1996, **6**, 1213.
- ² J. Harden, B. Mbanga, N. Eber, K. Fodor-Csorba, S. Sprunt, J. T. Gleeson, A. Jakli, *Phys. Rev. Lett.* 2006, **97**, 157802.
- ³ (a) M.-G. Tamba, W. Weissflog, A. Eremin, J. Heuer and R. Stannarius, *Eur. Phys. J. E* 2007, **22**, 85; (b) M.-G. Tamba, U. Baumeister, G. Pelzl, W. Weissflog, *Liq. Cryst.* 2010, **37**, 853; (c) J. Heuer, R. Stannarius, M.-G. Tamba, W. Weissflog, *Phys. Rev. E* 2008, **77**: 0562061; (d) R. Stannarius, J. Heuer, *Eur. Phys. J. E* 2007, **24**, 27; (e) R. Stannarius, A. Eremin, M.-G. Tamba, G. Pelzl, W. Weissflog, *Phys. Rev. E* 2007, **76**, 0617041; (f) M.-G. Tamba, W. Weissflog, A. Eremin, J. Heuer, R. Stannarius, *Eur. Phys. J. E* 2007, **22**, 85.
- ⁴ G. Pelzl, W. Weissflog in A. Ramamoorthy: *Thermotropic Liquid Crystals – Recent Advances*, Springer, 2007, 1.
- ⁵ C. V. Yelamaggad, S. K. Prasad, G. G. Nair, I. S. Shashikala, D. S. Shankar Rao, C. V. Lobo, S. Chandrasekhar, *Angew. Chem. Int. Ed.* 2004, **43**, 3429.
- ⁶ (a) M.-G. Tamba, B. Kosata, K. Pelz, S. Diele, G. Pelzl, Z. Vakhovskaya, H. Kresse and W. Weissflog, *Soft Matter* 2006, **2**, 60; (b) M.-G. Tamba, A. Bobrovsky, V. Shibaev, G. Pelzl, U. Baumeister, W. Weissflog, *Liq. Cryst.* 2011, **38**, 1531; (c) S. Haddawi, M.-G. Tamba, G. Pelzl, W. Weissflog, U. Baumeister, *Soft Matter* 2010, **6**, 1170.
- ⁷ B. Das, S. Grande, W. Weissflog, A. Eremin, M. W. Schröder, G. Pelzl, S. Diele, H. Kresse, *Liq. Cryst.* 2003, **30**, 529.

Chiral HPLC for a study of the optical purity of liquid-crystalline materials derived from lactic acid

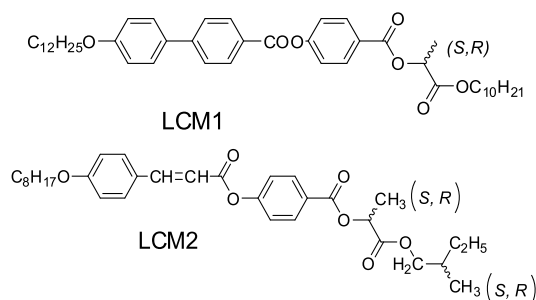
T. Vojtylová^{a,b}, M. Kašpar^a, V. Hamplová^a, V. Novotná^a and D. Sýkora^b

^a. Institute of Physics, Academy of Sciences of the Czech Republic, Na Slovance 1999/2; 182 21 Prague 8, Czech Republic.

^b. Institute of Chemical Technology, Technická 5; 166 28 Prague 6; Czech Republic.

e-mail: vojtyl@fzu.cz

Two new types of liquid-crystalline materials (LCM) were prepared by derivatization of lactic acid. General formulas of the materials labeled LCM1 and LCM2 are:



Compound LCM1 with one chiral centre in the molecule was prepared as racemic LCM1(RAC) and as the enantiomer LCM1(S). The other compound LCM2 derived from lactic acid having two chiral centers was prepared in four different variations: (RAC,S), (S,RAC) (RAC,RAC) and (S,S). Both materials exhibit of the $\text{SmA}^*-\text{SmC}^*$ or the $\text{TGBA}-\text{TGBC}$ phase sequences in a wide temperature range down to room temperature.

Although mesomorphic properties of ferroelectric materials can be affected by optical purity of the compounds [1–3], the control of enantiomeric impurities content is not common yet. In some previous works the dependence of liquid-crystalline properties on optical purity of liquid crystalline (LC) materials have been described, e.g. $\text{SmC}^*\alpha - \text{SmC}^*$ transition [4,5] or tilt-polarization-coupling in the SmC^* as well as the electroclinic effect in the SmA^* phase [2]. It has been described that some mesophases appear only with enantiomerically pure materials or after their slight racemization with the addition of the other enantiomer in amounts below 3 % (w/w).

Possibilities of separations of optical enantiomers and diastereomers of lactate based materials were studied by high performance liquid

chromatography (HPLC) using chiral stationary phase based on amylose modified silica gel. The separation of the individual enantiomers is based on their slight difference in retention on a suitable chiral stationary phase. The separation of LC materials is very challenging as typical LC compounds are relatively large molecules (average molecular mass around 500 – 700 g.mol⁻¹) possessing bulky achiral part and much smaller chiral moiety. Thus, the separation selectivity of the chiral stationary phase has to be very high to reach a successful separation of the individual enantiomers. Chiral sorbents based on derivatized polysaccharides, mainly amylose and cellulose, belong to the most widespread successfully used chiral stationary phases (CSPs) with very broad applicability [6, 7].

Separation conditions for LCM1 and LCM2 were optimized for two chiral columns, Lux Amylose-2 (LA) and Chiralpak AD-3 (CP). Chiral column LA with helically arranged amylose tris(5-chloro-2-methylphenyl-carbamate) coated on 3 μ m silica particles offers a complex chiral recognition pattern with high chance of achieving a chiral resolution. Similarly, the column CP is made of a spherical silica support onto which the polymeric chiral selector based on helically structured tris (3,5- dimethyl-phenylcarbamate) derivative of amylose as chiral stationary phase is physically coated. The optimal separation conditions with respect to the mobile phase composition and the temperature for LCM1(RAC) on both the chiral columns were found. An excellent separation was obtained for (R) and (S) enantiomers of LCM1 being sufficient even for the potential chiral chromatography in a preparative scale (Fig. 1).

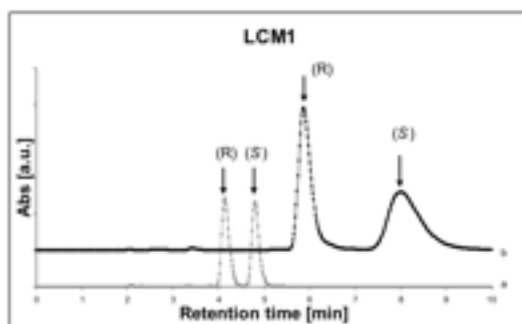


Figure 1: Separation of LCM1(RAC). Separation conditions: a) chiral column Chiralpak AD-3; mobile phase: hexane:isopropyl alcohol, 9/1 (v/v) at 35°C b) chiral column Lux Amylose-2, mobile phase: hexane:isopropyl alcohol, 8/2 (v/v) + 0,1% triethylamine, 0,2% trifluoroacetic acid at 35°C.

On the other hand despite much effort spent in the optimization of the separation conditions for LCM2 samples only two peaks at maximum were obtained for all the synthesized LCM2 materials differing in isomeric composition. The LCM2(RAC,S) material consisted of a mixture of diastereoisomers LCM2(S,S) and LCM2(R,S) with the ratio 1:1 and the baseline separation was obtained for these two diastereoisomers. For the identification of the individual peaks in the chromatogram for LCM2

compounds, the sole diastereoisomer LCM2(S,S) was prepared. A small peak at retention time ~5.0 min appeared for LCM2(S,S), which is probably related to a small amount of diastereoisomer LCM2(R,S). This proves that the individual components of LCM2(RAC,S), i.e. LCM2(R,S) and LCM2(S,S), can be effectively separated. This is very important finding from the practical point of view considering the significance of having a tool suitable to trace the optical purity specifically of the lactate part of the molecule. During the separation of LCM2(RAC,RAC) only two peaks with the area ratio 1:1 were obtained and finally chromatogram for LCM2(S,RAC) shows one major peak only, which corresponds to LCM2(S,S) and LCM2(S,R) diastereoisomers.

It is evident that the current chiral HPLC method is very sensitive to spatial arrangement of the substituents located on asymmetric carbon in lactate part of the molecule. On the other hand the method is unable to distinguish S and R configuration at the second chiral center derived from methylbutyl.

This work was supported by the Czech Science Foundation (grant CSF 13-14133S) and by the Ministry of Education of the Czech Republic, project MSM6046137307.

¹ M. Zurowska, R. Dabrowski, J. Dziaduszek, W. Rejmer, K. Czuprynski, Z. Raszewski and W. Piecek. *Mol. Cryst. Liq. Cryst.* 2010, **525**, 219-225.

² H. – R. Dubal, C. Escher and D. Ohlendorf. *Ferroelectrics* 1988, **84**, 43-165.

³ E. Gorecka, D. Pociecha, M. Cepic, B. Zeks and R. Dabrowski. *Phys. Rev. E* 2002, **65**, 061703-1-061703-4.

⁴ D. B. Amabilino. Wiley VCH Verlag GmbH & Co. KGaA, Weinheim 2009.

⁵ Y. Sasaki, K. Aihara, M. Isobe and K. Ema. *Mol. Cryst. Liq. Cryst.* 2011, **546**, 209-214.

⁶ K. M. Kirkland. *J. Chromatogr. A* 1995, **718**, 9-26.

⁷ M. Tang, J. Zhang, S. Zhuang and W. Liu. *TrAC* 2012, **39**, 180-194.

Optical and electronic properties of unilaterally and bilaterally extended perylene cores

J. Vollbrecht^{a*}, H. Bock^b, C. Wiebeler^a, S. Schumacher^a and H. Kitzerow^a

^a Center for Optoelectronics and Photonics Paderborn, University of Paderborn, Germany.

^b Centre de Recherche Paul Pascal, Université Bordeaux, France.

e-mail: Joachim.Vollbrecht@upb.de

Improvement of organic electronics in general and organic light emitting devices in particular requires that new compounds are synthesized and tested. One recent goal for many groups has been the fabrication of flexible displays based on organic light emitting diodes (OLED). Chemical stability, energy conversion and brilliance can be enhanced by the application of new compounds. It is well known that calamitic and discotic liquid crystals can improve the performance of OLEDs owing to their self-organizing properties.¹ In this study newly synthesized polyaromatic hydrocarbons with a bilaterally extended coronene core are characterized and the absorption, photoluminescence, electroluminescence spectra and electronic properties are compared to compounds with a perylene core and a unilaterally extended perylene core.²⁻⁵ For each core an ester and an imide compound have been investigated (Fig. 1). In addition simulations based on time-dependent density functional theory (TD-DFT) were employed to describe the observed differences between the cores.

173153

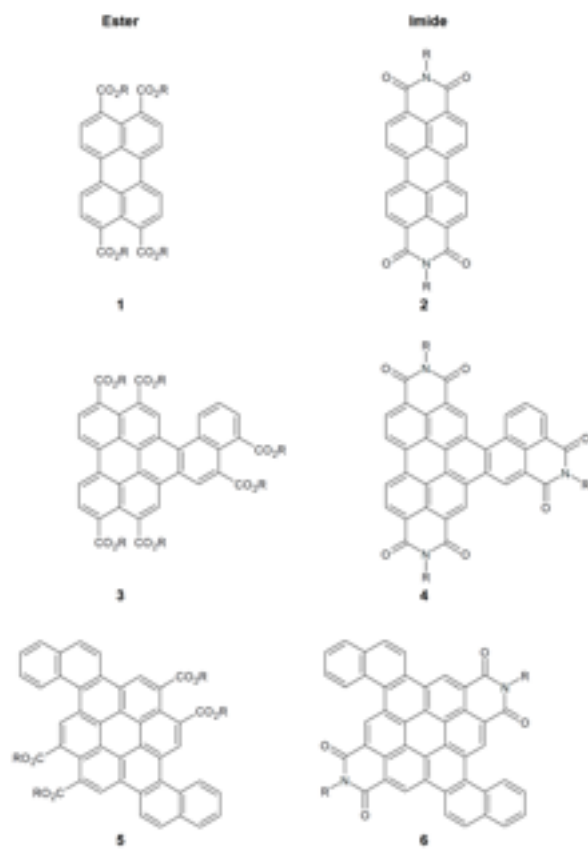


Figure 1: Molecular structure of compounds with different cores.

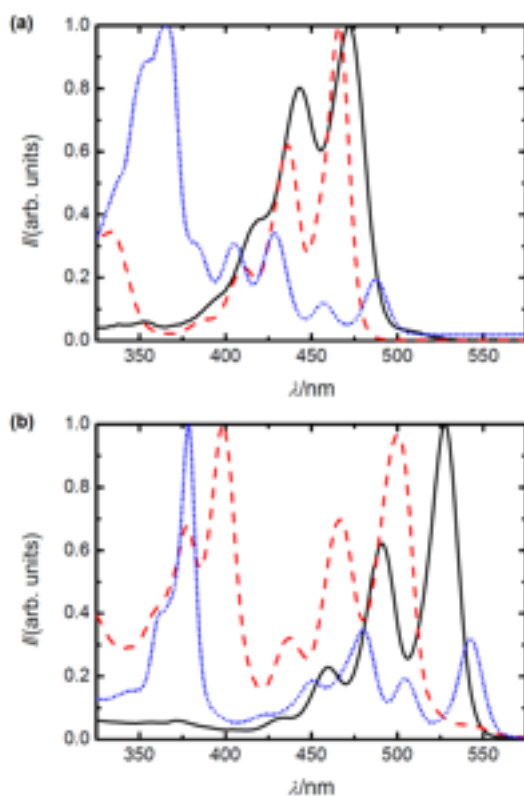


Figure 2: Absorption spectra of (a) esters **1** (solid line), **3** (dashed line), **5** (dotted line) and (b) imides **2** (solid line), **4** (dashed line) and **6** (dotted line).

The absorption spectra show that compounds **1**, **3**, **5** and **2**, **4**, **6** respectively, have peaks in the same wavelength region. However the intensity of the peaks varies significantly. While compounds **1** and **2** with a perylene core have their main peaks in the longer wavelength range, compounds **3**, **4** and **5**, **6** have their main peaks at shorter wavelengths. The experimental results are in reasonable agreement with theoretical calculations.

¹ T. Hassheider, S. A. Benning, H. Kitzerow, M.-F. Achard, H. Bock. *Angew. Chem. Int. Ed.* 2001, **40**, 2060.

² J. Kelber, M.-F. Achard, F. Durola, H. Bock. *Angew. Chem. Int. Ed.* 2012, **124**, 5290.

³ I. Seguy, P. Jolinat, P. Destruel, R. Mamy, H. Allouchi, C. Courseille, M. Cotrait, H. Bock. *ChemPhysChem.* 2001, **7**, 448.

⁴ W. E. Ford, P. V. Kamat. *J. Phys. Chem.* 1987, **91**, 6373.

⁵ M. Oltean, A. Calborean, G. Mile, M. Vidrighin, M. Iosin, L. Leopold, D. Maniu, N. Leopold, V. Chis. *Spectrochim. Acta Mol. Biomol. Spectros.* 2012, **97**, 703.

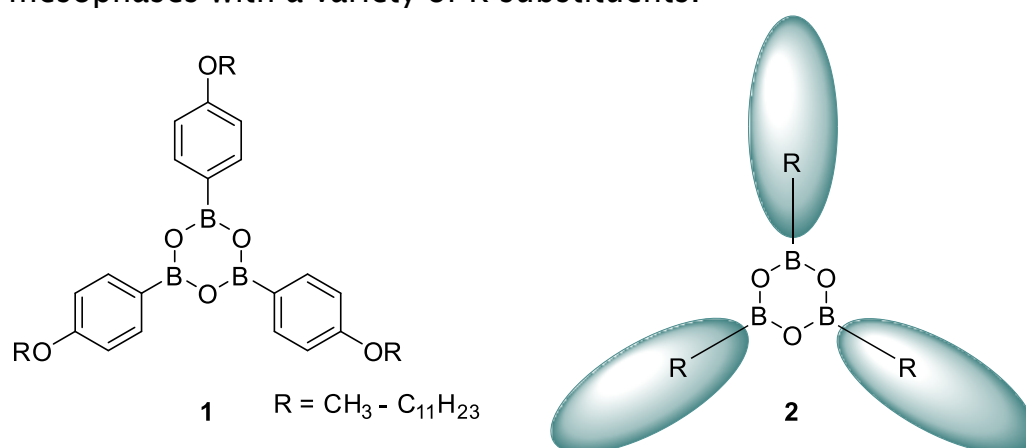
Novel liquid crystals containing a boroxine central unit

Tobias Wöhrle^{a*}, Sabine Laschat^a

^a Institut für Organische Chemie, Universität Stuttgart, Stuttgart, Germany

*e-mail: tobias.woehrle@oc.uni-stuttgart.de

Discotic liquid crystals have a broad field of application possibilities such as in electronics (e.g. air-stable semi-conductors), optoelectronics (e.g. organic light-emitting devices, photovoltaic devices) or newly as non-linear optics (NLOs).^{1,2,3} In order to obtain NLO properties studies showed structures with a D₃-symmetry as suitable.⁴ Hence we used boroxines as a core unit for our discotic compounds which provide quick and easy access to tripodal molecular architecture. Boroxines are the condensation product of three boronic acids and therefore consist of a 6-membered (-B-O-)₃ ring system. Since previous work showed that boroxines containing short alkyl-chains (**1**) were nonmesomorphic⁵ we varied the substituents (**2**) in order to induce a mesophase. The synthesis to the precursors was realised from cheap starting materials and standard reactions. However, the key step – the final condensation to desired boroxines – has not been very intensively researched for bulky substituents. Thus we present a successful synthetic route to liquid crystalline boroxines displaying broad mesophases with a variety of R substituents.



¹ Sergeyev, S.; Pisula, W. Geerts, Y. H.; Chem. Soc. Rev. **2007**, 36, 1902–1929.

² R. J. Bushby, K. Kawata, Liq. Cryst. **2011**, 38, 1415–1426.

³ J. Kopitzke, J. H. Wendorff, Chem. Unserer Zeit **2000**, 34, 4–16.

⁴ H. M. Kim, B. R. Cho, J. Mater. Chem. **2009**, 19, 7402–7409

⁵ M. Belloni, M. Manickam, Z. H. Wang, J. A. Preece, Mol. Cryst. Liq. Cryst. **2003**, 399, 93–114.

Coalescence of Lentil-Like Droplets on Freely Suspended Smectic Films

S. Dölle,^a Z. Qi^b, C. S. Park,^b J. E. Maclennan,^b M. A. Glaser,^b N. A. Clark,^b K. Harth,^a R. Stannarius^{a*}

^a *Otto-von-Guericke Universität Magdeburg, Institute for Experimental Physics, D-99016 Magdeburg, Germany.*

^b *Department of Physics, and the Liquid Crystal Materials Research Center, University of Colorado, Boulder, CO, 80309, USA.*

e-mail: sarah.doelle@ovgu.de

Pioneering theoretical studies on coalescence dynamics have been done by Hopper in 1993.¹ He found an analytic Solution for the Stoke's flow of two infinitely long, fluid cylinders coalescing in vacuum driven by surface tension. At early times, his analysis yields a linear growth of the bridge width with a logarithmic correction. The bridge width is the distance between the two edges where the cylinders are connected. Eggers, Lister and Stone showed that Hopper's results can be extended and transferred to the three-dimensional case.^{2, 3}

For a long time, experiments have been difficult to perform due to the deficient time resolution of observation systems. But with an ongoing improvement of high speed cameras this fundamental field of research was unclosed to experimentalists.

In the following, experiments on coalescence dynamics in restricted geometries are introduced. A study by Burton and Taborek treats lentil-like alkane droplets floating on water.⁴ The alkane lenses are used as a test system for quasi-two-dimensional (2D) fluids. The dimensionality should have an influence on singularities that occur during the coalescence process. However, the viscosity of the surrounding material cannot be neglected, resulting in a three-dimensional fluid flow around the lenses. And according to their experiments, the coalescence of floating lenses is not significantly different from the coalescence of axis symmetric, spherical droplets.

Freely suspended smectic films have been found to be excellent model systems to study quasi- 2D fluid dynamics.⁵ These smectic films form thicker, disc-like islands that can be considered as fluid cylinders floating in a 2D liquid. Experiments with these pancake-like islands show that the coalescence at early stages is much slower than Hopper's model would suggest for an ideal 2D process. The reason for this discrepancy is probably implied in the properties of the smectic material. The bridge width expands linearly until the two discs merge to an elliptic shape. Henceforth, the line tension drives the dynamics and the bridge width converges to a final value.

In our experiment, we investigate the coalescence of lentil-like oil droplets floating in a freely suspended smectic film. 8CB (4'-*n*-octyl-4-cyanobiphenyl, Sigma-Aldrich) was used as film material, which shows a smectic A phase at room temperature. The film thicknesses ranged from 9.5 nm to 37 nm. The films were drawn manually on a film holder and positioned in a sealed chamber. Oil (Highly-Refined Petroleum Lubricant Oils, 1407K Duoseal Vacuum Pump Oil, Welch-Ilmvac) was vaporized next to the film holder. The oil vapor condensed on the film and formed small oil droplets. The formed droplets were observed via reflective optical

microscopy using a high-speed camera (Phantom 12.1, Vision Research) with frame rates up to 20,000 frames/sec (fps).

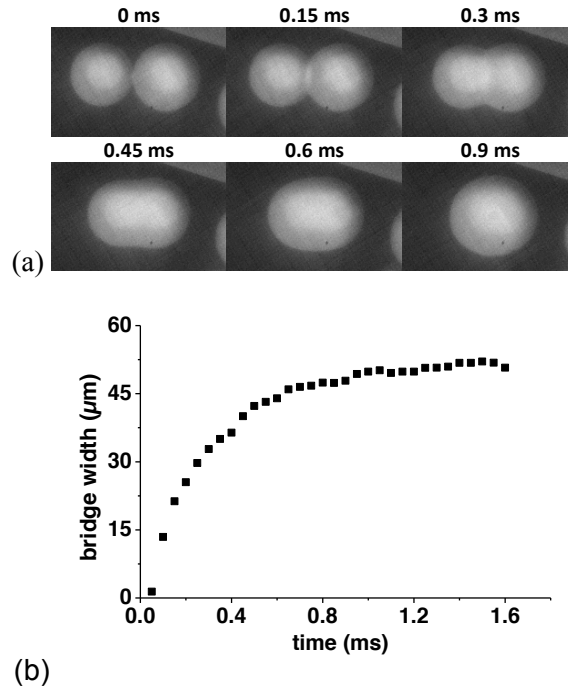


Figure 1: Coalescence of two lentil-like oil droplets in a freely suspended smectic film. (a) The images were taken with a frame rate of 20,000 fps. In the first image the radii of the oil lenses are $14\ \mu\text{m}$ and $16\ \mu\text{m}$ from the left to right. The curvature of the oil lenses scatters light and the objects appear darker towards the edges. (b) Bridge expansion over time of the coalescence in section (a). The coalescence starts with an exponential growth of the bridge width. Then the expansion slows down and the new formed inclusion relaxes towards its final circular shape with a radius of $26\ \mu\text{m}$.

The coalescence process of two lentil-like oil droplets is shown in Figure 1. The fluid film is very thin ($9.5\ \text{nm}$) compared to the thickness of the lenses, thus the film can be regarded as a 2D fluid. The oil lenses rest close to each other for an inexplicit time. After the first contact, the coalescence event completes almost within a millisecond. The width of the bridge grows exponentially until it reaches the tangent that connects the initial edges of the lenses ($t \approx 0.6\ \text{ms}$). From this point, the oil droplet converges slowly to its final circular shape. The bridge expansion velocity at early times seems to be faster than the velocity of two merging smectic islands.

¹ R. W. Hopper. *Journal of the American Ceramic Society*. 1993, **76**, 2947.

² J. Eggers, J. R. Lister, and H. A. Stone, *Journal of Fluid Mechanics*. 1999, **401**, 293.

³ J. Eggers. *Physical Review Letters*. 1998, **80**, 2634.

⁴ J. C. Burton, and P. Taborek, *Physical Review Letters*. 2007, **98**, 224502.

⁵ A. Eremin, S. Baumgarten, K. Harth, R. Stannarius, Z. H. Nguyen, A. Goldfain, C. S. Park, J. E. MacLennan, M. A. Glaser, and N. A. Clark. *Physical Review Letters*. 2011, **107**, 268301.

Dynamics of Free-Floating Smectic Bubbles

Kathrin May^a, Kirsten Harth^a, Torsten Trittel^a, Ralf Stannarius^a

^a Otto-von-Guericke-Universität Magdeburg, FNW/IEP/ANP, Postfach 4120, 39016 Magdeburg, Germany.

e-mail: kathrin.may@ovgu.de

Dynamics of closed interfaces is a topic of great interest in technical, chemical and biological investigations. Especially the theory of oscillating closed interfaces has been studied since many years. The oscillation frequency of interfaces with the approximations of no viscosity and small amplitudes is according to Lamb ¹:

$$\omega = \sqrt{\frac{n(n+1)(n-1)(n+2)\sigma}{((n+1)\rho_i + n\rho_o)a^3}} \quad (1)$$

where n is the mode number, σ the interface tension, ρ_i the density of the inner, ρ_o of the outer fluid, and a is the equilibrium radius. There have been many improvements in calculating the frequency and damping, but the special characteristics of smectic bubbles have not been taken into account yet.

Here, we investigate closed thin fluid membranes of smectic material. The characteristics of the liquid crystals make these smectic bubbles an interesting object of investigation, because the dynamics differ a lot from the dynamics of soap bubbles. The bubbles are created through the collaps of a film in the shape of a catenoid ². The experimental setup is shown in Fig. 1.

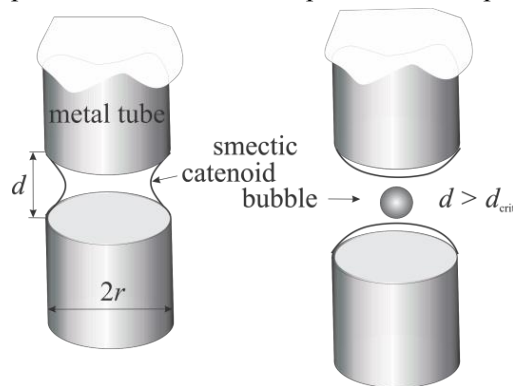


Figure 1: Experimental setup

An elongated bubble detaches from the catenoid holder. Two different bubble sizes are created, small soap and smectic microbubbles and smectic bubbles with a diameter of about 1cm. The large bubbles were prepared in zero g experiments during parabolic flights to avoid settling of the bubbles because of gravitation.

In the case of soap bubbles, the bubble immediately starts a damped oscillation to the spherical shape. The oscillation frequency is similar to what can be calculated by Lambs formula, although the film thickness lowers the frequency. In contrast to that, smectic bubbles deform and decrease their surface area very slowly in comparison with the frequency of Lamb. Only when the spherical shape is nearly reached, the bubble starts to oscillate with a frequency of about the one of Lamb. The reason for this slow relaxation is the reduction of the surface area,

which takes more time for the smectic film than for soap films, because islands have to be created, in which the excess material is stored. During the shrinking of the bubble, the islands grow and this slow process inhibits the fast oscillation of the bubble. On the centimetre sized bubbles, the creation and growth of islands can be observed. Thick islands grow slower than thin islands, and both stop to grow when the oscillation starts.

Another phenomenon can be seen by observing smectic A bubbles. Most of these bubbles, especially thin ones, rupture during the first deformations after the creation. Thin bubbles rupture easier than thick bubbles, because the deformations of thick bubbles are much slower. The reason for this is that less material has to be reorganised on the film.

The rupturing always takes place at the same shape of the bubble, see Fig. 2.

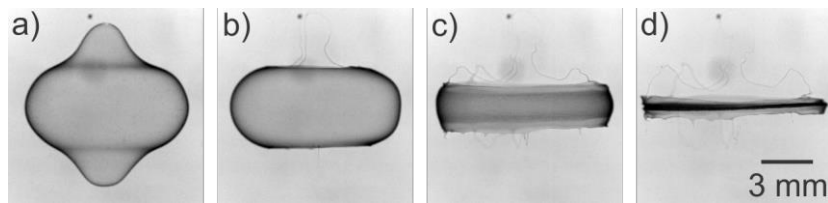


Figure 2: Rupture of a smectic A bubble

It begins either with two holes at the ends of the bubble, or many holes appear simultaneously all over the bubble. If only two holes occur, the bubble retracts to the middle and a darkening of the leftover smectic film can be observed. If many holes occur, all of them expand with the same speed. The material is then stored in thin filaments, so that a network of filaments occurs (Fig. 3).

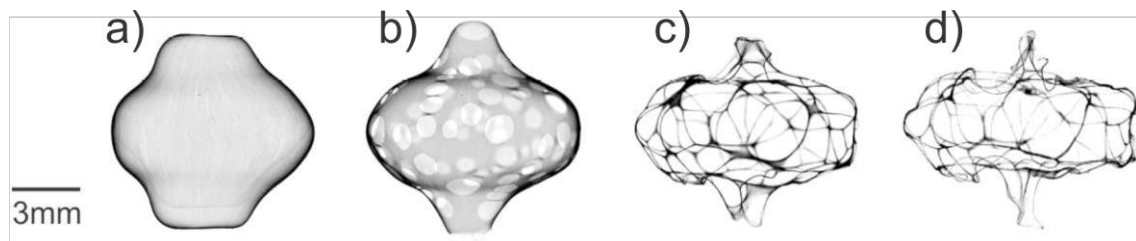


Figure 3: Filament network during the rupture of a smectic a bubble

In contrast to smectic A bubbles, smectic C bubbles usually do not rupture, even if they are very thin. This can be accounted to a higher stability of smectic C films,

¹ H. Lamb, *Hydrodynamics*, Cambridge University Press, Cambridge, 1879.

² K. May, K. Harth, T. Trittel, R. Stannarius, *Europhys. Lett.*, 2012, **100**, 16003.

Dynamics of Point Defects in Free-Standing SmC Films

Kirsten Harth^{a*}, Peter Salamon^b, and Ralf Stannarius^a

^a *Institute of Experimental Physics, Otto von Guericke University Magdeburg*

^b *Wigner Institute, Hungarian Academy of Sciences, Budapest*

e-mail: Kirsten.Harth@ovgu.de

Ordering phenomena that break certain symmetries often involve the dynamics of defects. Connections are made, e.g., to defects in crystals, colloidal crystals as well as symmetry breaking in string theory. In liquid crystals, such processes are easily visualized in polarised light microscopy. Point defect annihilation has been investigated experimentally and numerically, e. g., in thermotropic nematics [1], lyotropics[2] and active nematics[3].

Free-standing smectic films are ideal model systems to probe two-dimensional hydrodynamics. Films in the smectic C phase represent the simplest anisotropic fluid in two dimensions. Within elastic one-constant approximation and with neglect of hydrodynamic effects, the description of defect dynamics is identical to that of point charges in electrostatics. Whereas the equations for two point charges are easily solvable analytically, the case of three or more charges is equivalent to the classical three-body problem.

Within the c-director (unit vector along the projection of \mathbf{n} onto the tilt plane) field description, point defects in smC are represented as topological defects of a vector field. Only defects of strengths ± 1 occur. With neglect of material flow and in one-elastic constant approximation ($K_S = K_B = K$), the potential energy of a defect pair of topological strengths s_1, s_2 at separation d is given by [4]

$$W = \pi K (s_1 + s_2)^2 \ln \frac{R}{r_c} - 2\pi K s_1 s_2 \ln \frac{d}{2r_c},$$

where R is the film radius, and r_c is an estimate of the defect core radius. The first term is independent of the defect separation and does therefore not contribute to the interaction forces between the defects. The viscous drag on the moving defects due to the director reorientation (without material flow) is described as

$$f_v = \pi \gamma_1 s_1 s_2 \ln \frac{R}{r_c} \cdot \frac{\partial d}{\partial t},$$

where γ_1 is the rotational viscosity. In case of two defects of topological strengths with opposite signs, this leads to a square root scaling of the defect separation

$d(t) \propto \sqrt{t_0 - t}$, with the time until annihilation $t_0 - t$. The proportionality factor is defined by

the term
$$\sqrt{\frac{4K}{\gamma_1 \ln \frac{R}{r_c}}}.$$

Under this no-flow assumption, both defects would move at identical velocities, their annihilation would occur in the midpoint of the line connecting them.

When material flow is present, it has been predicted by Svenšek and Žumer [5] from a numerical simulation at small times and defect separations that

- i) due to advection, the +1 defect moves faster than the -1-defect and thus annihilation does not occur midway between their initial positions,
- ii) annihilation occurs faster than without flow,
- iii) for some examples it was shown that the details depend on the elastic anisotropy and viscosity coefficients.

We prepared homogeneously thick and non-patterned (non-chiral) smectic C films of several square millimeters size at room temperature. Film thicknesses were measured using a spectrometer range from 150 nm to several mm. We developed new techniques to create isolated defect pairs and groups of defects of topological strength +1 in a controlled way.

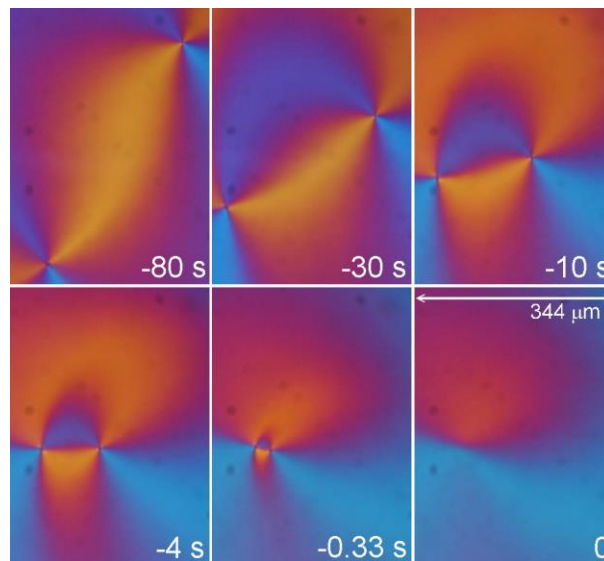


Figure 1: Annihilation of a +1 and a -1 c-director point defect in a smC free-standing film. Polarizers are parallel to the edges, a ($\lambda = 550$ nm)-phase plate is inserted at 45° . Time is taken respective to the annihilation.

For defect annihilation, the temporal evolution is recorded up to minutes before the annihilation using a CCD camera, see Figure 1 for an example. Initially, the elastic forces are small, so that large deviations from any power law scaling are observed, and individual measurements differ from each other due to random disturbances. Indeed, the +1 defect always moves more rapidly than the -1 defect. Additionally, the specific alignment of the hyperbolic axes in the director field of the -1-defect respective to the line connecting the pair (see Figure 2) influences the relaxation dynamics. When well-aligned pairs are selected, all plots coalesce to one curve. Shortly before annihilation, all measurements combine to a single master curve. Thus, the film

thickness, and typical membrane dynamic effects (e.g. the Saffman length, see Ref.[6]) are irrelevant.

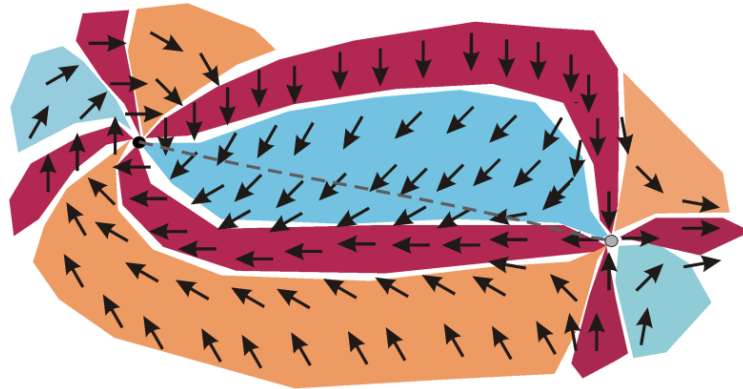


Figure 2: Sketch of a director field around a not well-aligned annihilating pair of defects (core positions in black (+1) and grey (-1)). The c-director field is not uniform along the line connecting their cores (dashed line), leading to a curved paths of coalescence for the defect pair.

The repulsion of sets of $n \geq 2$ defects of topological strength +1 leads to several (often regular) geometrical configurations. Figure 3 shows an example of eight +1 defects. Weighting the net forces of all defects respective to each other, a single approximately square root scaling of the defects' separation to their centroid position is retrieved. Hypothetically, this is attributed to a symmetric and weaker influence of material flow. Additionally, repulsion of +1 defects from larger positive net topological charges can be analyzed.

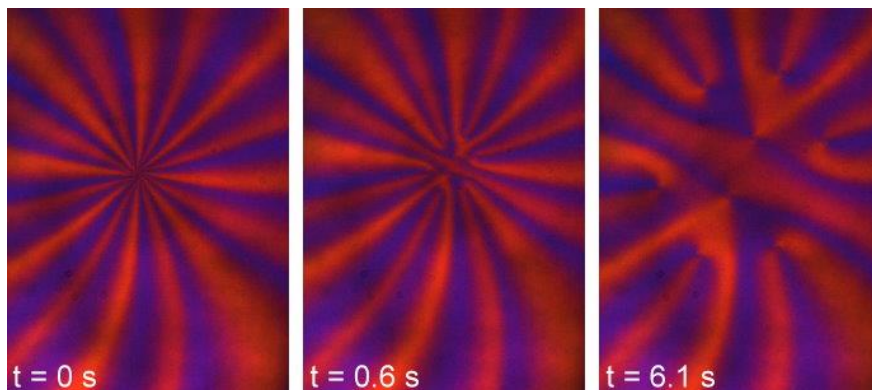


Figure 3: Repulsion of eight +1-defects. Images taken between crossed polarizers parallel to the edges and λ phase plate at 45° . The height of the images is $538 \mu\text{m}$. In the initial image, the defects are trapped at a layer step near the center of the pattern.

In order to quantify the effects of defect configurations, positions and material parameters, numerical simulations of defect dynamics on the time and length scales of the experimental findings are performed. In a 2D approach, the smectic becomes analogue of a 2D nematic, where the tilt cone angle is used as an order parameter. We solve the Ericksen-Leslie equations

(see e.g. Ref. [7]) using a finite elements approach on an adaptive mesh in COMSOL, where local refinement is enforced near the defect cores.

¹ P. Oswald, J. Ignes-Mullol, *Phys. Rev. Lett.* 2005, **95**, 027801; I. Dierking, et al., *Phys. Rev. E* 2012, **85**, 021703; A. Bogi, et al., *Phys. Rev. Lett.* 2002, **89**, 225501; G. Tóth, C. Denniston, J. Yeomans, *Phys. Rev. Lett.* 2002, **88**, 105504.

² H. V. Ribeiro, et al., *Phys. Rev. E* 2013, **87**, 054501.

³ L. Giomi, et al., *Phys. Rev. Lett.* 2013, **110**, 228101; L. M. Pismen, *Phys. Rev. E* 2013, **88**, 050502; Thampi, Golestanian, J. Yeomans, *Phys. Rev. Lett.* 2013, **111**, 118101.

⁴ M. Kleman, O. D. Lavrentovich, *Soft Matter Physics: An Introduction*, Springer Verlag 2003.

⁵ D. Svensek and S. Zumer, *Phys. Rev. Lett.* 2003, **90**, 155501.

⁶ A. Eremin, et al., *Phys. Rev. Lett.* 2011, **107**, 268301; Z. H. Nguyen, et al., *Phys. Rev. Lett.* 2010, **105**, 268304

⁷ I. W. Stewart, *The static and dynamic continuum theory of liquid crystals*, Taylor & Francis 2004.

Interface Tension of Smectic Membranes in Water

Kirsten Harth and Ralf Stannarius

Otto-von-Guericke-Universität Magdeburg, FNW/IEP/ANP, Postfach 4120, 39016 Magdeburg, Germany.

e-mail: kirsten.harth@ovgu.de

Liquid crystal research has opened up new fields of applications during the past years, far from electro-optic switching devices— one of these potential applications is the use of LC alignment and confinement properties for the construction of smart devices out of LC shells in aqueous environment [1], or for the detection of tiny concentrations of specific molecules through surface anchoring transitions in droplets or on flat films [2]. In all multi-phase hydrodynamic processes on the microscale, such as microfluidics, pick-off, or rupture phenomena, the interface tension between the involved liquids plays a central role.

Interestingly, while there have been several reports of liquid crystal surface tensions measured respective to air, very little is known about the interface tension between liquid crystals and other fluids. This is mainly due to the fact that in the classical pendant droplet method, the density difference between the host liquid and the LC is needed to calculate the surface tension. Both densities are very similar, therefore the results are often very inaccurate. The interface tension can be determined only to the order of magnitude: In a previous experiment [3], the 5CB interface tension to water was determined to be between 4...8 mN/m or 1.2 ...2.4 mN/m, depending on the choice of density data.

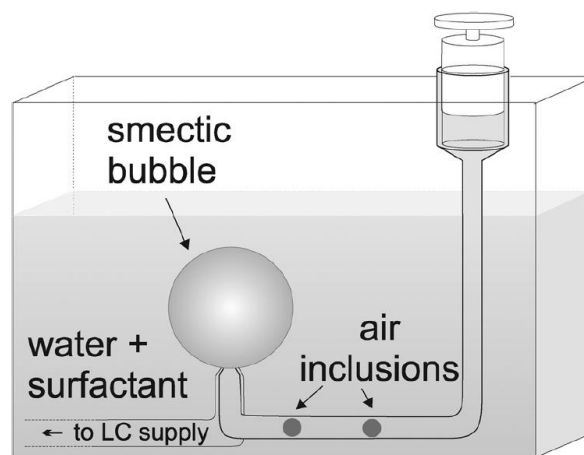


Figure 4: Sketch of a setup for measurements of the interface tension of smectics in a water / surfactant mixture: An amount of mesogenic material is placed on a nested capillary, a centimeter-sized bubble filled with fluid is created using a syringe, small air inclusions can be pumped into the smectic bubble the same way.

We developed a new, simple and accurate method to measure the interface tensions of smectics respective to water–surfactant mixtures [4]. The setup is sketched in Figure 1. For demonstration, we use a mixture of water and SDBS well above the critical micelle

concentration. A smectic bubble filled with fluid is prepared in a fluid-filled container. Small air volumina are injected into the centimeter-sized smectic bubbles. They settle under the top part of the smectic membrane and deform it to a non-spherical equilibrium shape (minimal surface), see Figure 2 for an example.

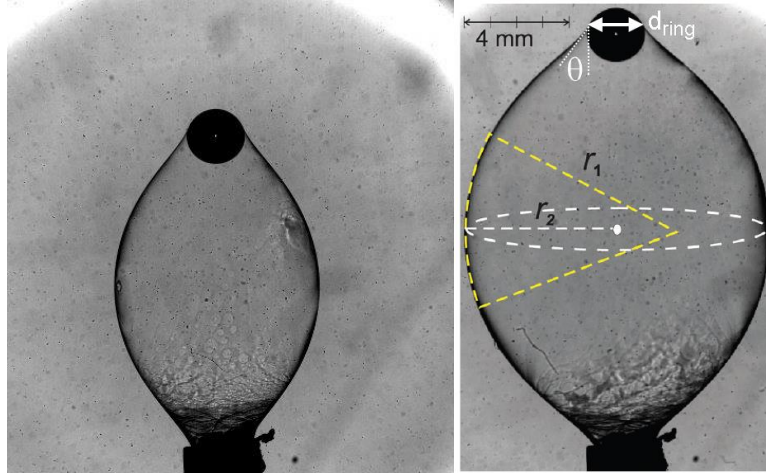


Figure 2: Water-filled smectic bubbles under water and the definition of measurement parameters (right). At the top, an air volume is trapped beneath the smectic film. It deforms the bubble surface. The same air volume (diameter $d=2.12$ mm) is trapped in both images, but the smectic bubble was inflated manually.

Due to the buoyancy of air bubbles of different sizes placed inside, the smectic bubbles are deformed in a well-defined manner. The interface tension is then easily and accurately determined from the film geometry:

$$G_{\text{air}} = 2\pi d_{\text{ring}} \sigma \left[\cos \theta - \frac{d_{\text{ring}}}{4} \left(\frac{1}{r_1} + \frac{1}{r_2} \right) \right].$$

Here, σ denotes the interface tension (half the film tension), d_{ring} is the diameter of the bubble at the contact point, θ is the angle of attack of the smectic film in the same position, and r_1 and r_2 are the principal radii of curvature of the smectic bubble, as shown in Figure 2.

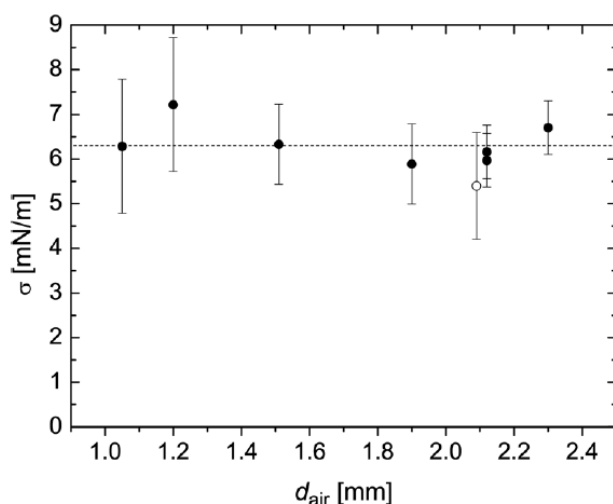


Figure 3: Calculated surface tensions for different sizes of inclusions and smectic bubbles, the dashed line denotes the average [4].

By varying the sizes of smectic bubbles and air inclusions, several measurement values were obtained, see Figure 4. We find an average of 6.3 ± 0.4 mN/m for our 1:1 mixture of 2-(4-n-hexyloxyphenyl)-5-n-octylpyrimidine and 5-n-decyl-2-(4-n-octyloxy-phenyl)-pyrimidine respective to water / SDBS mixtures above the critical micelle concentration.

Additional surface and interface tension data can be deduced from the positions and shapes of the air inclusions. When the smectic bubble is pierced, dynamic surface tension properties can be studied. After puncture of the films with trapped air bubbles, a dramatic rupture scenario is observed.

References

- ¹H.-L. Liang et al., *Phys. Rev. Lett.* 2011, **106**, 247801; T. Lopez-Leon, et al., *Phys. Rev. Lett.* 2011, **106**, 247802; D. R. Nelson, *Nano Lett.* 2002, **2**, 1125.
- ²I.-H. Lin, et al., *Science* 2012, **332**, 1297.
- ³J.-W. Kim, et al., *Langmuir* 2004, **20**, 8110.
- ⁴K. Harth and R. Stannarius, *Phys. Chem. Chem. Phys.* 2013, **15**, 7204

List of Presenting Authors

Alaasar, M.	O17
Atorf, B.	P1
Bahndorf, K.	P11
Bausch, A.R.	I3
Bogner, A.	O1
Bruckner, J.	O10
Chattham, N.	O5
Derouiche, Y.	O9, P4, P5
Dolganov, P.V.	O2
Dölle, S.	P29
Harth, K.	O12, P31, P32
Harjung, M.	P13
Hänle, J.C.	P12
Hügel, M.	P14
Jampani, V.S.R.	O4
Janietz, D.	P15
Jenz, F.	O15
Knecht, F.	P6
Kohout, M.	P6
Lagerwall, J.P.F.	I2
Lehmann, M.	O18
Lorentz, A.	O6
Maier, P.	P17
Maisch, S.	P18
May, K.	P30
Mehl, G.H.	O14
Menzel, A.M.	O16
Neidhardt, M.M.	O11
Pashmeah, R.	P19
Pieranski, P.	E1
Poppe, M.	P20
Poppe, S.	P21
Poryvai, A.	P22
Rieth, T.	P23
Rix, R.	O7
Roth, S.	P24
Schmidtke, J.	P7
Shukla, R.K.	O3, P8
Takezoe, H.	I1
Tamba, M.-G.	O19, P25
Urbanski, M.	P9
Vojtylová, T.	P26
Vollbrecht, J.	P27
Wahle, M.	O13
Wöhrle, T.	P28

Zimmermann, N. P10

